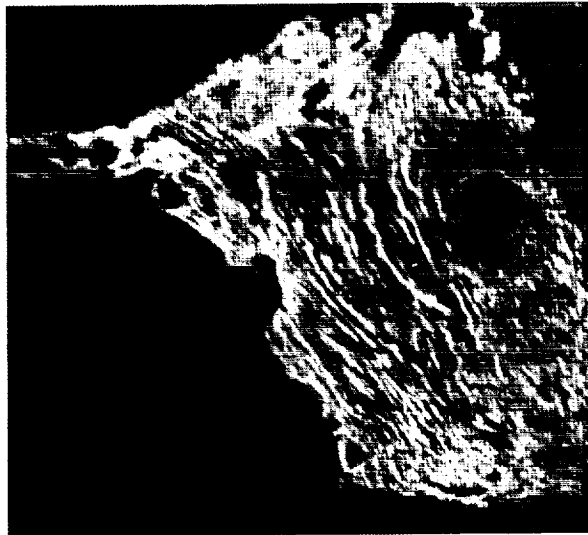


# ABSTRACTS FOR THE VENUS GEOSCIENCE TUTORIAL AND VENUS GEOLOGIC MAPPING WORKSHOP

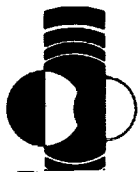
Flagstaff, Arizona

June 12-15, 1989



Sponsored by

Lunar and Planetary Institute and  
National Aeronautics and Space Administration

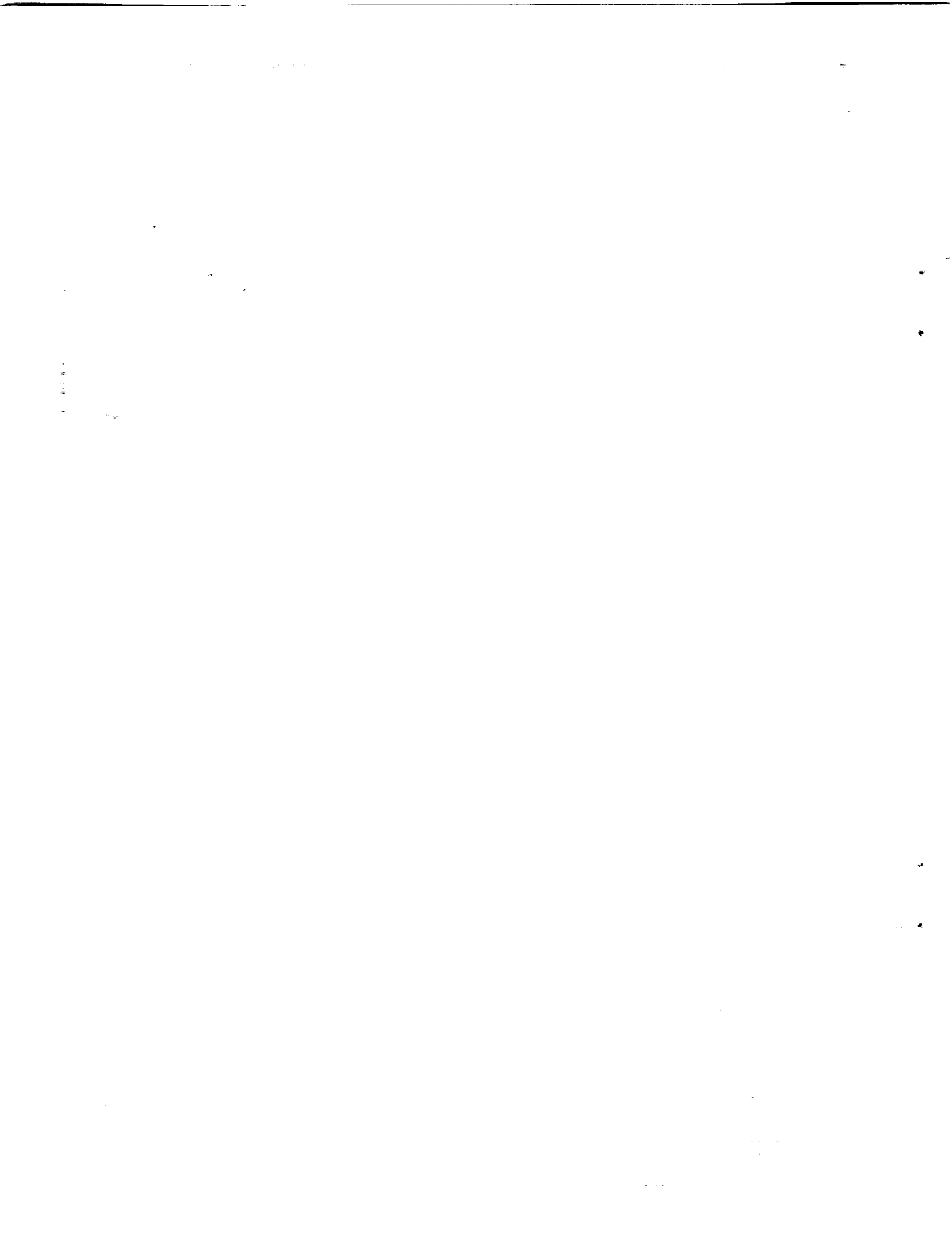


(NASA-CR-185432) ABSTRACTS FOR THE VENUS  
GEOSCIENCE TUTORIAL AND VENUS GEOLOGIC  
MAPPING WORKSHOP Abstracts Only (Lunar and  
Planetary Inst.) 62 p CSCL 03R



N90-12423  
--THRU--  
N90-12453  
Unclass  
0218571

G3/91



**ABSTRACTS FOR THE VENUS GEOSCIENCE TUTORIAL AND  
VENUS GEOLOGIC MAPPING WORKSHOP**

**Flagstaff, Arizona**

**June 12-15, 1989**

*Sponsored by*

*Lunar and Planetary Institute  
National Aeronautics and Space Administration*

*Hosted by the U. S. Geological Survey*

**LPI Contribution No. 708**

Compiled in 1989 by the  
Lunar and Planetary Institute  
3303 NASA Road 1  
Houston, TX 77058-4399

Material in this volume may be copied without restraint for library, abstract service, educational, or personal research purposes; however, republication of any paper or portion thereof requires the written permission of the authors as well as appropriate acknowledgment of this publication.

The Lunar and Planetary Institute is operated by the Universities Space Research Association under Contract No. NASW-4066 with the National Aeronautics and Space Administration.

Cover: Radar image of Maxwell Montes, Venus.  
(Courtesy Arecibo Observatory)

## **PREFACE**

This volume contains abstracts of invited tutorial and solicited posters that have been accepted for presentation at the Venus Geoscience Tutorial and Venus Geologic Mapping Workshop.

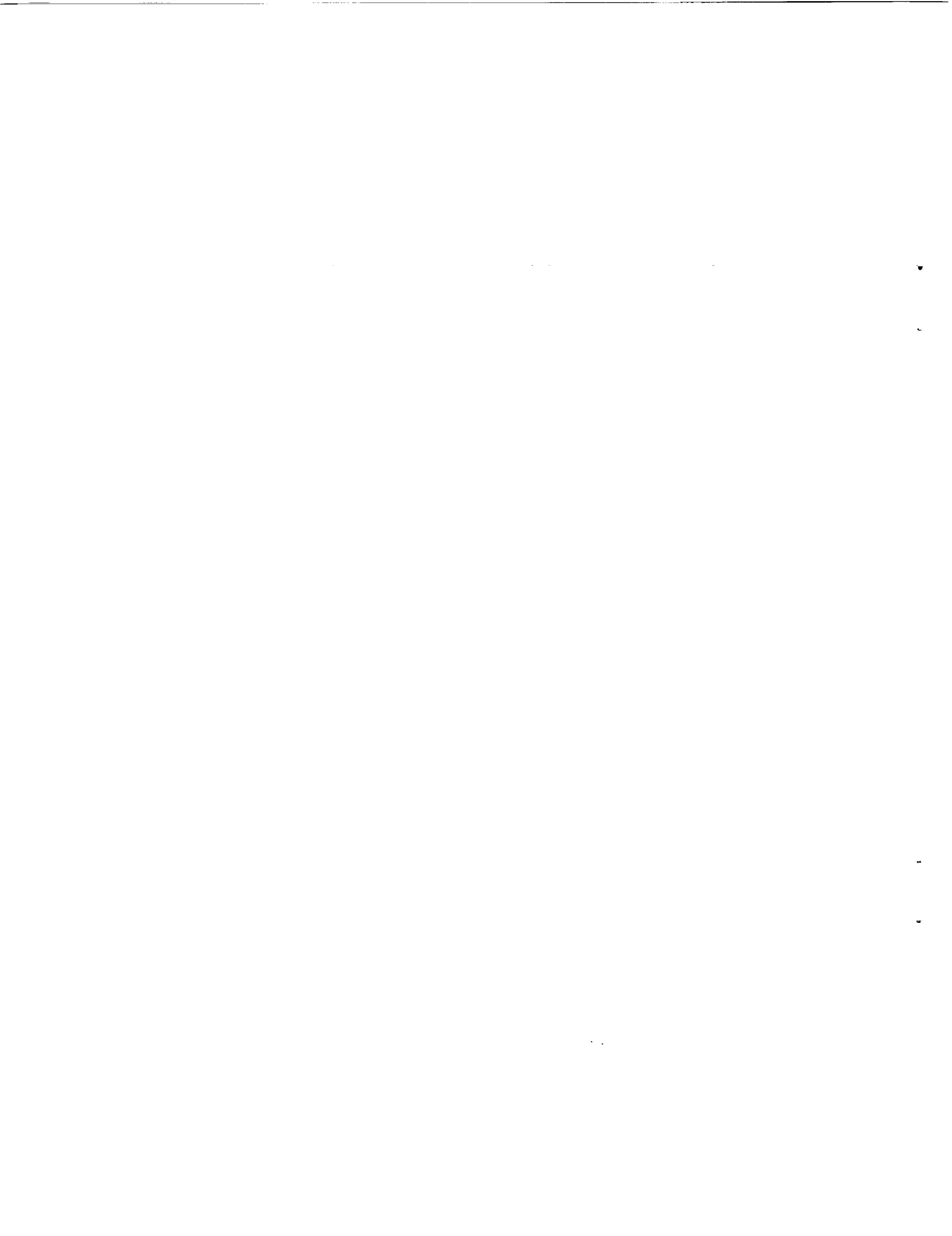
**Conveners:**

Gerald Schaber and Richard Kozak  
U. S. Geological Survey, Flagstaff

**Program Committee:**

Gerald Schaber, U. S. Geological Survey, Flagstaff  
James Head, Brown University  
Roger Phillips, Southern Methodist University  
Stephen Saunders, Jet Propulsion Laboratory

Logistics and administrative support were provided by the Projects Office staff at the Lunar and Planetary Institute.



# CONTENTS

P - Poster      T - Tutorial

T	<i>Geology of Southern Guinevere Planitia, Venus, Based on Analyses of Goldstone Radar Data</i> R. E. Arvidson, J. J. Plaut, R. F. Jurgens, R. S. Saunders, and M. A. Slade.....	1
P	<i>Characteristics, Distribution and Geologic/Terrain Associations of Small Dome-like Hills on Venus</i> J. C. Aubele and E. N. Slyuta.....	2
P	<i>Tessera Terrain: Characteristics and Models of Origin</i> D. L. Bindschadler and J. W. Head.....	4
T	<i>Divergent Plate Boundaries and Crustal Spreading on Venus: Evidence from Aphrodite Terra</i> L. S. Crumpler and J. W. Head.....	6
T	<i>Venus Volcanism: Rate Estimates from Laboratory Studies of Sulfur Gas-Solid Reactions</i> K. Ehlers, B. Fegley, Jr., and R. G. Prinn.....	8
P	<i>Potential for Observing and Discriminating Impact Craters and Comparable Volcanic Landforms on Magellan Radar Images</i> J. P. Ford.....	10
P	<i>Contrasting Landform Perception with Varied Radar Illumination Geometries and at Simulated Resolutions of Venera and Magellan</i> J. P. Ford and R. E. Arvidson .....	11
T	<i>Venus Surface Properties Deduced from Radar and Radiometry</i> P. G. Ford .....	12
P	<i>A Morphologic Study of Venus Ridge Belts</i> S. L. Frank and J. W. Head .....	13
P	<i>Evidence for Volcanism in NW Ishtar Terra, Venus</i> L. Gaddis and R. Greeley .....	15
P	<i>Analysis of Radar Images of the Active Volcanic Zone at Krafla, Iceland: The Effects of Look Azimuth Biasing</i> J. B. Garvin and R. S. Williams, Jr.....	17

P	<i>Radar Scattering Mechanisms Within the Meteor Crater Ejecta Blanket: Geologic Implications and Relevance to Venus</i> J. B. Garvin, B. A. Campbell, S. H. Zisk, G. G. Schaber, and C. Evans .....	19
T	<i>Aeolian Processes on Venus</i> R. Greeley.....	21
T	<i>Thoughts on the Venusian Surface and Early Earth</i> R. B. Hargraves.....	23
T	<i>Architecture of Orogenic Belts and Convergent Zones in Western Ishtar Terra, Venus</i> J. W. Head, R. Vorder Bruegge, and L. Crumpler .....	24
P	<i>Deducing the Age of the Dense Venus Atmosphere</i> R. Kahn .....	26
P	<i>Clotho Tessera, Venus: A Fragment of Fortuna Tessera?</i> R. C. Kozak and G. G. Schaber .....	27
T	<i>Tectonism on Venus: A Review</i> R. Kozak and G. G. Schaber .....	29
T	<i>Surface Composition and Petrology</i> J. S. Lewis .....	30
T	<i>Extensional Tectonism in the Southwestern United States</i> I. Lucchitta.....	31
P	<i>Crater Identification and Resolution of Lunar Radar Images</i> H. J. Moore and T. W. Thompson .....	32
T	<i>Venus: Mantle Convection, Hotspots, and Tectonics</i> R. J. Phillips.....	33
P	<i>Radar Scattering from Desert Terrains, Pisgah/Lavic Region, California: Implications for Magellan</i> J. J. Plaut, R. E. Arvidson, and S. Wall.....	35
P	<i>Lakshmi Planum: A Distinctive Highland Volcanic Province</i> K. M. Roberts and J. W. Head .....	37
T	<i>Volcanism on Venus: Large Shields and Major Accumulations of Small "Domes"</i> G. G. Schaber and R. C. Kozak .....	39
T	<i>Impact Cratering and the Surface Age of Venus: The Pre-Magellan Controversy</i> G. G. Schaber, E. M. Shoemaker, C. S. Shoemaker, and R. C. Kozak .....	41

P	<i>Geology of the Venus Equatorial Region from Pioneer Venus Radar Imaging</i> D. A. Senske and J. W. Head.....	43
T	<i>Venus Gravity: Measurements, Reductions and Results</i> W. L. Sjogren.....	45
T	<i>Venus and the Archean Earth: Thermal Considerations</i> N. H. Sleep.....	46
P	<i>Coronae on Venus: Observations and Models of Origin</i> E. R. Stofan .....	47
T	<i>Crustal Deformation: Earth vs. Venus</i> D. L. Turcotte.....	49
P	<i>Eastern Ishtar Terra: Tectonic Evolution Derived from Recognized Features</i> R. W. Vorder Bruegge and J. W. Head.....	50
P	<i>Stress Distribution and Topography of Tellus Regio, Venus</i> D. R. Williams and R. Greeley .....	52
P	<i>Three Ages of Venus</i> C. A. Wood and C. R. Coombs.....	54



## CHARACTERISTICS, DISTRIBUTION AND GEOLOGIC/TERRAIN ASSOCIATIONS OF SMALL DOME-LIKE HILLS ON VENUS

*J.C. Aubele, Dept. of Geol. Sciences, Brown University, Providence, R.I. 02912*

*E.N. Slyuta, Vernadsky Institute, USSR Academy of Sciences, Moscow, U.S.S.R.*

**Introduction.** Approximately 22,000 small dome-like hills have been recognized on the northern 20% of the surface of Venus imaged by Venera 15/16. These features have been described [1] as generally circular in planimetric outline, with a range in basal diameter from the effective resolution of the Venera images (1-2km) up to 20 km.

**General Characteristics.** The small hills have been called domes [1,2] following the lunar nomenclature, because of their broad apparent form. The nomenclature used here, "small dome-like hills", is preferred because of the strict volcanological definition of a dome and terrestrial lithologic connotations. The actual number of these features, and their true range of diameter and modal diameter is unknown; since there is undoubtedly a population, of unknown size, of dome-like hills  $\leq 1$  km that cannot be resolved in the Venera images. The maximum diameter of 20 km is, in a sense, an artificially imposed size range since similar features occur on Venus in the 20 to 100 km diameter range. However the 20 km cutoff reflects a significant change in the overall number of edifices, and in number versus basal diameter frequency distribution. Using diameter measurements in the along-range direction, best estimate modal diameter was determined for a typical cluster of small dome-like hills in Tethus Regio [3]. The 444 total ranged in basal diameter from 2-8 km, with a mode of 3-4 km. Based on constraints on the appearance of features imaged by this radar system, individual dome-like hill slopes are all less than  $10^\circ$ . Assuming these slopes, simple geometric models imply maximum height of approximately 1 km, and average height less than 1 km. Recent radarclinometric data confirms these estimates [4]; profiles of seven small dome-like hills, ranging in basal diameter from 7.2 to 19.2 km, show a slope that is slightly convex near the summit, relatively uniform (maximum slope  $5^\circ$ ) on the flank, and slightly concave (minimum slope  $1^\circ$ ) near the base. The maximum height ranges from 150 to 650 m; and increased height is generally related to increased basal diameter, with some variations. Most of the small dome-like hills show no individually associated features; however, a small number exhibit summit pits, low basal topographic rises or platforms, and radial or lobe-like bright features. Summit pits are infrequently observed in dome-like hills larger in basal diameter than 8 km, and more frequently in ones larger than 15 km. The total number with visible summit pits is less than 5%. Bright circular aureoles, without apparent topographic relief, appear to be associated with small dome-like hills northeast of Atalanta Planitia.

**Dome Distribution.** Slyuta, et al [2,5] have produced dome density contour maps and find that most dome-like hills occur in *groups* of several tens within areas of  $10^3$  km<sup>2</sup>. Adjacent *groups* form *clusters* consisting of 10-20 *groups* within areas of  $10^5$  km<sup>2</sup>. The greatest concentration of *clusters* of dome-like hills occurs in the general area of  $60^\circ\text{N}, 120^\circ\text{E}$ . Major concentrations of *clusters* are located in Tethus Regio ( $65^\circ\text{N}, 110^\circ\text{E}$ ), Atalanta Planitia ( $60^\circ\text{N}, 155^\circ\text{E}$ ), Ananke Tessera ( $55^\circ\text{N}, 138^\circ\text{E}$ ), and Akkriva Colles (from Niobe Planitia,  $35^\circ\text{N}, 130^\circ\text{E}$ , to Allat Dorsa,  $65^\circ\text{N}, 70^\circ\text{E}$ ). In general, these major areas of cluster concentration are approximately equidimensional in areal extent, with the exception of Akkriva Colles which is elongated in the NW-SE directions. Akkriva is also associated with a linear positive gravity anomaly of 25 mgal in the Pioneer Venus data set. The cluster concentrations in Tethus, Ananke and Akkriva are associated with broad regional topographic highs. However, many small groups or clusters of groups occur on low plains or inside circular depressions and the cluster concentration in Atalanta occurs in the general area of the topographically lowest region of Venus. Within a specific cluster, the dome-like hills appear to occur in relatively evenly scattered groups. Counts in a representative cluster in the Tethus Regio region show that overall density of the dome-like hills, within a specific cluster, is  $\approx 0.4/100$  km<sup>2</sup> and maximum density is  $1.0/100$  km<sup>2</sup> [3]. A few dome-like hills appear to exhibit alignment due to minor local structural control, but there is no evidence of large-scale structural control or dominant trend directions.

**Terrain Unit and Geologic Feature Associations.** Almost all of the areas of cluster concentration occur on mottled plains units designated as "rolling plains interpreted to be of volcanic origin" [6]. The outline of the major region of cluster concentration also generally corresponds to the Plains-Corona-Tessera Assemblage described by Head [7]. Major clusters frequently occur on plains units at the margins of areas of tessera, while very small groups occasionally occur in intra-tessera plains near the margins of large tessera units. Where it is possible to evaluate

GEOLOGY OF SOUTHERN GUINEVERE PLANITIA, VENUS, BASED ON ANALYSES OF GOLDSTONE RADAR DATA; R. E. Arvidson, J. J. Plaut, McDonnell Center for the Space Sciences, Department of Earth and Planetary Sciences, Washington University, St. Louis, Missouri 63130, R. F. Jurgens, R. S. Saunders, M. A. Slade, Jet Propulsion Laboratory, Pasadena, California 91103

The ensemble of forty-one backscatter images of Venus acquired by the S Band (12.6 cm) Goldstone radar system covers approximately 35 million square kilometers and includes the equatorial portion of Guinevere Planitia, Navka Planitia, Heng-O Chasma, and Tinatin Planitia, and parts of Devana Chasma and Phoebe Regio. The images and associated altimetry data combine relatively high spatial resolution (1 to 10 km) with small incidence angles (less than 10 degrees) for regions not covered by either Venera Orbiter or Arecibo radar data. Systematic analyses of the Goldstone data show that: (a) Volcanic plains dominate, including groups of small volcanic constructs, radar bright flows on a NW-SE arm of Phoebe Regio and on Ushas Mons and circular volcano-tectonic depressions. The radar bright, flow-like features have length scales similar to those seen in Venera Orbiter and Arecibo data covering Sedna Planitia. The relative abundance of volcanic features is similar to that found in Venera radar images in northern Guinevere Planitia and in Sedna Planitia; (b) Some of the regions imaged by Goldstone have high radar cross sections, including the flows on Ushas Mons and the NW-SE arm of Phoebe Regio, and several other unnamed hills, ridged terrains, and plains areas. While some of the high returns are probably associated with surfaces tilted toward the radar nadir, other regions with high cross sections are not associated with obvious topography and retain high values over a range of incidence angles. These areas expose materials with high dielectric constants. The global trend observed in Pioneer-Venus data, where higher elevations are found to preferentially expose such materials, may be because higher elevations are simply sites of vigorous volcanism and thus maximum exposure of these materials; (c) A 1000 km diameter multiringed structure is observed and appears to have a morphology not observed in Venera data. The northern section corresponds to Heng-O Chasma; (d) A 150 km wide, 2 km deep, 1400 km long rift valley with upturned flanks is located on the western flank of Phoebe Regio and extends into Devana Chasma. The floor has low backscatter values. At the low incidence angles for Goldstone observations, backscatter is controlled by quasi-specular reflections and low returns correspond to surfaces that are rough at length scales many times the radar wavelength. Thus, rifting processes, associated volcanism, and perhaps mass wasting seem to be ongoing processes that continue to generate rough topography; (e) A number of structures can be discerned in the Goldstone data, mainly trending NW-SE and NE-SW, directions similar to those discerned in Pioneer-Venus topography throughout the equatorial region. The structural orientations suggest deformation due to a large-scale stress system. For example, with an appropriately thin lithosphere, equatorial to mid latitude strike-slip faulting may have occurred as the planet's equatorial bulge relaxed as the spin rate slowed to its present value; and (f) The abundance of circular and impact features is similar to the plains global average defined from Venera and Arecibo data, implying that the terrain imaged by Goldstone has typical crater retention ages, measured in hundreds of millions of years. The rate of resurfacing is  $\leq 4$  km/Ga.

## SMALL DOME-LIKE HILLS ON VENUS: Aubele, J.C. and Slyuta, E.N.

the evidence, it appears that the plains, on which the dome-like hills occur, post-date the formation of the tessera terrain. Smaller cluster concentrations occur in regions of predominant arachnoids, in the area between Sedna Planitia and Bell Regio and in the area south of the ridge belt province at 40°N, 215°E; and also occur at Beta Regio. Although domes occur on the plains to the north and south of Ishtar Terra, Lakshmi Planum and the horizontal compressional fold belts [8] of Akna and Freyja Montes exhibit one of the lowest densities of small dome-like hills on Venus. No major concentrations of dome-like hills occur in the major ridge belt areas, although small groups and isolated dome-like hills occur near the ends of a few ridge belts. Small groups of dome-like hills always appear to be associated [9] with the following specific geologic features: (1) coronae - dome-like hills occur predominantly inside the annular concentric ridges of coronae [10]; (2) arachnoids - dome-like hills occur predominantly in the areas of lineations on the plains surrounding and between adjacent arachnoids; (3) intermediate (20-100 km) sized hills interpreted to be volcanic constructs - these generally occur as isolated features on plains units near groups or clusters of small dome-like hills; (4) large volcanic centers ( $\geq 100$  km) - dome-like hills occur predominantly on the lower flanks, or beyond the distal edges, of the bright radial markings associated with these centers; (5) calderas - isolated dome-like hills generally occur on the rims and periphery [11]; and (6) large circular features of uncertain origin - dome-like hills occur predominantly within these features. The spatial association between these specific geologic features and groups of dome-like hills is ubiquitous, even when one of these geologic features occurs in an area with low overall density of small dome-like hills. Geologic mapping provides evidence that formation of the dome-like hills post-dated the development of tessera terrain; may have coincided with the emplacement of plains units interpreted to be volcanic; but may have pre-dated the final development of many large volcanic centers found spatially associated with the dome-like hills.

**Discussion.** Because they are so numerous, the origin and mechanism of formation of the small dome-like hills of Venus is a significant question that has implications for the geologic processes and evolution of the planet. Since many clusters of dome-like hills occur on plains units that are adjacent to, and appear to be younger than, tessera terrain, it is reasonable to question whether they merely represent partially buried and isolated topography. The large number of these features, their randomly scattered occurrence, their consistent circularity, the apparent lack of major structural alignments, and the frequent occurrence of summit pits suggest that the dome-like hills do not merely represent partially flooded pre-existing ridges. Large volcanic features have been previously recognized on Venus, such as the calderas in Lakshmi Planum and the large volcanic edifices associated with Bell Regio. Smooth plains, frequently appearing to embay other terrain units, have been interpreted to be volcanic in origin. Circular features, such as corona or arachnoids, have also been interpreted to be associated in some way with volcanism [8]. In addition, detailed study of the Venera images has resulted in the recognition of approximately 1000 edifices, with diameter  $\geq 20$  km, that are interpreted to be volcanic. As the geologic associations described above have demonstrated, the small dome-like hills of Venus occur spatially associated with other features which are recognized as volcanic or interpreted to be volcanic by other researchers. The dome-like hills can, therefore, be reasonably interpreted to be small volcanic edifices themselves. Examples of small edifices, interpreted to represent predominantly effusive volcanism, occur on Earth in the form of low shield volcanoes and seamounts, and also occur on Mars and Earth's moon. The morphology of volcanic edifices is a complex function of fundamental volcanological properties and variables; however, the general appearance and characteristics of these dominantly effusive volcanic edifices appear to be similar to those of the Venus dome-like hills [3]. The existence of dome-like hills ( $\leq 20$  km), intermediate sized volcanic edifices (20-100 km), and large volcanic centers ( $\geq 100$  km) implies a continuum of volcanic edifices on Venus. There is a distinct distribution of number versus size range such that the number of edifices increases as the size decreases; this is similar to that observed for volcanic edifices on Earth.

**References.** [1] Barsukov, V.L. et al, 1986, Proc. LPSC XVI, JGR, 91, B4, D378; [2] Slyuta, E.N., et al, 1988, LPSC XIX (Abst), 1097; [3] Aubele, J.C., et al, 1988, LPSC XIX (Abst), 21; [4] Sinilo and Slyuta, 1989, LPSC XX (Abst), 1016; [5] Slyuta, E.N., et al, 1988, *Aston. Vestnik*, 22, #4, 287 (in Russian); [6] Barsukov, V.L and Basilevsky, A., 1986, *Piroda*, 24; [7] Head, J.W., 1989, LPSC XX (Abst), 392; [8] Crumpler, L.S., et al, 1986, *Geology*, 14, 1031; [9] Aubele, J.C., 1989, LPSC XX (Abst), 28; [10] Stofan, E.R. and Head, J.W., 1989, Submitted to *Icarus*; Stofan, E.R. and Head, J.W., 1988, LPSC XIX (Abst), 1127; [11] Magee, K.P. and Head, J.W., 1988, LPSC XIX (abst), 711 and 713; Roberts, K.P.M. and Head J.W., 1989, LPSC XX (abst), 910.

## Tessera Terrain: Characteristics and Models of Origin.

D.L. Bindschadler, and J.W. Head, Brown University Dept. of Geological Sciences,  
Providence, RI, 02912 (SPAN BRNPSG::BINDSCH)

Tessera terrain consists of complexly deformed regions characterized by sets of ridges and valleys that intersect at angles ranging from orthogonal to oblique [1], and were first viewed in Venera 15/16 SAR data. Tesserae cover more area (~15% of the area north of 30°N) than any of the other tectonic units mapped from the Venera data [2,3] and are strongly concentrated in the region between longitudes 0° E and 150° E. Tessera terrain is concentrated between a proposed center of crustal extension and divergence in Aphrodite [4,5] and a region of intense deformation [6], crustal convergence, and orogenesis in western Ishtar Terra [7,8]. Thus, the tectonic processes responsible for tesserae are an important part of Venus tectonics. As part of an effort to understand the formation and evolution of this unusual terrain type, we have compared the basic characteristics of the tesserae to the predictions made by a number of tectonic models. Here we describe the basic characteristics of tessera terrain and then briefly discuss the models and some of their basic predictions.

### Observational Data

**Altimetry and Surface Roughness:** Pioneer Venus data show that the regions tessera lie at higher elevations than surrounding plains, are typically plateau-like in topographic cross section, and are characterized by high values of rms slope [3] (a measure of roughness at a scale of ~0.5 m to 10's of m) [9,10]. Tesserae are also characterized by greater cm-scale roughness than the plains which we interpret to be due to erosion linked to extensive deformation and possibly to greater relative age [11]. Craters are sufficiently sparse to make determination of the relative age of the tesserae unreliable [12].

**Gravity Anomalies:** For the largest regions of tessera, line of sight (LOS) gravity data may be used to infer depths of compensation. Of the three largest regions of tessera (Tellus Regio, Laima Tessera and Fortuna Tessera) LOS gravity data extend far enough north for Tellus, partly cover Laima Tessera, and do not cover Fortuna Tessera. Anomalies associated with the ~2.5 km of topography in Tellus are < 5 mgal, leading Sjogren et al. [13] to suggest that the region is compensated at shallower depths than most large-scale uplands in the equatorial region. Anomaly values over Laima Tessera are also < 5 mgal [13].

**Morphology:** Examination of Venera data for the large regions of tessera reveals three morphologic subtypes for the terrain. These are the sub-parallel ridged terrain ( $T_{SR}$ ), trough and ridge terrain ( $T_{TR}$ ), and disrupted terrain ( $T_{DS}$ ).

The sub-parallel ridged terrain ( $T_{SR}$ ) is similar to ridge belts in that it consists of sub-parallel ridges. However,  $T_{SR}$  ridges are less sinuous and do not intertwine. Ridges tend to be disrupted along linear zones of consistent orientation and often form an echelon groups, perhaps indicating strike-slip offset. The three structural orientations are consistent with compression (ridges) and conjugate strike-slip or shear motion (lineations). Type locale: Fortuna Tessera, east of Maxwell Montes.

Structures in the trough and ridge terrain ( $T_{TR}$ ) are expressed as troughs in one direction and as ridges and/or valleys with approximately orthogonal orientations. Troughs appear both as broad (~50km) and narrow (< 20 km) structures. Ridges occasionally show an echelon offset and tend to be spaced approximately 5 to 10 km apart. Troughs are spaced at least 10-20 km). Type locale: Eastern Laima Tessera

The disrupted terrain ( $T_{DS}$ ) is characterized by a general lack of continuous ridges or valleys longer than ~50 km. The terrain is often blocky to chaotic in appearance, depending upon the consistency of ridge orientations. Even if ridge orientations are chaotic, lineations defined by short troughs, ridges and by discontinuities in ridges preserve consistent orientations over the region of tessera. Disrupted terrain is usually transitional with the  $T_{TR}$  or  $T_{SR}$ . Type locale: Central Tellus Regio.

Contacts between tessera and plains are characterized by two types of boundaries. In Type I boundaries, the contact is highly irregular at the 100 km scale, consisting of numerous ovoidal to polygonal plains regions that often separate small regions of tessera from the main body of a block. Structures within the tessera take on a subdued appearance near the boundary and show little relation to the shape of the tessera-plains boundary. Type I boundaries thus appear to be an expression of embayment of the tessera by plains-forming materials. Type II boundaries are much more regular at the 100 km scale and typically characterized by the presence of the  $T_{SR}$  subtype of tessera as well as steep topography and the presence of small ridges or ridge belts within the adjacent plains. These boundaries appear to be places where the tesserae have formed at the expense of the plains.

## Models

A number of models have been suggested for the formation of tessera terrain [2,14,15]. From these and other tectonic models, we set forth working hypotheses for the formation of tessera, which are divided into three formational models (those which produce the high topography of the tessera) and two modificational models (those in which deformation results from high topography).

**Horizontal convergence and crustal thickening** may be driven by in-plane lithospheric stresses (as on Earth) or by flow within the mantle of Venus [16,17]. In general, convergent motion is expected to result in high topography, steep topographic slopes, and fold-and-thrust deformation at the surface. Crustal compensation of topography should result in a relatively small LOS anomaly over regions of tessera, given predicted crustal thicknesses for Venus of  $\leq 30$  km [18]. In addition, both strike-slip and extensional deformation are observed in terrestrial orogens such as the India-Asia collision and the Andean orogen, and might also be expected to occur on Venus

**Mantle upwelling** may be manifested as the upwelling limb of a convection cell, a long-lived hotspot, or a diapir-like body. Such an upwelling will result in the formation of a dome-shaped region of high topography, characterized by extensional deformation, and possibly by volcanism [19]. Relatively large LOS gravity anomalies are anticipated, unless the characteristic depth of the source is quite shallow. Numerous workers have identified Beta, Bell, and Atla Regiones as likely surface manifestations of mantle upwelling. Such regions are thus likely to represent some part of the evolution of any tessera formed due to upwelling.

**Seafloor spreading** or an analogous process is suggested to occur within Aphrodite Terra [5] and to be responsible for the structural fabric of Laima Tessera [20]. On Earth, seafloor spreading results in the formation of an approximately orthogonal structural fabric consisting of transform faults and fracture zones in one direction, and abyssal hill topography in the other. Tessera formed near Aphrodite and transported north is predicted to be old compared to the undeformed plains that surround it. High topography is explained as being due to a relatively thick crust, suggesting that topography at plains-tessera contacts should be gently sloping. Steep topography might be expected to occur at transforms due to juxtaposition of lithosphere of different ages and to thermal stress-supported bending of plate segments [21]. Finally, a common feature of the terrestrial ocean floor are volcanic seamounts, which may be observable as small domes on the surfaces produced by a spreading process.

**Gravity sliding** is defined here as a thin-skinned, predominantly brittle process involving the downslope movement and deformation of a wedge of material above a decollement. This process is expected to produce extensional features (e.g. a detachment fault) at or near local topographic highs, with structures becoming increasingly compressional toward local topographic lows. If topographic slopes are approximately radial about the highest topography, radial graben would also be expected to form, as observed in the aureole surrounding Olympus Mons on Mars [22].

**Gravitational relaxation** of compensated topography is distinguished from gravity sliding as a predominantly ductile process driven by gradients in vertical normal stress due to surface and/or crust-mantle boundary topography. In the case of crustally compensated topography, calculations predict extension of high topography and increasingly compressional deformation toward the edges of a topographic high. Highest rates of extension occur at the highest elevations, but extension may occur even in relative lows if they lie above the level of the surrounding plains. If the high topography of the tessera is due to uplift rather than crustal thickness variations, a somewhat different scenario is predicted, see [19].

## References

- [1] Basilevsky, A.T., et al., *JGR* **91**, D399-D411, 1986; [2] Sukhanov, A.L., Sukhanov, A. L., *Geotectonics* **20**, 294-305, 1986; [3] Bindschadler, D.L. and J.W. Head, *Icarus* **77**, p. 3-20, 1989; [4] Schaber, G.G., *GRL* **9**, 499-502, 1982; [5] Head, J. W., Crumpler, L. S., *Science* **238**, 1380-1385, 1987; [6] Pronin, A.A., *Geotectonics* **20**, 54-59, 1986; [7] Campbell, D.B., et al., *Science* **221**, 644-647, 1983; [8] Crumpler, L.S., et al., *Geology* **14**, 1031-1034, 1986; [9] Pettengill, G., et al., *JGR* **85**, 8261-8270, 1980; [10] Head, J.W., et al., *JGR* **90**, 6873-6885, 1985; [11] Bindschadler, D.L., and J.W. Head, *Earth Moon Planets* **42**, 133-149, 1988; [12] Ivanov, B.A., et al., *JGR* **91**, D413-D430, 1986; [13] Sjogren, W.L., et al., *JGR* **88**, p. 1119-1128, 1983; [14] Basilevsky, A. T., *Geotektonika* **20**, 282-288, 1986; [15] Kozak, R.C. and G.G. Schaber, *Lunar Planet Sci. XVII*, 444-445, 1986; [16] Phillips, R.J., *GRL* **13**, 1141-1144, 1986; [17] Bindschadler, D.L. and E.M. Parmentier, *EOS Trans. AGU* **69**, 1450, 1988; [18] Zuber, M. T., *JGR* **92**, E541-E551, 1987; Grimm, R.E. and S.C. Solomon, *JGR* **93**, 11911-11929, 1988; [19] Bindschadler, D.L. and E.M. Parmentier, *Lunar Planet. Sci. XX*, 78-79, 1989; [20] Head, J.W., *Lunar Planet. Sci. XX*, 394-395, 1989; [21] Haxby, W.F., and E.M. Parmentier, *JGR* **93**, 6419-6429, 1988; [22] Francis, P.W. and G. Wadge, *JGR* **88**, 8333-8344, 1983;

**DIVERGENT PLATE BOUNDARIES AND CRUSTAL SPREADING ON VENUS:  
EVIDENCE FROM APHRODITE TERRA.** L.S.Crumpler and J.W.Head, *Department of Geological Sciences, Brown University, Providence, RI 02912*

**Introduction.** The modes of lithospheric heat transfer and the tectonic styles may differ between Earth and Venus, depending on how the high surface temperature ( $700\text{K} = 430^\circ\text{C}$ ), dense and opaque atmosphere ( $\sim 10\text{ MPa} = 100\text{ bars}$ ), lack of water oceans, and the other known ways in which Venus differs from Earth, influence basic lithospheric processes, thermal gradient, upper mantle temperature, thermal and chemical evolution, and convection. A fundamental question is whether the lithosphere of Venus is horizontally stable, like the other terrestrial planets, or is mobile like that on Earth. Previous studies have suggested on the basis of the presence of rift-like topography [1, 2] that Aphrodite Terra may be a zone of relatively recent lithospheric extension and potential volcanism. Large positive correlations between gravity and topography [3] similarly suggest that the current topography is supported dynamically by mantle convection perhaps with associated volcanism [4,5,6]. Tectonic deformation in these models is mainly vertical and the crustal extension is limited, representing either traction from mantle convection beneath [7] or rifting resulting from stresses associated with gravitational spreading of high-standing regional topography [8, 9]. Recently, the detailed characteristics of Aphrodite Terra and the equatorial highlands have been analyzed and interpreted to be analogous to divergent plate boundaries on Earth [9, 10, 11, 12], a model which is distinguished primarily by the requirement of large horizontal motions of the surface and lithosphere similar to that associated with plate tectonics on Earth. This interpretation is based on (a) the presence of linear discontinuities crossing the approximately east-west strike of Aphrodite Terra with many of the characteristics of oceanic fracture zones, (b) bilateral symmetry in directions parallel to these linear discontinuities similar to that associated with (i) evolving thermal boundary layers and (ii) splitting and separating of features along rise crests by crustal spreading at divergent boundaries, and (c) a variety of map [11] and geophysical [13] relationships consistent with the presence of features linked to both crustal spreading and the thermal evolution of lithosphere migrating over great distances laterally away from a zone of extension and crustal creation.

**Crustal Spreading and Plate Boundary Characteristics.** Zones of crustal spreading and divergent plate boundary characteristics display organized relationships, many of which may be predicted on the basis of the existence of rise crest offsets at transform faults and fracture zones in the presence of horizontal divergent motions of a thermal boundary layer. If Western Aphrodite Terra represented processes similar to a spreading center and divergent plate boundary, we would expect to see (i) a broad symmetric altimetry associated with a thermal boundary layer in which regional symmetry and overall altimetry may be approximated as a surface which descends as the square root of distance and at a rate consistent with the form of a thermal boundary layer, (ii) offset of this symmetry at nearly right angles along linear transform faults, (iii) continuation of the transform zone beyond the offset ends of the rise crest as fracture zones, (iv) regional step up or down in altimetry of the surface across the CSD's depending on the sense of the rise crest offset, and (v) differences between the detailed features of the surfaces in adjacent rise crest segments which are (vi) individually symmetric about the rise crest and the result of splitting and drifting apart of topography associated with anomalous crustal production.

**Observed Characteristics of Aphrodite Terra.** These predicted characteristics of the organized relationship between divergent plate boundaries processes may be compared with observed altimetric and radar image characteristics in Western Aphrodite Terra which include (i) broad symmetry which is quantitatively similar to that predicted for thermal boundary layer topography [14, 15, 16] diverging at rates of a few centimeters per year in the environment of Venus [17, 18]. Least squares analysis of altimetric profiles show that the plateau-like highlands of Western Aphrodite are similar also in slope to adjacent lowlands and differ mainly in absolute altitude (Fig. 2). This symmetry occurs along linear axes and is also frequently (ii) offset at right angles along through-going and linear and parallel discontinuities (CSD's) which (iii) can be traced for several thousand kilometers across the highlands and into the surrounding lowlands. Altimetric profiles in the lowlands across the CSD's show that there is frequently a (iv) regional altimetric step up or down across the CSD's depending on whether the horizontal sense of offset across the CSD moves the rise crest closer or farther away respectively. Removal of the broad symmetry of a thermal boundary layer from the altimetric profiles across Aphrodite Terra results in a (v) residual short wavelength topography which is shown to be symmetric about the same symmetry axis (Fig. 3), and (vi) which differs in character from one domain to the next.

**Conclusions.** The variety of characteristics, their detailed integrated relationships, and their predictable behavior throughout Western Aphrodite Terra are similar to those features known to occur in association with the terrestrial seafloor at spreading centers and divergent plate boundaries. We conclude that Western Aphrodite Terra represents the site of crustal spreading and displays many of the characteristics of divergent plate boundaries [11]. The extent of similar characteristics and processes elsewhere on Venus outside of the 13,000 km long Western and Eastern Aphrodite Terra rise is unknown at the present, but their presence in other areas of the equatorial highlands, suggested from recent analysis [12], may be tested with forthcoming Magellan data.

DIVERGENCE/CRUSTAL SPREADING: Crumpler, L.S., and Head, J.W.

**References:** [1] Schaber, G.G, 1982, *Geophys. Res. Lett.*, 9, 499-502; [2] McGill, G.E. et al., 1983, *Venus, Hunten et al. eds., U. Az. Press*, 69-130; [3] Sjogren, W.L. et al., 1983, *J. Geophys. Res.*, 88, 1119-1128; [4] Kiefer, W.S. et al., 1986, *Geophys. Res. Lett.*, 13, 14-17; [5] Banerdt, W.B., 1986, *J. Geophys. Res.*, 91: 403-419; [6] Morgan, P., and R.J. Phillips, 1985, *J. Geophys. Res.*, 88: 8305-8317; [7] Phillips, R.J., 1986, *Geophys. Res. Lett.*, 13: 1141-1144; [8] Smrekar, S. and R.J. Phillips, 1988, *Geophys. Res. Lett.*, 15: 693-696; [9] Crumpler, L.S. et al., 1987, *Venus. Geophys. Res. Lett.*, 14: 607-610; [10] Crumpler, L.S., and J.W. Head, 1988, *Venus. J. Geophys. Res.*, 93: 301-312; [11] Head, J.W., and L.S. Crumpler, 1987, *Science*, 238: 1380-1385; [12] Head, J.W., and L.S. Crumpler, 1989, *Earth. Moon Planets*, in press; [13] Sotin, C. et al., 1989, *Earth Planet. Sci. Letts.*, submitted; [14] Davis, E.E., and C.R.B. Lister, 1974, *Earth and Planet Sci. Lett.*, 21: 405-413; [15] Parker, R.L., and D.W. Oldenburg, 1973, *Nature*, 242: 137-139; [16] Parsons, B., and J.G. Sclater, 1977, *J. Geophys. Res.*, 82: 803-827; [17] Kaula, W.K., and R.J. Phillips, 1981, *Geophys. Res. Lett.*, 8: 1187-1190; [18] Phillips, R.J., and M.C. Malin, 1983. In *Venus*, edited by D.M. Hunten, et al., University of Arizona Press, Tucson: 159-214.

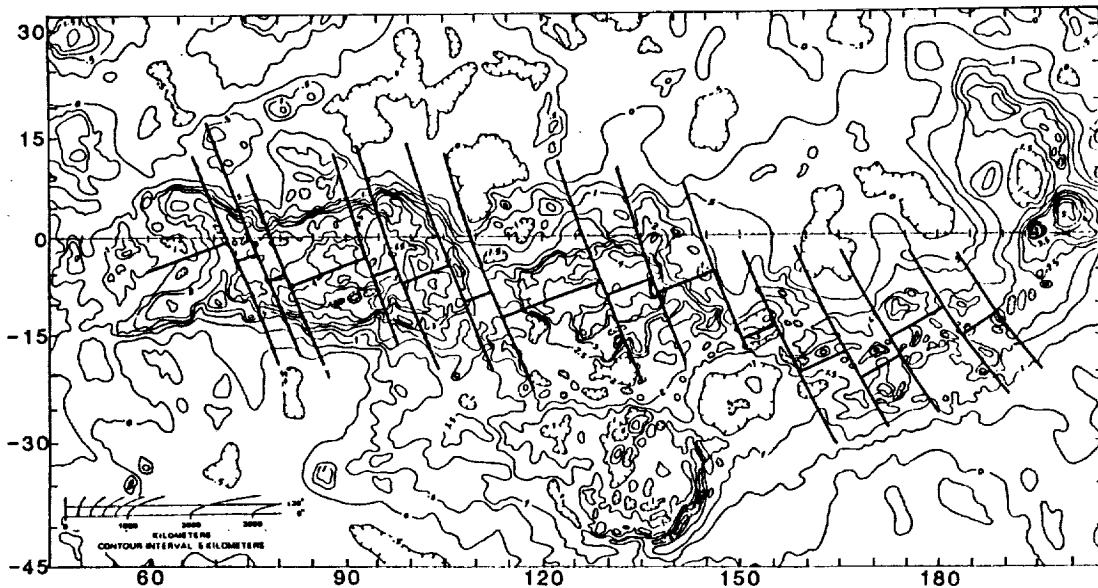


Figure 1. Altimetric map of Aphrodite Terra showing location of identified CSD's and axes of bilateral symmetry.

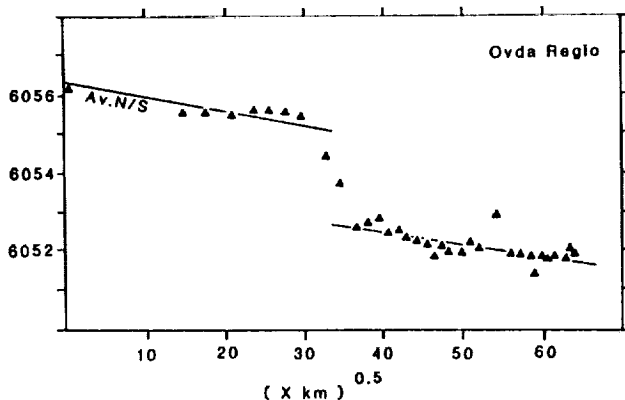


Figure 2. Example of altimetry in direction parallel to CSD's plotted as a function of the square root of distance. Lines are best fitting linear trend through the data for the highlands and lowlands evaluated separately.

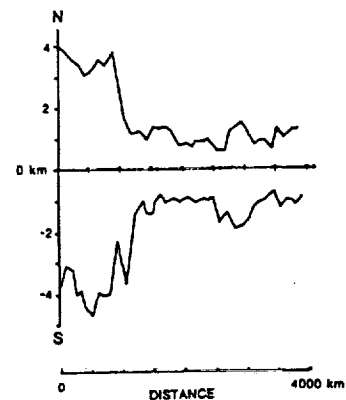


Figure 3. Example of residual altimetry after removal of the thermal boundary layer-like component,  $f(X^{0.5})$ . The data from the north and south flanks are plotted together, one inverted beneath the other.

VENUS VOLCANISM: RATE ESTIMATES FROM LABORATORY STUDIES OF SULFUR GAS-SOLID REACTIONS. K. Ehlers, B. Fegley, Jr., and R.G. Prinn, Department of Earth, Atmospheric, and Planetary Sciences, Massachusetts Institute of Technology, Cambridge, MA 02139

Thermochemical reactions between sulfur-bearing gases in the atmosphere of Venus and calcium-, iron-, magnesium-, and sulfur-bearing minerals on the surface of Venus are an integral part of a hypothesized cycle of thermochemical and photochemical reactions responsible for the maintenance of the global sulfuric acid cloud cover on Venus (1-3). As schematically illustrated in Figure 1, SO<sub>2</sub> is continually removed from the Venus atmosphere by reaction with calcium-bearing minerals on the planet's surface. Maintenance of the global H<sub>2</sub>SO<sub>4</sub> clouds, which are formed by the ultraviolet-sunlight-powered conversion of SO<sub>2</sub> into H<sub>2</sub>SO<sub>4</sub> cloud particles (4), requires a comparable sulfur source to balance this SO<sub>2</sub> sink. The most plausible endogenic source is volcanism, which has occurred on Venus in the past (5), and which may have led to increased SO<sub>2</sub> levels above the Venus cloud-tops observed by the Pioneer Venus orbiter (6,7). The rate of volcanism required to balance SO<sub>2</sub> depletion by reactions with calcium-bearing minerals on the Venus surface can therefore be deduced from a knowledge of the relevant gas-solid reaction rates combined with reasonable assumptions about the sulfur content of the erupted material (gas + magma).

We are carrying out a laboratory program to measure the rates of reaction between SO<sub>2</sub> and possible crustal minerals on Venus. At present we have studied the reaction CaCO<sub>3</sub>(calcite) + SO<sub>2</sub> → CaSO<sub>4</sub> (anhydrite) + CO (see Figure 2). Experimental details and preliminary results have been given by Fegley (8) and Fegley and Prinn (9). We find that the temperature dependence of the reaction is given by the equation  $R = 10^{19.64(\pm 0.28)} \exp(-15,248(\pm 2970)/T)$  molecules cm<sup>-2</sup>s<sup>-1</sup> and that the reaction rate exhibits no statistically significant variation with either O<sub>2</sub> or CO<sub>2</sub> partial pressure. If this reaction rate represents the SO<sub>2</sub> reaction rate with calcium-bearing minerals on the Venus surface (an assumption which we are currently investigating by studying SO<sub>2</sub> reactions with other minerals such as anorthite and diopside) then all SO<sub>2</sub> (and thus the clouds) in the Venus atmosphere will disappear in 1.9x10<sup>6</sup> years unless volcanism replenishes the lost SO<sub>2</sub>. The Venus surface composition at the Venera 13, 14, and Vega 2 landing sites implies a volcanism rate of approximately 1 km<sup>3</sup> yr<sup>-1</sup>; a range of 0.4-11 km<sup>3</sup>yr<sup>-1</sup> is implied by assuming S/Si ratios appropriate for ordinary chondrites or for the terrestrial crust (9).

Acknowledgments. This work was originally supported by the NASA Innovative Research Program and by NSF Grant No. ATM-87-10102 to MIT.

References. (1) R.G. Prinn (1985) in Recent Advances in Planetary Meteorology, ed. G.E. Hunt, Cambridge Univ. Press, pp. 1-15. (2) R.G. Prinn (1985) in The Photochemistry of Atmospheres, ed. J.S. Levine, Academic Press, pp. 281-336. (3) R.G. Prinn (1985) Scientific American 252, 46-53. (4) L.W. Esposito et al. (1983) in Venus, ed. D.M. Hunten et al., Univ. of Arizona Press, pp. 474-564. (5) A.T. Basilevsky and J.W. Head (1988) Ann. Rev. Earth Planet. Sci. 16, 295-317. (6) L.W. Esposito (1984) Science 223, 1072-1074. (7) L.W. Esposito et al. (1988) J. Geophys. Res. 93, 5267-5276. (8) B. Fegley, Jr. (1988) Lunar Planet. Sci. XIX, 315-316. (9) B. Fegley, Jr. and R.G. Prinn (1989) Nature 337, 55-58.

## VENUS VOLCANISM K. Ehlers, B. Fegley, Jr. R.G. Prinn

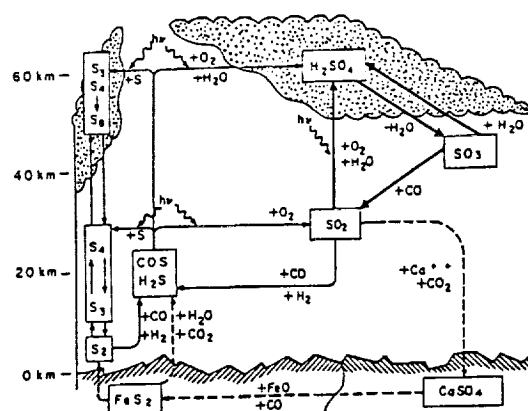


Figure 1. The cycle of sulfur compounds in the Venusian atmosphere (Prinn 1985). Volcanic eruptions or reactions of  $\text{H}_2\text{O}$  and  $\text{CO}_2$  with volcanic surface rocks yields  $\text{COS}$ ,  $\text{H}_2\text{S}$ ,  $\text{S}_2$ , and  $\text{SO}_2$ . Various photochemical reactions convert these species to concentrated  $\text{H}_2\text{SO}_4$  or elemental sulfur particles in the Venusian clouds. The  $\text{H}_2\text{SO}_4$  evaporates at the cloud base, producing  $\text{SO}_3$ , which can then either recondense or be reduced to  $\text{SO}_2$ . Reactions of  $\text{SO}_2$  with  $\text{Ca}^{2+}$  in rocks provides a sink that must be balanced by the volcanic and surface sources.

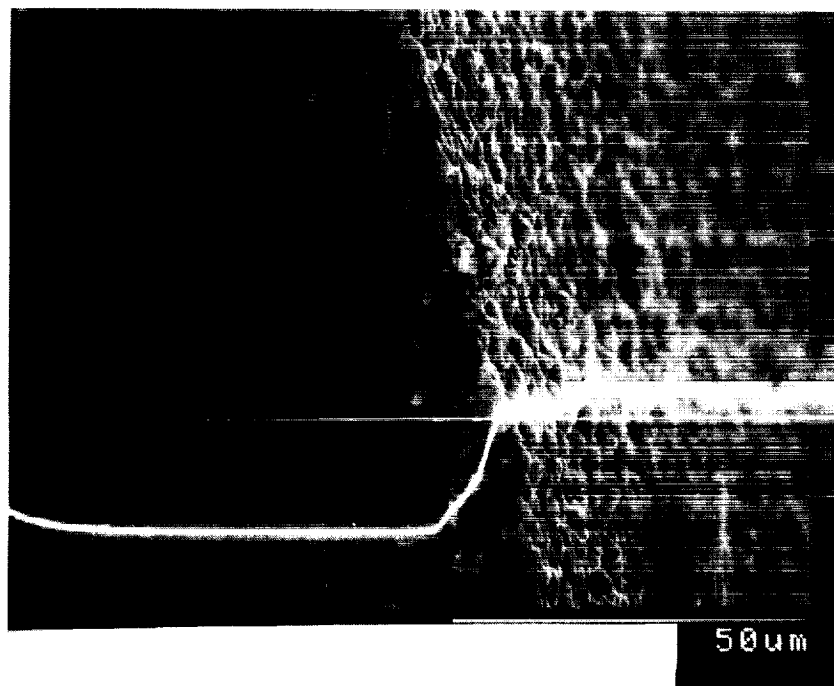


Figure 2. Scanning electron micrograph of the fracture surface of a reacted calcite crystal. The scale bar is 50 micrometers long. The horizontal white line on the micrograph shows the position of an X-ray line scan for the element sulfur. The wavy white line shows that sulfur X-rays are produced only at the reacted surface where grains of the mineral anhydrite ( $\text{CaSO}_4$ ) are formed as a result of the gas-solid reaction.

ORIGINAL PAGE  
BLACK AND WHITE PHOTOGRAPH

POTENTIAL FOR OBSERVING AND DISCRIMINATING IMPACT CRATERS AND COMPARABLE VOLCANIC LANDFORMS ON MAGELLAN RADAR IMAGES. J.P.Ford, Jet Propulsion Laboratory, California Institute of Technology, Pasadena, California 91208.

Observations of small terrestrial craters by Seasat synthetic-aperture radar (SAR) at high resolution (~25 m) and of comparatively large Venusian craters by Venera 15 and 16 images at low resolution (1000-2000 m) and shorter wavelength show similarities in the radar responses to crater morphology. At low incidence angles ( $< \sim 15$  deg), the responses are dominated by large-scale slope effects on the order of meters; consequently it is difficult to locate the precise position of crater rims on the images. Abrupt contrasts in radar response to changing slope (hence incidence angle) across a crater produce sharp tonal boundaries normal to the illumination. Crater morphology that is radially symmetrical appears on images to have bilateral symmetry parallel to the illumination vector. Craters are compressed in the distal sector and drawn out in the proximal sector. At higher incidence angles ( $> \sim 35$  deg) obtained with the viewing geometry of SIR-A, crater morphology appears less compressed on the images.

At any radar incidence angle, the distortion of a crater outline is minimal across the medial sector, in a direction normal to the illumination. Only the medial sector may yield an accurate measure of the diameter, provided there is sufficient contrast to locate the crater rim. It is important in radar images to distinguish between departures from crater circularity that are real and image distortion that relates to the scene illumination.

Radar-bright halos surround some craters imaged by SIR-A and by Venera 15 and 16. The brightness probably denotes the radar response to small-scale surface roughness of the surrounding ejecta blankets [1, 2, 3]. In some cases the halos appear to be bilaterally symmetrical about an axis that parallels the illumination vector, with reduced brightness from the foreslopes to the backslopes.

Similarities in the radar responses of small terrestrial impact craters and volcanic craters of comparable dimensions (~ 2 km diameter, observed by Seasat SAR and SIR-A) emphasize the difficulties in discriminating an impact origin from a volcanic origin in the images [4]. Similar difficulties will probably apply in discriminating the origin of small Venusian craters, if they exist.

Because of orbital considerations, the nominal incidence angle of Magellan radar at the center of the imaging swath will vary from about  $45^\circ$  at  $10^\circ$  N latitude to about  $16^\circ$  at the north pole and at  $70^\circ$  S latitude. At latitudes from  $20^\circ$  N to  $10^\circ$  S the viewing geometry will approach the SIR-A configuration. North of  $60^\circ$  N and south of  $40^\circ$  S the viewing geometry will be analogous to Seasat SAR. At the latitudinal extremities of imaging in both hemispheres the viewing geometry will approach the Venera 15 and 16 configuration. With this variable viewing geometry, radially symmetrical landforms on Magellan images can be expected to show outlines that vary with latitude. Impact craters and comparable volcanic landforms will show bilateral symmetry parallel to the illumination vector and will appear increasingly compressed toward higher latitudes.

#### REFERENCES

- [1] Lambert, Ph. et al., 1980, *Meteoritics*, 15, 157-178; [2] Ivanov, B.A. et al., 1986, *Jour. Geophysical Research*, 91 (B4), D413-D430; [3] Basilevsky, A.T. et al., 1987, *Jour. Geophysical Research*, 92, (B12) 12869-12901; [4] Greeley, R. et al., 1987, *Earth, Moon and Planets*, 37, 89-111.

CONTRASTING LANDFORM PERCEPTION WITH VARIED RADAR ILLUMINATION GEOMETRIES AND AT SIMULATED RESOLUTIONS OF VENERA AND MAGELLAN. J.P.Ford, Jet Propulsion Laboratory, California Institute of Technology, Pasadena, California 91208, and R.E.Arvidson, Department of Earth and Planetary Sciences, Washington University, St. Louis, Missouri 63130..

The high sensitivity of imaging radars to slope at moderate to low incidence angles enhances the perception of linear topography on images. It reveals broad spatial patterns that are essential to landform mapping and interpretation. As radar responses are strongly directional, the ability to discriminate linear features on images varies with their orientation. Landforms that appear prominent on images where they are transverse to the illumination may be obscure to indistinguishable on images where they are parallel to it. Linear features should be examined carefully because faults and other features such as dipping strata, dikes or linear joint patterns may be expressed in a similar manner on images [1]. In the absence of relief, nontopographic lineaments may appear in response to local contrasts of small-scale surface roughness [2]. In the case of sand dunes, radar responses are rigorously constrained by specific angular relations between the illumination and the orientation and angle of repose of dune faces [3].

Landform detection is also influenced by the spatial resolution in radar images. Seasat radar images of the Gran Desierto Dunes complex, Sonora, Mexico; the Appalachian Valley and Ridge Province; and accreted terranes in eastern interior Alaska were processed to simulate both Venera 15 and 16 images (1000 to 3000 km resolution) and image data expected from the Magellan mission (120 to 300 m resolution) [4]. The Gran Desierto Dunes are not discernable in the Venera simulation, whereas the higher resolution Magellan simulation shows dominant dune patterns and specular reflections from dune faces oriented normal to the radar illumination. Antiforms and synforms are evident in both simulations over the Appalachians largely because of patterns produced from differential erosion of the rocks. The Magellan simulation also shows that fluvial processes have dominated erosion and exposure of the folds. Mountainous terrains and their degree of erosion are discernable in both simulations over Alaska, although the Magellan simulation shows that fluvial, glacial, and eolian processes have all been active in shaping the landscape. Neither simulation provides evidence that diverse lithotectonic terranes in Alaska were juxtaposed (i.e. accreted), since the primary evidence needed is lithological, whereas radar returns are dominated primarily by topography and small-scale surface roughness.

#### REFERENCES

- [1] Ford, J.P., 1980, *Amer. Assoc. Petroleum Geologists Bull.*, 64, 2064-2094; [2] Sabins, F.F., et al., 1980, *Amer. Assoc. Petroleum Geologists Bull.*, 64, 619-628; [3] Blom, R.G., 1988, *Int. Jour. Remote Sensing*, 9, 945-965; [4] Arvidson, R., et al., 1988, *Icarus*, 75, 163-181.

VENUS SURFACE PROPERTIES DEDUCED FROM RADAR AND RADIOMETRY;  
P. G. Ford, MIT Center for Space Research, Cambridge, Mass. 02139

The brightness of surface features on side-looking radar images of Venus is determined by many factors: the angles of incidence and reflection, polarization, surface geometry and composition, and so forth. The contribution from surface properties themselves can only be deduced by combining several types of measurement. For instance, without additional information, it is impossible to distinguish the effects of changes in surface roughness from those in dielectric constant.

In common with the Moon and Mars, the surface of Venus appears to scatter radar waves in two ways: small-scale surface inhomogeneities, i.e. those smaller than the incident wavelength, depolarize and scatter the energy over a wide range of angles. The Pioneer results are best described by Muhleman's (1) phenomenological function  $\sigma_m(\theta) = (0.0188 \cos\theta)/(\sin\theta + 0.111 \cos\theta)^3$ , where  $\theta$  is the angle of incidence. When  $\theta$  is less than about  $20^\circ$ , a different mechanism dominates—quasi-specular scattering from numerous surface "facets". The scattering cross section from this mechanism depends on the distribution of the tilts of these facets. Pioneer results tend to confirm the Hagfors model (2) in which surface heights obey a gaussian distribution, while tilts are correlated exponentially, leading to a scattering cross-section  $\sigma_h(\theta) = \frac{1}{2}C\rho (\cos^4\theta + C\sin^2\theta)^{3/2}$ .  $C$  corresponds to the inverse of the mean square of the distribution of meter-scale surface slopes, in radians, and  $\rho$  is the bulk Fresnel reflectivity of the surface material.

The Pioneer Venus radar mapper experiment made three overlapping sets of measurements of the equatorial region of Venus from  $15^\circ\text{S}$  latitude to  $45^\circ\text{N}$ —the backscatter cross section at a range of incidence angles, the shape and intensity of radar echoes from the nadir, and the microwave brightness temperature of the surface (3). For each element of the surface, these measurements have been combined as follows—(a) backscatter measurements at several incidence angles serve to locate the datum on the Muhleman curve and determine that fraction of the surface,  $\alpha$ , that is rough at the small scale; (b) the reflectivity  $\rho$  derived from fitting nadir echoes to the Hagfors curve may be corrected for the incident energy lost through diffuse scattering; (c) this correction may be verified from the radiometer measurements of the surface emissivity,  $e$ , since, for sufficiently rough surfaces,  $\rho = (1-e)$ ; (d) finally, the bulk surface dielectric constant,  $\epsilon$ , may be computed from the relation  $\rho = |(\epsilon-1)/(\epsilon+1)|^2$ .

These techniques developed during the analysis of Pioneer Venus data will be used during the Magellan mission to extract measurements of surface slopes and dielectric constants over all areas covered by the SAR and altimeter antennae, with a resolution of about 10 km. A knowledge of the mechanisms that govern surface scattering will also be useful in the analysis of higher resolution side-looking radar images, particularly in distinguishing the effects of changing roughness from those caused by a long-range surface tilt or changing dielectric constant.

<sup>1</sup> Muhleman, D. O., Radar Scattering from Venus and the Moon, *Astron. J.*, 69, 34-41, 1969.

<sup>2</sup> Hagfors, T. A., A study of the depolarization of lunar surfaces, *Radio Sci.*, 2, 445-465, 1967.

<sup>3</sup> Pettengill, G. H., P. G. Ford, and B. D. Chapman, Venus: Surface Electromagnetic Properties, *J. Geophys. Res.*, 93, B12, 14881-14892, 1988.

**A Morphologic Study of Venus Ridge Belts:** S.L. Frank and J.W. Head, Department of Geological Sciences, Brown University, Providence, RI, 02912

Ridge belts, first identified in the Venera 15/16 images [1,2] are distinguished as linear regions of concentrated, parallel to anastomosing ridges. They are tens to several hundreds of km wide, hundreds to over one thousand km long, and composed of individual ridges 5-20 km wide and up to 200 km long. The ridges appear symmetrical in the radar images and are either directly adjacent to each other or separated by mottled plains. Cross-strike lineaments, visible as dark or bright lines, are common within the ridge belts, and some truncate individual ridges. In places the ridge belt may be offset by these lineaments, but such offset is rarely consistent across the ridge belt. The angle between the lineaments and the ridge belts is usually 30° to 90°. Localized plains units from several km to 100's of km wide are bounded by arcuate ridges, forming elliptical-shaped plains regions within the ridge belts. Between 0°E and 90°E in the Tessera-Ridge Belt assemblage [3], the ridge belts form an orthogonal pattern surrounding large blocks of tesserae, while in the Plains-Ridge Belt assemblage, between 150°E and 250°E, the belts trend predominantly N-S, occasionally coalescing and dividing to form a fan pattern [3,4]. Ridge belts most often occur at elevations within 2 km of the planetary mean. Some ridge belts lie on broad highs up to 1.5 km high, many lie on topographic slopes, and a few occur in topographic depressions. The origin of these ridge belts is a matter of controversy, with both compressional origins [2,5] and extensional origins [6] proposed. Once the mode of formation of these ridge belts is understood, their distribution and orientation will help to constrain the homogeneity and orientation of the stresses over the period of ridge belt formation.

The look direction for the Venera system was to the west, so ridges appear as pairs of bright and dark lineaments, with the bright line to the east of the dark. A major difficulty with radar imagery, especially at small incidence angles, is foreshortening, in which the radar-facing slope is shortened and the away-facing slope lengthened [7]. This effect reaches a maximum when the look angle (in this case 10°) equals the radar-facing slope. The apparent symmetry of the ridges thus implies either that all the ridges are asymmetrical, with shallow radar-facing slopes, or that all slopes are considerably shallower than 10°. Since it is unlikely that all ridges in an area of tens of millions of square kilometers are asymmetrical in the same direction, we conclude that the ridges have gentle slopes and are mostly symmetrical.

Above, the term 'ridge' has been used in a general sense to refer to a linear rise. In the following discussion, the use of this term is restricted to rises which have a sharp transition from bright to dark at the crest, and are 5-15 km wide. These ridges are either continuous or discontinuous. The continuous ridges are over 30 km long and form coherent ridge belts, while the discontinuous ridges are less than 30 km long and do not form a coherent ridge belt. We have divided the continuous ridges into three components [8]. (1) *Anastomosing ridges*, in which the individual ridges are sinuous and often meet and cross at small angles, are the most common component. The ridges in this component are often separated by 5-20 km of plains, but sometimes form adjacent to one another, with no plains visible in between. (2) The *parallel ridge* component also consists of well-defined ridges, often with plains separating the individual ridges, but the ridges are more linear and rarely intersect one another. (3) *Parallel ridged plains* are composed of indistinct ridges, some of which do not have a distinctive bright-dark pattern. The distance between adjacent ridges is usually greater than 10 km. *Broad arches* are a fourth component also present within the ridge belts. They are more than 10 km wide, and there is no sharp bright-dark boundary at the crest, but rather a gradual transition from light to dark. They are similar to wrinkle ridges on the moon, Mars, and Earth, with their broadly curving crests, sinuosity and shallow slopes [9,10]. There are several possible origins for each of these components, ranging from extension and magmatism to compressional folding and faulting. We are assessing these

origins by comparing component morphology with compressional and extensional features on the other terrestrial planets.

Much discussion has surrounded the origin of the ridge belts [5,6]. Evidence for compressional origin discussed by Frank & Head [5] is as follows: (1) the broad morphology of the arches is similar to the maria wrinkle ridges, which are interpreted to be formed by compressional and vertical movements [i.e. 9,10,11]; (2) the more detailed morphology of ridges within the belts is similar to the mountains surrounding Lakshmi Planum, which all workers have interpreted as compressional [12]; (3) ridge belts and the ridges within them are generally sinuous, as are compressional features on the Moon and Mars, while extensional features on the Moon and Mars tend to be more linear or broadly arcuate (this is consistent with Anderson's [13] observation that low-angle faults (i.e. thrust faults) tend to have more sinuous traces than vertical strike-slip faults); (4) lineaments that cut across ridge belts and adjacent plains often form a conjugate set, trending  $60^\circ$  to the ridge belts, and where there is evidence of some strike-slip motion it is often in a direction consistent with compression and shortening across the ridge belt (under extensional stresses, one would expect either a conjugate set of faults at  $30^\circ$  to the ridge belts, or transform-type faults near  $90^\circ$  to the ridge trend); (5) the curvature of ridges around the elliptical plains regions resembles deformation of less competent material around more rigid bodies. In this case the elliptical plains regions are interpreted as less deformed or undeformed blocks. In addition, in places the components and topography show an asymmetric pattern across the ridge belts, as expected in regions of low-angle thrust faults.

Sukhanov and Pronin [6] have proposed that ridge belts are of extensional origin on the basis of the following evidence: (1) some ridge belts are symmetrical about a central line, suggesting spreading within the belt; (2) volcanic structures are visible along ridge belts; (3) where ridge belts cross other structures, these structures are not visible within the ridge belts; and (4) ridges within belts sometimes turn into graben. These aspects, however, are not all unique indicators of extension. The graben, for example, are often oriented at an angle to the overall trend of the ridge belts, and could represent pull-apart basins which have developed along strike-slip faults. Furthermore, volcanic activity is not limited to regions of extension, but is common in compressional environments (e.g. island arcs). The symmetrical pattern, however, is a strong indicator of extensional origin, and the apparent symmetry of the ridges argues against large-scale thrust faults, although the sinuosity of the ridges supports low-angle faults.

The nature of deformation within the ridge belts is complex and not fully understood at present. Some belts show distinct signs of compression, while others have symmetrical patterns expected in extensional environments. Thus the ridge belts may have formed by more than one style of deformation; some may be extensional, while others are compressional. We are now systematically mapping of all the ridge belts, concentrating on symmetry relationships, in order to determine the locations of compressional and extensional deformation within the ridge belts.

**References:** [1] Barsukov, *et al* (1986) *JGR* 91, D378-D398. [2] Basilevsky, *et al* (1986) *JGR* 91, D399-D411. [3] Head (1989) *LPSC XX* 392-393. [4] Frank & Head (1989) *LPSC XX*, 311-312. [5] Frank & Head (1988) *LPSC XIX*, 350-351. [6] Sukhanov & Pronin (1989) *Proc. LPSC XIX* (in press). [7] Sabins (1978) *Remote Sensing--Principles and Interpretation*; MacDonald (1980) in *Remote Sensing in Geology*, Siegal & Gillespie, eds. [8] Frank & Head (1988) *LPSC XIX*, 348-349. [9] Watters (1988) *JGR* 93, 10,236-10,254. [10] Plescia & Golombek (1986) *GSA Bull* 97, 1289-1299. [11] Lucchitta (1976) *Proc. LPSC VII*, 2761-2782; Sharpton & Head (1986) *Proc. LPSC XVIII*, 307-317. [12] Campbell, *et al* (1983) *Science* 221, 644-647; Crumpler & Head (1986) *Geology* 14, 1031-1034; VorderBruegge & Head (1986) *LPSC XVII*, 917-918; Pronin (1986) *Geotektonika* 4, 24-41 (in Russian). [13] Anderson (1942) *The Dynamics of Folding and Dyke Formation, with Application to Britain*, Oliver and Boyd, Edinburgh.

**EVIDENCE FOR VOLCANISM IN NW ISHTAR TERRA, VENUS;**  
*L. Gaddis and R. Greeley, Department of Geology, Arizona State University, Tempe, AZ 85287*

Venera 15/16 radar data for an area in NW Ishtar Terra, Venus (74°N, 313°E; at the intersection of Akna and Freyja Montes), show an area with moderate radar return and a smooth-textured surface which embays low-lying areas of the surrounding mountainous terrain (figure.1). Although this unit may be an extension of the lava plains of Lakshmi Planum to the southeast, detailed study suggests a separate volcanic center in NW Ishtar Terra. Lakshmi Planum, on the Ishtar Terra highland, exhibits major volcanic<sup>1,2,3,4</sup> and tectonic<sup>5,6</sup> features. It is a smooth-surfaced plateau (3 to 5.5 km in elevation) surrounded by major mountain belts including Akna, Freyja, and Maxwell Montes<sup>5,6,7</sup>. Volcanic features<sup>1,2,3,4</sup> on Lakshmi Planum include calderas of Colette (130x180 km) and Sacajawea (120x200 km) Paterae, lava flows (Colette flows average 15 km in width, 100-300 km in length<sup>3</sup>), and associated smaller vents. These volcanoes may be the surface expression of hot spots, as observed in Hawaii, in which the growing volcanic edifice deformed the surrounding areas<sup>8</sup>; alternatively, compressional deformation may have resulted in crustal thickening and melting, and the formation and deposition of volcanic materials<sup>3</sup>.

On the Venera radar image (figure 1) radar brightness is influenced by slope and roughness; radar-facing slopes (east-facing) and rough surfaces (~8 cm average relief) are bright, while west-facing slopes and smooth surfaces are dark. The moderate radar return indicates a smooth unit embaying low-lying areas of the adjacent "ridge-and-trough" terrain; these characteristics are consistent with a volcanic origin for this unit. To the northwest, bright, lobate features extend further northwestward more than 300 km. A geologic sketch map (figure 2) shows smooth terrain for the volcanic units, and the darker units represent adjacent, possibly associated volcanic flows.

A series of semi-circular features, apparently topographic depressions, do not conform in orientation to major structural trends in this region of NW Ishtar Terra. Topography<sup>9</sup> (figure 3) shows elevations from about 5.5 km in the SE (toward Lakshmi Planum) to 2 km (to NW). If the 3.0 km elevation is assumed to be the outer boundary of a complex caldera in the center of the smooth terrain, a feature about 200 x 250 km in size is measured; the smaller depression to the southeast (an associated vent?) is about 50 km in diameter.

The large depression (caldera?) in NW Ishtar Terra is similar to the calderas of Colette and Sacajawea Paterae, as all three structures are large irregular depressions. Although Colette and Sacajawea have been described as shields, their flank slopes are low (<0.5°). All 3 calderas have depths of 1 to 1.5 km, but the caldera in NW Ishtar is both more complex and larger than Colette (130x180 km) and Sacajawea (200x120 km). If a relationship between caldera diameter and magma chamber diameter and depth exists for Venus<sup>10</sup>, then the chamber under the NW Ishtar caldera is larger/deeper than those of Colette and Sacajawea. Although the types and volumes of volcanic products from the structures and the presence or absence of rifting and associated volcanism cannot be constrained with Venera data, the large calderas indicate that centralized eruptions were predominant. Age relationships are difficult to establish; although the muted appearance and lower relief of Sacajawea support an older age than for Colette, it is not possible to determine a relative age for the NW Ishtar Terra volcano.

NW Ishtar Terra appears to be the site of a volcanic center with a complex caldera structure, possibly more than one eruptive vent, and associated lobed flows at lower elevations. The morphologic similarity between this volcanic center and those of Colette and Sacajawea suggests that centralized eruptions have been the dominant form of volcanism in Ishtar. The location of this volcanic center at the intersection of two major compressional mountain belts and the large size of the caldera (with an inferred large/deep magma source) support a "crustal thickening/melting" rather than a hot-spot origin for these magmas.

**References:** 1) Barsukov *et al.*, 1986, LPSC Proc. 16th, JGR, 91, D378; 2) Magee and Head, 1988, LPSC XIX, 711; 3) Magee and Head, 1988, LPSC XIX, 713; 4) Gaddis, 1989, LPSC XX, 317; 5) Crumpler *et al.*, 1986, Geology, 14, 1031; 6) Head, 1988, LPSC XIX, 469; 7) Vorder Bruegge and Head, 1988, LPSC XIX, 1218; 8) Pronin, 1986, Geotektonika, 4, 26 (in Russian); 9) Fotokarta Veneri B4, Lakshmi Planum, 1987; 10) Wood, 1984, JGR, v. 89, 8391.

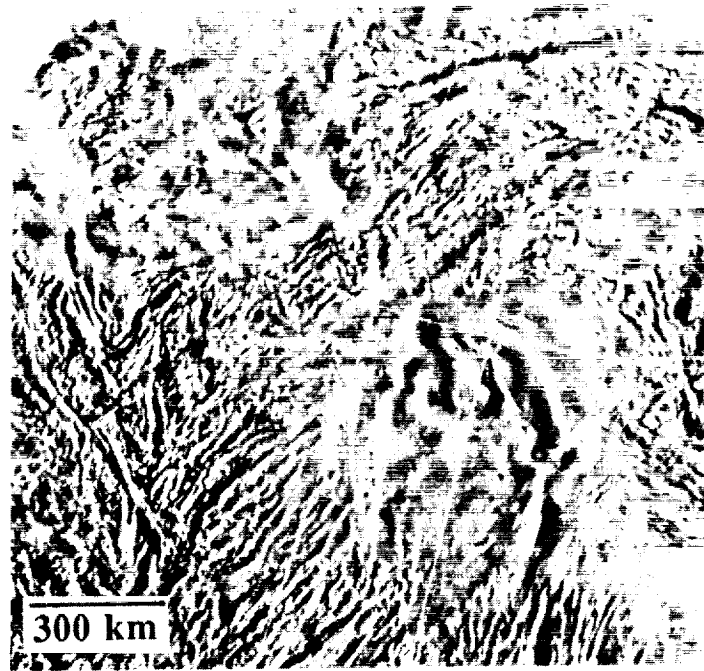


Figure 1

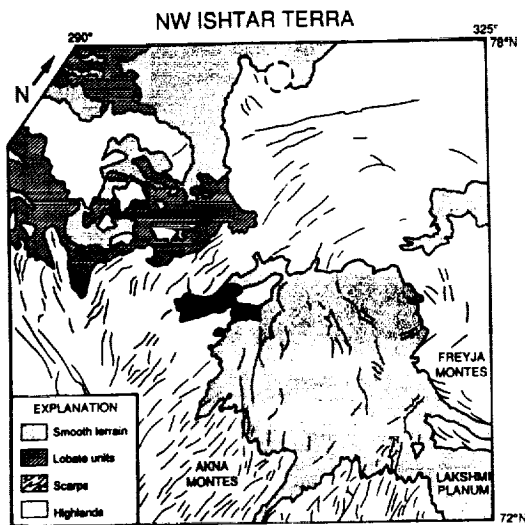


Figure 2

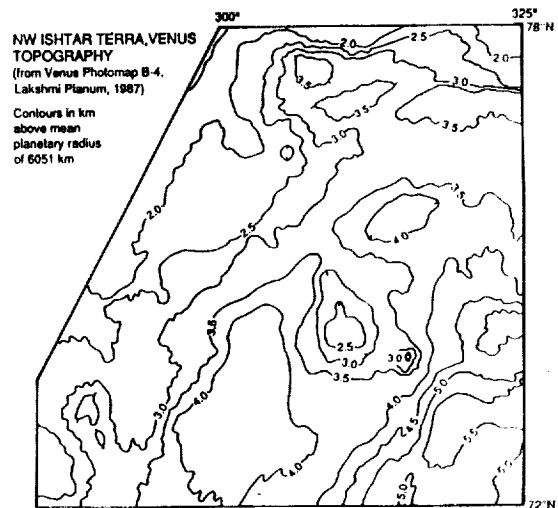


Figure 3

**Analysis of Radar Images of the Active Volcanic Zone at Krafla, Iceland: The Effects of Look Azimuth Biasing:** J. B. Garvin# and R. S. Williams Jr.\*, #NASA/GSFC, Geodynamics Branch, Greenbelt, MD 20771; \*Geophysics Division, 927 National Center, USGS, Reston, VA 22092.

The geomorphic expression of Mid-Ocean-Ridge (MOR) volcanism in a subaerial setting occurs uniquely on Earth in Iceland, and the most recent MOR eruptive activity has been concentrated in the Northeastern Volcanic Zone in an area known as *Krafla*. Within the *Krafla* region are many of the key morphologic elements of MOR-related basaltic volcanism, as well as volcanic explosion craters, sub-glacial lava shields, tectonic fissure swarms known as *gjar*, and basaltic-andesite flows with well-developed ogives (pressure-ridges). Deposits of basaltic tephra and hyaloclastite can also be found, and an incipient collapse caldera (*Krafla* itself) is well-established. The most recent series of eruptions were of the fissure type, with extensive flows of both a'a and pahoehoe covering a 10 km long zone to the east of the Gaesafjoll sub-glacial lava shield. The diverse range of pristine basaltic volcanic constructs that are manifested in the *Krafla* region has motivated our geomorphic analysis of the area from the perspective of high-resolution, airborne SAR imagery, in comparison with vertical airphotos and orbital panchromatic imagery collected by the SPOT satellite. One of our prime objectives has been to use the synoptic perspective offered by remote sensing imagery of different kinds to evaluate how severely look-azimuth biasing effects recognition of basic structure and geomorphology of an active volcanic zone. For this reason, our collaborators on this project, INTERA Technologies, collected X-band digital SAR imagery at a 15 degree incidence angle (average) and at 8 m per pixel resolution in *three different look directions*: from the *East*, *West*, and *South*. Since orbital constraints prevent the Magellan SAR from imaging known venusian volcanic areas of interest (e.g., at *Beta Regio* etc.) at more than one look azimuth, there is a real concern that many diagnostic structures may appear "invisible" in the Magellan imaging dataset (especially those features oriented parallel to the look direction). In fact, our experience with one look direction INTERA SAR imagery of the *Reykjanes* region in southwestern Iceland clearly indicates that major tension fractures that cut many of the recent volcanic features such as the lava shields cannot be observed, in spite of their clear expression in airphotos and orbital SPOT multispectral imagery [Garvin et al., 1989]. Therefore, our objective has been to quantify the degree to which the basic volcanic and structural features can be mapped from directional SAR imagery as a function of the look azimuth. To accomplish this, we have independently mapped the current expression of volcanic and tectonic constructs within the *Krafla* region on the E, W, and N-looking SAR images, as well as from SPOT Panchromatic imagery acquired in 1987. The INTERA SAR images were acquired in October of 1988 and provide imagery for the region that supercedes the most recent airphoto survey conducted by the Landmaelingar Islands Aerial Photographic Service; thus we have no recent maps to compare with except for those which describe the various lava flow emplacement episodes from 1981-1984 in the *Krafla* region. A second phase of this study (to commence shortly) will involve digital co-registration of the 3 INTERA SAR images (designated E, W, and N on the basis of their look direction) to the SPOT Panchromatic image. This analysis will permit an even more quantitative assessment of the degree to which major features can be observed as a function of look azimuth. We believe that our results will have a bearing on the reliable interpretation of Magellan images of volcanic zones on Venus, many of which appear (on the basis of 1 km resolution *Venera* and *Arecibo* images) to be of a basaltic, fissure-fed variety (e.g., the volcanic plains of *Sedna* etc.).

Our initial observations of the E, W, and N images indicates that fresh a'a lava surfaces are extremely radar-bright (rough at 3 cm to meter scales) independent of look direction -- this suggests that these flows do not have strong flow-direction related structures at meter and cm scales, which is consistent with typical Icelandic a'a lava surfaces in general. The November 1981 *Krafla* flow has the most pronounced radar-bright appearance (saturated in the optically correlated INTERA imagery). The structural expression of the incipient *Krafla* caldera cannot be observed in any of the SAR images, independent of look direction. The oriented (mostly N-S) tectonic fissures and cracks (*gjar*) are well-expressed at all three look directions; this result is rather surprising given their strong preferred orientation, but the high spatial resolution and extreme obliquity of the INTERA SAR imagery serves to enhance the expression of these extensional features, even in the N-looking image. The lava shields

(i.e. *Theistareykjabunga*) and the sub-glacial varieties can all be identified at all three look directions as well. The appearance of the *Hverfjall* tephra ring and nearby *Ludent* (both ~ 1 km in diameter craterform structures involving a hydromagmatic eruption phase) are distinctive at each of the three look directions, although the basal surge deposit that lies beyond the rim crest of these depressions is quite variable. Our basic impression from a preliminary analysis of the effects of look azimuth biasing on interpretation of the geology of an active MOR volcanic zone is that up to 30% of the diagnostic features can be missed at any given look direction, but that having two orthogonal look direction images is probably sufficient to prevent gross mis-interpretation. In fact, the strong directional orientation of structural elements within the Krafla region may provide on an end-member test of the effects of azimuth biasing, as older volcanic zones (on Earth and Venus) may have undergone several eruptive phases with different structural fabrics (i.e., not just a single N-S fabric as at Krafla). Our analysis is continuing, and results of our digital co-registration are expected by late 1989, and in time to assist Magellan scientists with image interpretation. (This research was partially supported through NASA Code EEL RTOP 677-43-28 to Garvin and Williams. We gratefully acknowledge the cooperation and support of INTERA Technologies, and Garth Lawrence; we are also grateful for the permission to work in Iceland granted us by the Iceland National Research Council.)

#### REFERENCES:

Garvin J. B. , R. S. Williams, and J. Jónsson (1989) *Geologic Remote Sensing of Iceland: An Imaging Radar and Laser Altimeter Approach to Problems in Planetary Volcanology*, *in press* in Proc. of 28th International Geological Congress, July, 1989, Washington, DC, 6 pp.

**Radar Scattering Mechanisms within the Meteor Crater Ejecta Blanket: Geologic Implications and Relevance to Venus:** J. B. Garvin\*, B. A. Campbell#, S. H. Zisk#, G. G. Schaber@, and C. Evans%: \*Geodynamics Branch, NASA/GSFC, Code 621, Greenbelt, MD 20771; #Planetary Geosciences Div., Hawaii Instit. of Geophysics, U. Hawaii, Honolulu, HI 96822; @Branch for Astrogeology, U. S. Geological Survey, Flagstaff, AZ, 86001; %Univ. Maryland Dept. of Astronomy and NASA/GSFC, Greenbelt, MD 20771.

Simple impact craters are known to occur on all of the terrestrial planets and the morphologic expression of their ejecta blankets is a reliable indicator of their relative ages on the Moon, Mars, Mercury, and most recently for Venus [e.g., 1,2]. In addition, the geology of impact crater ejecta blankets has been shown to reveal details of the physics of the ejecta emplacement process as manifested by distinctive facies and morphologies (e.g. hummocks) [1-3]. The Magellan S-band SAR dataset to be acquired for Venus is expected to provide 120-360 m resolution images of hundreds to thousands of craterforms, many of which are likely to be of hypervelocity impact origin. It will be crucial for the interpretation of the geology of Venus to develop a reliable means of distinguishing smaller impact landforms from volcanic collapse and explosion craters, and further to use the observed SAR characteristics of *crater ejecta blankets* (CEB) as a means of relative age estimation. With these concepts in mind, we have initiated a study of the quantitative SAR textural characteristics of the ejecta blanket preserved at *Meteor Crater*, Arizona, the well-studied 1.2 km diameter simple crater that formed ~49,000 years ago from the impact of an octahedrite bolide [3,4]. While Meteor Crater was formed as the result of an impact into wind and water-lain sediments [3] and has undergone recognizable water and wind-related erosion [3-5], it nonetheless represents the only well-studied simple impact crater on Earth with a reasonably preserved CEB. Recent field geomorphic investigations of the Meteor Crater CEB by Grant and Schultz [6] have challenged the previous work by Roddy and colleagues [4,5] that suggested about 20% of the ejecta has been removed, and the new, albeit controversial, evidence indicates that the ejecta is still in a pristine state [6]. Therefore, we are also interested in exploring whether the scattering behavior of the CEB can provide an independent perspective on its preservation state and style of erosion. Finally, we have used airborne laser altimeter profiles of the microtopography of the Meteor Crater CEB [7] to further quantify the sub-radar pixel scale topographic slopes and RMS height variations for comparisons with the scattering mechanisms computed from SAR polarimetry. This report summarizes a preliminary assessment of the L-band radar scattering mechanisms within the Meteor Crater CEB as derived from a NASA/JPL DC-8 SAR Polarimetry dataset acquired in 1988, and compares the dominant scattering behavior with microtopographic data (laser altimeter profiles and 1:10,000 scale topographic maps).

Campbell and colleagues [8] have demonstrated that polarimetric SAR backscatter data from volcanic lava surfaces can be reasonably represented by a model in which the entire coherent echo from the surface is separated into quasi-specular (QS), quasi-dihedral (DI), and Bragg-resonant (BR) components. Details of this approach are summarized in [9], and a general description of the analysis of multipolarization SAR data in Stokes matrix format is given by van Zyl and colleagues [9-11], and will not be reviewed here. Campbell and colleagues [8] have convincingly shown that this radar model produces quantitative information about the relative surface roughness of lava flows, and that it should be extensible to the Meteor Crater if the CEB can be modelled as dielectrically homogeneous. Furthermore, they have demonstrated that RMS height variations and other topographic parameters can be deduced from the types of scattering components. We have used terrain properties computed from meter-resolution laser altimeter profiles [7] to quantify the Meteor Crater CEB as a function of range (from the rim crest) and azimuth. For a 500 m long section of the eastern CEB, the RMS height variations are approximated by a power law of the form:  $RMS = 0.032 (\Delta x)^{1.06}$  in meters, where  $\Delta x$  is the spatial scale over which the RMS height variation is desired. In a similar manner, the scale-dependent local topographic slope can be described by a power law of the form:  $Slope = 6.8 (\Delta x)^{-0.106}$  in degrees. Thus, the 10 cm spatial-scale RMS height variations (on the average) for the near-rim ejecta range from 0.14 to 0.47 cm as a function of azimuth around the crater, and the 1 m scale RMS variations range from 2 to 4.3 cm. At the scale of a 10 m SAR polarimeter pixel, the RMS height variations range from 23 to 49 cm, with the eastern and northeastern ejecta the roughest (40-49 cm RMS per 10 m). Local slopes at 10 cm scales vary from 4

to 8 degrees. Even at 10 m spatial scales, local slopes range from 3.4 to 7.2 degrees as a function of azimuth around the crater. These values for the Meteor Crater CEB are dramatically different by factors of up to 10 from similar statistics derived from microtopographic statistics for lava flows such as SP (AZ). The blocky SP lava flow averages over 18 cm of RMS height variation at 1 m scales, and 71 cm of RMS relief at 10 m (DC-8 SAR pixel) scales. Local slopes at radar pixel scale average 11 degrees, while those at 1 m scale lengths are typically 36 degrees. Therefore, our prediction is that the Meteor Crater CEB is much more benign at radar wavelengths than blocky or a'a lava flows.

We have applied the model described in [8] to the DC-8 SAR polarimetry (at L-band only) of Meteor Crater and its CEB (out to 5 crater radii), after having corrected these data for HH and VV phase errors and cross-talk using algorithms developed by J. van Zyl [11]. In order to evaluate the effect of dielectric homogeneity of the surface layer in the vicinity of the crater, we have computed model solutions for  $E' = 4, 6, \text{ and } 8$ ; for reference, only very dense, competent rocks have dielectric permittivities as high as  $E' = 8$ , and there is no obvious physical evidence for high dielectric phases at the surface of the CEB. A simple color (RGB) composite image involving the QS, BR, and unpolarized (UN) components of the radar model reveals the dominant textural variations of the CEB. The DI component is extremely subdued in the CEB, perhaps due to a general absence of natural "corner reflectors" except at the rim. We examined the differences between the composite BR, QS, and UN images as a function of dielectric permittivity  $E'$ , and in correlation with topography and geology. The  $E' = 8$  model is most sensitive to local variations in surface texture, and best depicts the spatial variability and asymmetry of the ejecta [3-5]. There is a sense of bilateral symmetry to the ejecta as revealed in the scattering mechanism images, about an axis oriented E-W. This is not consistent with the theory of a directed impact from the SE [5], but the effect may be due to an erosional imprint or radar look azimuth biasing. The expression of the CEB in the composite image (BR, QS, UN) is strongest to the NE and South/SE, and is most subdued to the West. This is consistent with the results of a radial topographic analysis of the CEB [7]. A significant component of the scattering in the CEB is represented by the unpolarized (UN) echo, although most of terrain appears to behave as QS facets. The  $E' = 8$  model suggests that the "roughest" areas of the ejecta have a higher dielectric permittivity, which is consistent with their occurrence as isolated ridges of rock outcrops within the more friable (eolian lag covered) ejecta deposit. An apparently random spatial distribution of isolated, lower dielectric regions exists around the crater, and these areas are not correlated with the limits of the CEB.

Our preliminary examination of the radar scattering characteristics within a partially preserved impact crater ejecta blanket suggest a few cautions. First, the Meteor Crater ejecta blanket may not be the ideal analogue for such terrain types on planets such as Venus or the Moon. This is because of the generally benign nature of the Meteor Crater CEB, at least relative to lava and block field surfaces. While the scattering behavior of the CEB is distinct from the surrounding terrain, it is not representative of a blocky surface unit, as is suggested from existing radar observations of probable venusian impact craters [2]. It is possible that a partially fluidized mode of late-stage ejecta emplacement at Meteor Crater has subdued the expression of the ejecta block field within one crater radius from the rim. In spite of the possible uniqueness of the preserved CEB at Meteor Crater, the suggestion that ejecta blankets may have dielectric permittivities that are larger than their surroundings warrants further examination in light of enhanced radar reflectivities observed around probable venusian impact craters. {This work was partially supported by NASA/GSFC DDF 88-04 and RTOP 677-43-24}.

**REFERENCES:** [1] Melosh H. J. (1989) *Impact Cratering*, Oxford Univ. Press. [2] Ivanov B. A. et al. (1986) *JGR* 91, D413-D430. [3] Shoemaker E. M. and S. E. Kieffer (1974) *Guidebook to the Geology of Meteor Crater*, ASU Center for Meteorite Studies, Public. no. 17, Tempe, 66 pp. [4] Roddy D. J. et al. (1975) *Proc. 6th LPSC*, 2621-2644. [5] Roddy D. J. (1978) *Proc. 9th LPSC*, 3891-3930. [6] Grant J. and P. Schultz (1989) *LPSC XX*, 355-356, LPI, Houston. [7] Garvin J. B. et al. (1989) *LPSC XX*, 243-244, LPI, Houston. [8] Campbell B. A. et al. (1989) *PIERS* abstract, "Lava Roughness Mapping...", 2 pp. [9] van Zyl J. et al. (1987) *Radio Sci.* 22, 529-543. [10] Evans D. L. et al. (1988) *IEEE GRS* 26, 774-789. [11] van Zyl J. (1989) *IEEE GRS* 27, 36-45.

**AEOLIAN PROCESSES ON VENUS; R. Greeley, Department of Geology,  
Arizona State University, Tempe, Arizona 85287-1404**

This review assesses the potential aeolian regime on Venus as derived from spacecraft observations, laboratory simulations, and theoretical considerations. The two requirements for aeolian processes--a supply of small, loose particles and winds of sufficient strength to move them--appear to be met on Venus. Venera 9, 10, 13, and 14 images show particles considered to be sand-and-silt size on the surface (1-5). In addition, "dust spurts" (grains 5-50  $\mu\text{m}$  in diameter) observed via lander images (6) and inferred from the Pioneer-Venus nephelometer experiments suggest that the particles are loose and subject to movement. Although data on near-surface winds are limited, measurements of 0.3 to 1.2 m/sec from the Venera lander and Pioneer-Venus probes (7) appear to be well within the range required for sand and dust entrainment.

The Venus Wind Tunnel (VWT) is an apparatus used to simulate the movement of particles on Venus (8); it operates with carbon dioxide gas at 35 bars pressure and 27°C (ambient laboratory temperature); this produces a *fluid density* (the critical factor in aeolian processes) that is equivalent to the nominal Venus case of 90 bars at 475°C. Experiments have been run to determine threshold (e.g., minimum wind speeds) for particle entrainment as a function of grain size: results show that in the dense venusian atmosphere particles are easily moved ( $u_{*t} = 2.8 \text{ cm s}^{-1}$  for  $\sim 80 \mu\text{m}$  grains, the optimum size). However, experiments also reveal a mode of aeolian transport unusual on Earth (and presumably unusual on Mars), i.e., *rolling*, in which grains roll along the surface and are *not* impacted by saltating grains (9). The threshold wind speed ( $u_*$ ) is about 20% *lower* than that for saltation, suggesting that aeolian processes could occur with greater frequency than otherwise expected on Venus.

Once set into motion, what is the potential for transport of surficial material and for erosion by windblown particles? Experiments show that the *flux* of grains is lower than predicted, primarily due to a "choking" effect that occurs in high-density grain flow. Nonetheless, the velocity of the grains in motion very quickly achieves 75-100% of the wind speed, in contrast to windblown particles on Earth and Mars (10). Evidently, the coupling of particles with the atmosphere is directly proportional to atmospheric density.

From analyses of Venera lander images, there was speculation on the existence of various aeolian bedforms such as ripples and dunes (3). The postulation of the existence of "microdunes" is supported by simulations that show the development of dunelike features 10-20 cm long by a few cm high (11). The existence of "slip faces", foreset beds, flow separation, and distinctive grain size distributions all are appropriate for dunes as opposed to ripples. However, experiments also show that microdunes and other bedforms developed under venusian conditions are highly dependent on wind speed, particle diameter, and atmospheric density. Consequently, the formation and preservation of small bedforms may be limited and ephemeral.

Aeolian activity involves the interaction of the 1) atmosphere, 2) lithosphere, and 3) loose particles. Thus, there is the potential for various physical and chemical weathering processes that can effect not only rates of erosion, but changes in the composition of all three components. The *Venus Simulator* is an apparatus used to simulate weathering under venusian conditions at full pressure (to 112 bars) and temperature (to 800 K). In one series of tests, the physical modifications of windblown particles and rock targets were assessed and it was shown that particles become abraded even when moved by gentle winds (12, 13). However, little abrasion occurs on the target; rather, the comminuted material from the particles readily adheres to the target faces. Thus, compositional "signatures" for target rocks may be more indicative of the windblown particles than of the "bedrock".

From these and other considerations, aeolian modifications of the venusian surface may be expected to occur as weathering, erosion, transportation, and deposition of surficial materials. Depending upon global and local wind regimes, there may be distinctive "sources"

and "sinks" of windblown materials. Radar imaging, especially as potentially supplied via the Magellan mission, may enable the identification of such areas on Venus.

### References

1. Basilevsky, A.T., and J.W. Head (1988) The geology of Venus. *Ann. Rev. Earth Planet Sci.*, 16, 295-317.
2. Florensky, C.P., L.B. Ronca, A.T. Basilevsky, G.A. Burba, O.V. Nikolaeva, A.A. Pronin, A.M. Trakhtman, V.P. Volkov, and V.V. Zazetsky (1977) The surface of Venus as revealed by Soviet Venera 9 and 10. *Bull. Geol. Soc. of Amer.*, 88, 1537-1545.
3. Florensky, C.P., A.T. Basilevsky, V.P. Kryuchkov, R.O. Kusmin, O.V. Nikolaeva, A.A. Pronin, I.M. Chernaya, Yu.S. Tyufin, A.S. Selivanov, M.K. Naraeva, and L.B. Ronca (1983) Venera 13 and Venera 14: Sedimentary rocks on Venus. *Science*, 221, 57-59.
4. Garvin, J.B., J.W. Head, M.T. Zuber, and P. Helfenstein (1984) Venus: The nature of the surface from Venera panoramas. *J. Geophys. Res.*, 89, B5, 3381-3399.
5. McGill, G.E. (1983) The geology of Venus. *Episodes*, 4, 10-17.
6. Garvin, J.B. (1981) Landing induced dust clouds on Venus and Mars. *Proc. Lunar Planet. Sci. Conf.*, 12B, Houston, TX, 1493-1505.
7. Counselman III, C.C., S.A. Gourevitch, R.W. King, G.B. Lorient, and R.G. Prinn (1979) Venus winds are zonal and retrograde below the clouds. *Science*, 205, 85-87.
8. Greeley, R., J. Iversen, R. Leach, J. Marshall, B. White, and S. Williams (1984) Windblown sand on Venus: Preliminary results of laboratory simulations. *Icarus*, 57, 112-124.
9. Greeley, R., J.R. Marshall (1985) Transport of venusian rolling 'stones' by wind. *Nature*, 313, 6005, 771-773.
10. Greeley, R., S.H. Williams, and J.R. Marshall (1983) Velocities of windblown particles in saltation: Preliminary laboratory and field measurements. in *Eolian Sediments and Processes* (M.E. Brookfield and T.S. Ahlbrandt, eds.), Elsevier Science Publ., Amsterdam, 133-148.
11. Greeley, R., J.R. Marshall, and R.N. Leach (1984) Microdunes and other aeolian bedforms on Venus: Wind tunnel simulations. *Icarus*, 60, 152-160.
12. Greeley, R., J.R. Marshall, and J.B. Pollack (1987) Venus: Physical and chemical modification of the surface by windblown particles. *Nature*, 327, 6120, 313-315.
13. Marshall, J.R., R. Greeley, and D.W. Tucker (1988) Aeolian weathering of Venusian surface materials: Preliminary results from laboratory simulations. *Icarus*, 74, 495-515.

THOUGHTS ON THE VENUSIAN SURFACE AND EARLY EARTH,  
R.B.Hargraves, Department of Geological and Geophysical Sciences,  
Princeton University, Princeton, NJ 08544

The possibility that improved understanding of the tectonic style on Venus may have particular relevance to the Archean Earth, adds to the interest and excitement of the Magellan mission. The speaker - no expert on Venus - will present his views of this aspect based on limited reading and what he learns at this Tutorial.

ARCHITECTURE OF OROGENIC BELTS AND CONVERGENT ZONES IN WESTERN ISHTAR TERRA, VENUS;  
 J. W. Head, R. Vorder Bruegge, and L. Crumpler, Dept. of Geological Sciences, Brown University,  
 Providence, R. I. 02912

Linear mountain belts in Ishtar Terra were recognized from Pioneer-Venus topography<sup>1</sup>, and later Arecibo images showed banded terrain interpreted to represent folds<sup>2</sup>. Subsequent analyses<sup>3</sup> showed that the mountains represented orogenic belts<sup>4</sup>, and that each had somewhat different features and characteristics<sup>5,6</sup>. Orogenic belts are regions of focused shortening and compressional deformation and thus provide evidence for the nature of such deformation, processes of crustal thickening (brittle, ductile), and processes of crustal loss. Such information is important in understanding the nature of convergent zones on Venus (underthrusting, imbrication, subduction?), the implications for rates of crustal recycling, and the nature of environments of melting and petrogenesis. In this study we identify and examine the basic elements of four convergent zones and orogenic belts in western Ishtar Terra, and then assess the architecture of these zones (the manner in which the elements are arrayed), and their relationships. The basic nomenclature of the convergent zones is shown in Fig. 1.

Danu Montes ranges in width from about 75 to 175 km and extends for over 1200 km along the southern and southwestern edge of Lakshmi Planum, rising up to 2.5-3.0 km above the adjacent plains. It is characterized by parallel to sinuous linear bands interpreted to be folds. The inboard foreland area of Lakshmi Planum generally tilts slightly upward toward Colette and Sacajawea calderas, and volcanic plains can be seen to embay parts of the mountains<sup>7</sup>. Outboard of Danu, there is no plateau region, and the terrain descends directly to the base of the adjacent foredeep along Vesta Rupes, a 50-150 km wide scarp whose base is 2-2.5 km below the elevation of Lakshmi Planum. Outboard of the foredeep, a broad rise (Ut Rupes) about 200-300 km wide parallels Danu Montes at a distance of 450-500 km. Danu Montes rises topographically from the west toward the east, and is most well-developed at the bend at the southeast edge of Lakshmi Planum. At this bend, and to the east, Clotho Tessera is developed between Danu and Ut Rupes, and the foredeep characteristic of western Danu is replaced by the complex positive topography of the tessera sloping down to the adjacent plains. The general direction of compression appears to be normal to the strike of western Danu Montes, and as Danu turns towards the north it, and the adjacent tessera, are characterized by a series of parallel linear features interpreted to be strike-slip faults, and the tessera region appears to be an approximately 300 km wide shear zone. Where Danu is best developed, it is interpreted to be at least partly transpressional in nature.

Akna Montes trends in a NE direction, ranges in width from about 200-250 km, and extends for 800-900 km along the western edge of Lakshmi Planum, rising up to 2.5-3.0 km above the adjacent plains. High topography is best developed in its southern half and it is characterized by a series of features typical of orogenic belts<sup>4</sup>. The inboard foreland area of Lakshmi Planum is characterized by a broad depression opening to the south between Akna and Colette caldera. Volcanic plains can be seen to embay parts of the mountains, and parts of the orogenic belt has deformed the plains<sup>7</sup>. Outboard of Akna there is a distinctive plateau region (Atropos Tessera) extending about 900-1000 km outboard of Akna. At the western edge of Atropos, the terrain descends slowly to the the adjacent plains (Snegorochka Planitia) dropping down about 2 km over a distance of several hundred km. Neither the outboard scarp, nor the foredeep and rise are distinctly developed here. The southwestern edge of Atropos Tessera is characterized by a NW trending linear scarp in excess of 1000 km in length against which Akna Montes terminates; this has been interpreted as a shear zone<sup>8</sup> and syntaxis structures<sup>9</sup> are developed where it coincides with Atropos Tessera.

Freyja Montes trends in an EW direction and connects along its western edge with Akna Montes in a zone characterized by a syntaxis structure<sup>9</sup>. Freyja extends over 800 km along the northern edge of Lakshmi Planum, is 200-300 km wide, and rises up to 2.5-3.0 km above the adjacent plains. High topography is best developed in its eastern half and like Danu and Akna it is characterized by a series of features typical of orogenic belts<sup>4</sup>. The inboard foreland area of Lakshmi Planum is characterized by a gentle slope extending to the south and the volcanic plains have been tilted upward and deformed

## Orogenic Belts and Convergent Zones

J. W. Head et al.

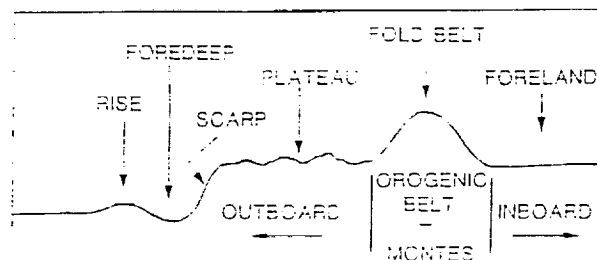
into ridged plains<sup>7</sup>. Outboard of Freyja there is a distinctive plateau region (Itzpapalotl Tessera) 200-400 km wide characterized by a range of terrain types interpreted to represent compressional deformation and zones of localized faulting<sup>6</sup>. At the northern edge of Itzpapalotl, the terrain descends abruptly to the adjacent plains dropping down about 3 km over a distance of less than 100 km (Uorsar Rupes), and there is a foredeep filled with young lava plains and an adjacent outboard rise<sup>6</sup>. Freyja Montes and the associated terrain have been interpreted to represent generally N-S oriented convergence resulting in flexure, underthrusting, and crustal imbrication<sup>6</sup>. At its eastern edge, the topographic trend of the edge of the plateau turns SSE, producing a broad topographic indentation into Ishtar Terra. Along the western edge of this indentation, the deformation changes style to produce a series of transpressional ridges.

Maxwell Montes is broader and more equant in planform than the other mountain ranges and rises over 6 km above the surrounding plain. Although Maxwell shares the common characteristics of an orogenic belt<sup>4</sup>, it also contains distinctive cross-strike structures that have been interpreted to represent strike-slip deformation of an Akna-like linear mountain range as it was transported westward between two converging shear zones<sup>5,10</sup>. Inboard of Maxwell the plains dip slightly inward toward Lakshmi, but locally there are depressions in the plains along the base of the steep Planum-facing scarp. Outboard of Maxwell is an arcuate plateau and the complex and distinctive structure and topography of Fortuna Tessera<sup>3</sup>. The distinctive scarp, foredeep and rise typical of Danu and Freyja Montes are not readily visible here; instead the deformation is much more widespread and distributed. Analysis of the Fortuna has led to the interpretation that it represents complex deformational patterns associated with convergence, lateral transport of material, and large-scale ductile deformation and crustal thickening<sup>11</sup>.

Identification and mapping of the basic elements of convergent zones illustrates the different architecture of the orogenic belts and suggests that different processes or different levels and styles of similar processes are operating in different belts. We tentatively order the orogenic belts in a sequence from simple to complex as follows: Danu, Freyja, Akna, Maxwell. The rise, scarp, and foredeep characteristic of Danu and Freyja Montes suggests that large-scale flexure<sup>12</sup>, underthrusting<sup>13</sup>, and crustal loss are typical of these environments. The distinctive altitude differences between the outboard plains and the foreland region suggest that the orogenic belt represents the boundary between crusts of two different thicknesses. Akna and Maxwell Montes display similar topographic elevations both inboard and outboard and this may represent convergence of crust of more equal thickness, and the consequent emphasis on more distributed deformation and ductile crustal thickening, particularly in the case of Maxwell Montes.

References: 1) G. Pettengill, *et al.* (1980) *JGR*, 85, 8261. 2) D. Campbell *et al.* (1983) *Science*, 221, 644. 3) A. Basilevsky *et al.* (1986) *JGR*, 91, D399. 4) L. Crumpler *et al.* (1986) *Geology*, 14, 1031. 5) R. Vorder Bruegge *et al.* (1989) submitted to *JGR*. 6) J. Head (1988) *LPSC XIX*, 467. 7) K. Magee and J. Head (1988) *LPSC XIX*, 713. 8) E. Stofan *et al.* (1987) *Earth, Moon, Planets*, 38, 183. 9) J. Head (1988) *LPSC XIX*, 469. 10) R. Vorder Bruegge and J. Head (1988) *LPSC XIX*, 1218. 11) R. Vorder Bruegge and J. Head (1988) *LPSC XIX*, 1220. 12) S. Solomon and J. Head (1989) *LPSC XX*, 1032. 13) J. Head (1989) The formation of mountain belts on Venus: Evidence for large-scale convergence, underthrusting, and crustal imbrication in Freyja Montes, Ishtar Terra, submitted to *Geology*.

**Figure 1.** Cross section and nomenclature of convergent zones and orogenic belts in the Ishtar Terra region of Venus.



ORIGINAL PAGE IS  
OF POOR QUALITY

DEDUCING THE AGE OF THE DENSE VENUS ATMOSPHERE: R. Kahn, Jet Propulsion Laboratory/California Institute of Technology, 4800 Oak Grove Drive, Pasadena CA. 91109

The dense atmosphere of Venus has a discernable effect on the size of impact craters produced by incoming meteors. This means that if parts of the modern Venus surface are old enough to preserve the record of crater impacts dating back 3 to 4 billion years, it is possible to determine whether or not the dense atmosphere was around to shield the surface during the late heavy bombardment period of solar system history.

Based on simple but reasonable models for crater production, and the effects of atmospheric drag and breakup on incident meteors, I calculate the expected surface crater size-frequency distributions for scenarios in which the dense atmosphere formed early and late in the planet's history. I include models where simple obliteration mechanisms affect the surface crater populations to varying degrees. If the atmosphere is young, then any uneroded (old) surfaces will have crater densities upward of  $10^{-4}$  km<sup>-2</sup>, and a ratio of small (4 km) to large (128 km) craters near  $10^3$ , according to the models. If the atmosphere is old, and atmospheric breakup is the dominant mechanism for destroying incident meteors, then absolute crater frequencies on the Venus surface will be diminished by several orders of magnitude relative to the young atmosphere case. If atmospheric drag dominates breakup and the atmosphere is old, the absolute crater frequency will be lowered by perhaps an order of magnitude relative to the young atmosphere case, and the ratio of small to large craters will be reduced to a value near  $10^{1.5}$ .

Even when adequate data are available, much work will probably be required to sort out the effects of surface erosion, which are likely to be regional, from any remaining signature of the atmospheric history. However, once a large fraction of the Venus surface has been imaged at kilometer resolutions, as the Magellan Mission promises to do, it may be possible to make a crude determination of the age of the dense Venus atmosphere.

Such a deduction would be of more than academic interest. Gram for gram, the Earth and Venus have about the same amount of carbon; on Earth it is in carbonate rocks (limestone) while on Venus it is in the atmosphere. The single most important question one can ask about this difference is: 'Did the dense Venus atmosphere form as part of original outgassing, or did it form later as a result of some climate instability that moved carbon from the surface rock into the atmosphere?' Even a very crude determination of the age of the dense Venus atmosphere would be a step toward answering this question. If the dense atmosphere postdates the heavy bombardment, core formation, and the period when rapid outgassing of the planet is most likely, then the possibility that the atmospheric carbon dioxide results from some instability in climate must be taken seriously.

Reference: R. Kahn (1982) *Icarus* 49, p.71-85.

**Clotho Tessera, Venus: A fragment of Fortuna Tessera?;**

Richard C. Kozak and G.G. Schaber, U.S. Geological Survey, Flagstaff, AZ 86001

Clotho Tessera, adjacent to southeast Lakshmi Planum, may provide additional evidence for lateral crustal motions, and a model for the origin of small tessera fragments.

Clotho Tessera and Lakshmi Planum are so noticeably different, and in such close proximity, it is difficult to derive a reasonable model of their formation in situ. Squeezing of material out from beneath Lakshmi has been suggested as an origin for Moira Tessera [1], which is also adjacent to Lakshmi and 1400 km west of Clotho. However, a logical model of juxtaposition of the two different terrains, originally from points once distant, can be made for Clotho and Lakshmi (and perhaps other small tesserae as well).

The 4.5-km-high Danu Montes between Clotho and Lakshmi clearly indicate convergence. Parallel to the WSW trend of the eastern Danu Montes is a distinct lineament, across which the character of the terrain changes (in some places radically), and the tessera ridges appear deflected. The deflection of ridges along a 50-km segment of this Danu lineament suggests drag caused by right-lateral offset. At the northeast extent of both Danu Montes and Clotho Tessera is a 120-km-wide diffuse lineament zone (DLZ) trending southeast. These lineaments are traceable for 700 km before they disappear, apparently buried for almost 500 km by flows from the northeast that are related to a large volcano-tectonic depression whose southeast rim is roughly defined by Valkyrie Fossae. Beyond Valkyrie Fossae, a similar lineament zone continues an additional 800 km southeastward before abruptly terminating 150 km short of Sigrun Fossae. (The abrupt termination follows a line subparallel to Sigrun Fossae -- itself nearly perpendicular to the lineament zone -- and is probably one of the faults which form the Sigrun rift valley). This eastern segment of the DLZ is 100 km wide near Valkyrie and fans out eastward to as much as 400 km or more wide near Sigrun.

I suggest that Clotho Tessera was once part of Fortuna Tessera, but was cut off by a transcurrent fault zone (the DLZ) striking perpendicular to the Sigrun "rift" [1,2] and carried westward where it collided with Lakshmi Planum (forming Danu Montes). A gravity anomaly along the southern border of Lakshmi, in the area of Danu Montes, has been interpreted as indicating subduction there [3], providing additional supporting evidence for the collision hypothesis. The Danu Montes right-lateral fault(?) is explained by the obliquity of the collision of Clotho with Lakshmi (the path of least resistance for the migrating terrain being toward the southwest).

Diffusion of the DLZ with proximity to Sigrun Fossae may be due to either higher ductility near the postulated Sigrun "rift", or to burial by flows away from the rift nearer to Valkyrie Fossae. (The latter hypothesis is reinforced by inselbergs of the sheared-type terrain near Valkyrie). If this is indeed the case, it indicates that the visibility of transcurrent structures resulting from crustal movements may be difficult to see in the plains, due to much higher ductility there and/or to burial by the plains-forming flows.

Other possible examples of migrating tesserae occur elsewhere: small pieces of Ananke Tessera can be fit back together as though they had rifted apart, and the spreading apart of Ananke and Virilis Tesserae has been suggested because of their symmetric locations about the axis of an inferred spreading zone [4]. Other tessera fragments appear to have been isolated by rifting, with little, if any, significant lateral motion (e.g., Meni and Tellus Tesserae, and Tethus and Fortuna Tesserae). The migrating terrain model for Clotho Tessera supports Sukhanov's [5] interpretation of tesseral fragments as rafts of lighter crustal material.

## References

- [1] Pronin, A.A., et al., 1986, A geologic and morphological description of Lakshmi Planum, Astron. Vestnik, 20, 83-98.
- [2] Kozak, R.C., and Schaber, G.G., 1987, A spreading center on Venus?, Lunar Plan. Sci., XVIII, 513-514.
- [3] Janle, P., and Janssen, D., 1984, Tectonics of the southern escarpment of Ishtar Terra on Venus from observations of morphology and gravity, Earth, Moon, and Planets, 31, 141-155.
- [4] Sukhanov, A.L., 1986, Parquet: areas of regional plastic deformation, Geotektonika, 1986, no. 4, 60-76.
- [5] Sukhanov, A.L., et al., 1986, Geologic-morphological description of Laima Tessera area and Bereghiniya Planitia, Astron. Vestnik, 20, 272-286.

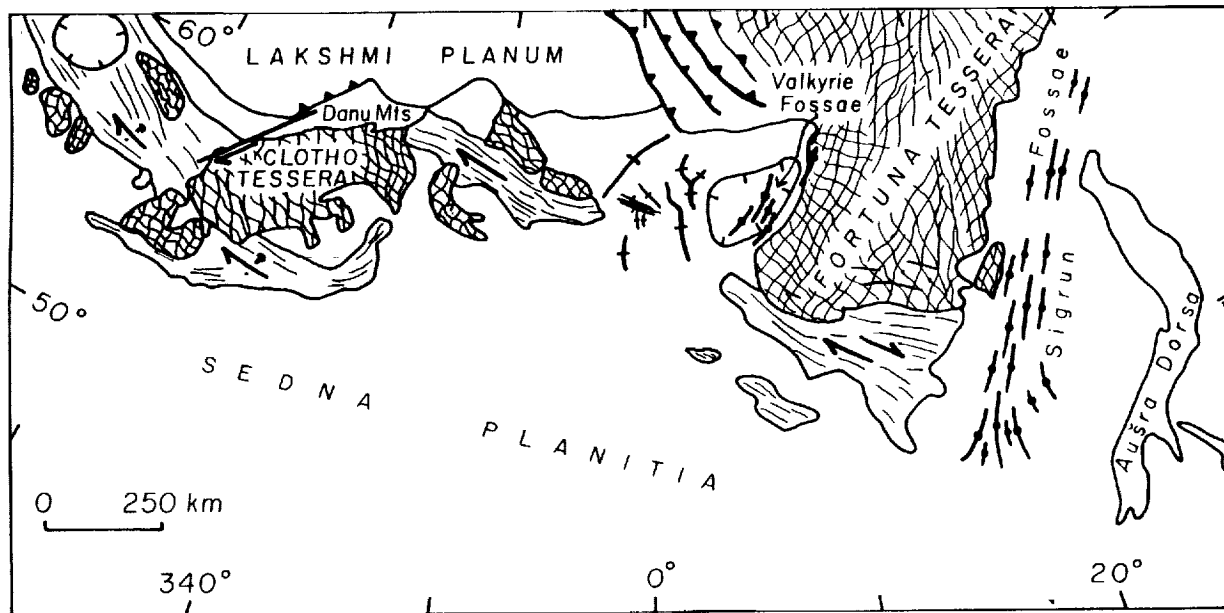
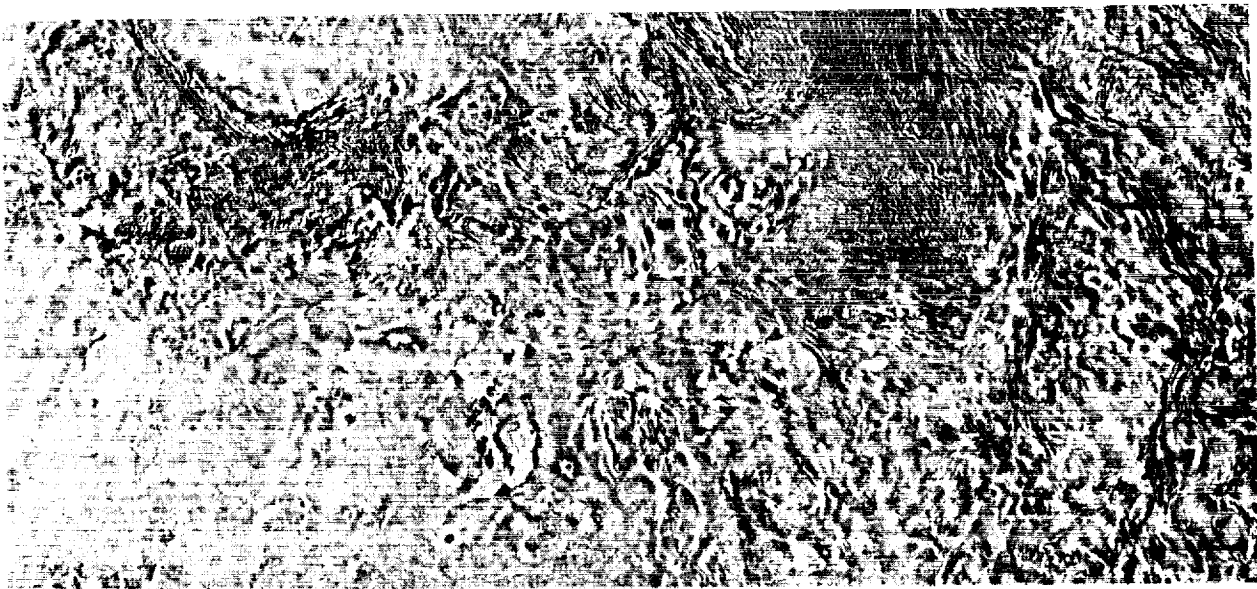


Figure 1. (top) Venera 15/16 mosaic of the suggested "Clotho-Sigrun shear zone" area. (bottom) Interpretive sketch map of the area.

TECTONISM ON VENUS: A REVIEW; Richard Kozak and Gerald G. Schaber,  
U.S. Geological Survey, Flagstaff, AZ 86001.

Venus is more similar to Earth than to any other planet. It has elevated regions associated with marginal fold and thrust belts, fracture zones that extend tens of thousands of kilometers, crustal swells and shields that are hundreds of kilometers in diameter and 1 to 2 km high, and sublinear accumulations of volcanic cones and domes that stretch for thousands of kilometers across the plains. The Venusian surface is, however, distinctly different from Earth's in that (1) its elevated terrains cannot be distinguished from its low plains on a hypsometric curve; (2) trenches have not been found plainsward of the marginal belts; (3) fracture zones bear no resemblance to mid-oceanic ridges; and (4) some features, such as the ridge-belt zone near 210° E, seem to have no terrestrial analog. Phillips and Malin (1983) stated that hypsograms may reflect the structure, composition, and erosion of a planet's lithosphere more than its tectonics. This statement might be modified as follows: observed global-scale morphology may reflect less the existence of (plate) tectonics on a planet than the environment in which the tectonic features were formed. Brass and Harrison (1982) and Phillips and Malin (1983), among others, have dealt with the problem of how manifestations of Venusian plate tectonism might differ theoretically from those of terrestrial plate tectonism, and they put restrictions on what can be occurring, given the data available.

Kaula and Phillips (1981) and Phillips and Malin (1983) estimated that current tectonic activity on Venus can be no more than 15% that of Earth's; other workers, using various approaches, have come to similar conclusions. Some, such as Phillips et al. (1981), have suggested that plate tectonics on Venus ceased more than 1 Ga ago, while others, such as Meissner (1983), believe that Venus is still in its "alpha" tectonics stage wherein shallow subduction is dictated by higher temperatures (as is postulated for the early Earth). The former hypothesis is supported by the crater-age estimates of Ivanov et al. (1986) and Basilevsky et al. (1987), whereas surface-age estimates by Shoemaker and Shoemaker (in press) tend to support the latter contention. Maxwell Montes (about 12 km above mean radius) seems to exemplify young tectonism, because such relief does not appear capable of having survived more than a few hundred million years under the the present thermal environment (Solomon and Head, 1982). Because presently there are good arguments for both views, the placing of the observed "impact craters" in context by careful mapping from the Magellan images will go a long way toward resolving this issue.

#### References

- Basilevsky, A.T., et al. (1987) Jour. Geophys. Res., 92, 12,869-12,901;  
 Brass, C.G., and Harrison, C.G.A. (1982) Icarus, 49, 86-96.  
 Ivanov, B.A., et al. (1986) Jour. Geophys. Res., 91, D413-430.  
 Kaula, W.M., and Phillips, R.J. (1981) Geophys. Res. Lett., 8, 1187-1190.  
 Meissner, R. (1983) Annales Geophysicae, 1, no. 2, 121-127.  
 Phillips, R.J., et al. (1981) Science, 212, 879-887.  
 Phillips, R.J., and Malin, M.C. (1983) in Venus, Univ. of Arizona Press,  
 Tucson, Ariz.  
 Shoemaker, E.M., and Shoemaker, C.S. (in press) in The New Solar System, Sky  
 Publishing Corp., Cambridge, Mass.  
 Solomon, S.C., and Head, J.W. (1982) Jour. Geophys. Res., 87, 9236-9246.

SURFACE COMPOSITION AND PETROLOGY John S. Lewis, Lunar and Planetary Lab., University of Arizona, Tucson AZ 85721. The available lines of evidence regarding the bulk composition, mineralogy and petrology of the surface of Venus are reviewed critically. The principal sources of data on the surface chemistry are Earth-based spectroscopic studies and Venera and Pioneer Venus entry probe studies of the atmospheric composition, in-situ radiochemical assays for potassium, uranium, and thorium by Venera landers, and Earth-based radar reflectivity measurements. The inferential process by which these disparate types of information are used to draw petrological conclusions is described, with emphasis upon the uncertainties inherent in such indirect methods. Recent works relevant to the planetary water budget and the hydrogen isotopic composition of the atmosphere are reviewed because of their intimate connection with the oxidation and hydration state of surface minerals and the equilibrium maintenance of hydrogen halides via atmosphere-surface interactions.

CRATER IDENTIFICATION AND RESOLUTION OF LUNAR RADAR IMAGES  
H. J. Moore, U. S. Geol. Survey, Menlo Park, CA 94025  
T. W. Thompson, Jet Propulsion Laboratory, Pasadena, CA 91109

Our study has three principal results: (1) The percentage of craters that can be identified increases with diameter or relief for any given resolution, but craters are not identified at all diameters and relief. (2) Relations between the percentage of identified craters and their dimensions depend on the size-frequency distributions of both diameters and relief and their interrelations. (3) Identification of craters is strongly dependent on the resolutions of the radar images. Our data also indicate that crater identification depends on crater age, that the effect of background terrain is uncertain, and that angle of incidence of radar illumination has a modest effect, if any, on crater identification. The ability to recover an actual crater size-frequency distribution from radar images diminishes with increasing size of the resolution elements because of the results listed above. Good agreement between the actual distribution and the one derived from radar images is attained if the crater diameters are at least 10 times larger than the resolution of the radar images. Our results are important considerations in geologic interpretations of radar images because conclusions about geologic processes, estimates of ages of planetary surfaces based on crater statistics, and assessments of size-frequency distributions of other landforms depend on resolution. We expect that the high-resolution radar images of Venus to be acquired from orbit during the Magellan mission will reveal at least 64 times more craters and volcanic landforms than are known today.

(Abstract from: Moore, H. J. and Thompson, T. W., 1988, Crater identification and resolution of radar images: Proc. 18th Lunar and Planet. Sci. Conf., p. 383-395).

EXTENSIONAL TECTONISM IN THE SOUTHWESTERN UNITED STATES;  
Ivo Lucchitta, U.S. Geological Survey, Flagstaff, Arizona 86001.

The Basin and Range Province of the American Cordillera is a textbook example of extensional tectonics: regional exposures are good and structural relations with the more stable terrane to the east provide useful constraints on models for the extension.

The tutorial will provide a sketch of the development of ideas regarding the nature of the extensional orogen, with a bias toward western Arizona and eastern California (with which I am most familiar). The sketch will be followed by a brief description of salient features, including the characteristics of the Highly Extended Terranes ('Metamorphic core complexes'), the 'classic' Basin and Range terrane (horst-and-graben structure), the Arizona Transition Zone, and the Colorado Plateau, together with an analysis of models that have been advanced to explain these terranes and their mutual relationships. If time permits, I will conclude with my own (probably outrageous) thermomechanical model.

VENUS: MANTLE CONVECTION, HOTSPOTS, AND TECTONICS  
R.J. Phillips, Dept. of Geological Sci., Southern Methodist Univ., Dallas, TX 75275

**Introduction.** The putative paradigm that planets of the same size and mass have the same tectonic style led to the adaptation of the mechanisms of terrestrial plate tectonics as the *a priori* model of the way Venus should behave. Data acquired over the last decade by Pioneer Venus, Venera, and ground-based radar have modified this view sharply and have illuminated our lack of detailed understanding of the plate tectonic mechanism.

**Earth.** For reference, we briefly review terrestrial mechanisms. The ocean basins make up 70% of the Earth's surface and the vast majority of interior heat escaping from this region does so from the midocean ridges in the process of seafloor spreading (more than 60% of the Earth's total heat loss [1]). Hotspot heat flow (e.g., Hawaii) produces a minor component. The relationship of seafloor spreading and subduction to mantle convection has long been debated. In one view, the oceanic lithosphere is the thermal boundary layer of either upper mantle or whole mantle convection. Another view is that the lithospheric plates are uncoupled from the underlying mantle by a low viscosity zone (~ the asthenosphere), that midocean ridge rifting is a passive phenomenon, and that seafloor spreading does not *directly* reflect the underlying mantle convection. Besides the obvious arguments regarding the midocean ridges, there is considerable debate as to the direct role of convection in any tectonic process observed on the Earth. This applies to both hotspot swells such as Hawaii [2] and direct convective coupling into the lithosphere [3].

Lithospheric evolution is well understood in the terrestrial ocean basins in terms of a conductively cooling, moving thermal boundary layer, at least for ocean floor ages less than about 70 Ma. The evolution of continental lithosphere is more problematical, but might best be understood in terms of arc accretion and compositional stabilization of cratons through the extraction of the basaltic component of the mantle [4], a process which becomes less efficient through time.

**Venus: Lithospheric Divergence.** On Venus there is nothing akin to the Earth in terms of a globally interconnected oceanic ridge system at constant elevation [5]. It has been suggested that Aphrodite Terra is a region of lithospheric divergence [6,7,8], but this hypothesis has been strongly challenged [9]. In any event, the existence of (companion?) subduction zones has not been established by the observation of trenches, despite imaging radar resolution of a few kilometers [10]. If a seafloor spreading cycle exists on Venus, then return of crustal material to the venusian mantle takes place by a process whose surface manifestations are not easily recognized (e.g., lithospheric delamination [11].)

**Venus: Hotspot Model.** It has been proposed [12,13] that in the absence of plate tectonics, hotspots (convective plumes passing their heat flux through a thermally thinned lithosphere) are the primary way in which Venus removes its internal heat. This hypothesis is based partly on large apparent depths (> ~ 100 km) of compensation (ADCs), as interpreted from gravity data, of many topographic features. The implication is that, given the present surface temperature and chondritic or Earth-like heat sources [13], the compensating density anomalies supporting topography cannot be passively or isostatically maintained. Hence they must be part of a convective flow system dynamically supporting hotspot topography. A more recent interpretation [14] suggests that compensation of regional topographic highs is provided in many places by a combination of thermal isostasy from a thinned lithosphere [15] and dynamic compensation from sublithospheric flow. The ADC value for any feature furnishes a guide to the relative contribution of each mechanism.

In summary, Venus may lose most of its heat by conduction through the litho-

sphere, with enhanced heat loss provided at hotspots [15]. Calculations show that the hotspot surface area occupies about 35 times the area of the Hawaiian swell. An additional observation supporting conductive heat loss is that the resurfacing rate of Venus is low; crater statistics suggest a volcanic flux no greater than  $2 \text{ km}^3/\text{yr}$  [16], compared to a value of  $17 \text{ km}^3/\text{yr}$  associated with the generation of oceanic crust on Earth.

**Venus: Horizontal Deformation.** This tidy picture of the way Venus works was interrupted by the scenes revealed in high resolution radar images from Veneras 15/16 and Arecibo. It is clear that certain regions of the planet have undergone intense tectonic disruption; such deformation is undoubtedly the result of large-scale compressional and extensional horizontal forces [17,18]. What we do not know is the age of the tectonism.

If we cannot find evidence for lithospheric divergence on Venus, then it would be fruitful to demonstrate a link between hotspot tectonism and the postulated large horizontal forces. However, at long wavelengths, where flexural effects may be unimportant, simple compensated uplift of a lithospheric layer will lead to tensional stresses in the "uplands." But there will be no stress in the surrounding "plains," unless the lithosphere starts to creep. This is because the local potential energy anomaly associated with topography is supported by local stresses [19]. Out in the plains there is no potential energy anomaly (or defect). Topographic highs might be expected to spread into the lowlands, particularly by creep in the lower portions of a crust. Such effects, however, cannot be expected to affect the plains more than a distance of approximately the horizontal dimension of the uplift [20].

We can speculate, then, that any link between hotspots (with associated convective flow in the mantle) and horizontal disruption of the lithosphere must be a direct one; i.e., the tectonic response must occur in the same region as the mantle dynamical process. We have proposed [21,22] that direct coupling by convective flow with the lithosphere indeed provides sufficient horizontal stress to induce a significant tectonic response. The magnitude of the response can be estimated directly from free air gravity data. Additionally, it has been suggested that the formation and evolution of Ishtar Terra can be directly related to mantle flow processes [17,23,24]. Alternative scenarios for Ishtar Terra require large scale motion of crust [25], but the driving forces have not been identified. The ridge belts of the northern plains are a possible region of considerable extension [26], but lack the thermal topographic signature associated with lithospheric spreading on the Earth. Alternatively, this activity happened in the geological past, and we are observing the fossilized tectonic remains.

**References.** [1] Sclater, J.G., and B. Parsons, *J. Geophys. Res.*, 86, 11,535-11,552, 1981; [2] Sandwell, D.T., and M.L. Renkin, *J. Geophys. Res.*, 93, 2775-2783, 1988; [3] Buck, W.R., and E.M. Parmentier, *J. Geophys. Res.*, 91, 1961-1974, 1986; [4] Jordan, T.H., *Phil. Trans. R. Soc. Lond. A*, 301, 359-373, 1981; [5] Kaula, W.M., and R.J. Phillips, *Geophys. Res. Lett.*, 8, 1187-1190, 1981; [6] Head, J.W., and L.S. Crumpler, *Science*, 238, 1380-1385, 1987; [7] Crumpler, L.S., and J.W. Head, *J. Geophys. Res.*, 93, 301-312, 1988; [8] Crumpler, L.S., and J.W. Head, *Lunar and Planetary Sci. XX*, Lunar and Planetary Institute, Houston, 214-215, 1989; [9] Grimm, R.E., and S.C. Solomon, *J. Geophys. Res.*, in press, 1989; [10] Barsukov, V.L., and 29 others, *J. Geophys. Res.*, 91, D378-D398, 1986; [11] Turcotte, D.L., *J. Geophys. Res.*, 94, 2779-2785, 1989; [12] Phillips, R.J., and M.C. Malin, in *Venus*, D.M. Hunten et al., eds., 159-214, Univ. of Arizona Press, Tucson, 1983; [13] Phillips, R.J., and M.C. Malin, in *Ann. Rev. Earth. Planet. Sci.*, 12, 411-443, 1984; [14] Smrekar, S., and R.J. Phillips, *Lunar Planet. Sci. Conf. XX*, Lunar and Planetary Institute, Houston, 1028-1029, 1989; [15] Morgan, P., and R.J. Phillips, *J. Geophys. Res.*, 88, 8305-8317, 1983; [16] Grimm, R.E., and S.C. Solomon, *Geophys. Res. Lett.*, 14, 538-541, 1987; [17] Basilevsky, A.T., *Geotectonics*, 20, 282-288, 1986; [18] Markov, M.S., *Geotectonics*, 20, 306-313, 1986; [19] Artyushkov, E.V., *J. Geophys. Res.*, 78, 7675-7708, 1973; [20] Bindshadler D.L., J.W. Head, and E.M. Parmentier, *Icarus*, in press, 1989; [21] Phillips, R.J., *Geophys. Res. Lett.*, 11, 1141-1144, 1986; [22] Phillips, R.J., *J. Geophys. Res.*, in press, 1989; [23] Kiefer, W.S., and B.H. Hager, *Lunar Planet. Sci. Conf. XX*, Lunar and Planetary Institute, Houston, 520-524, 1989; [24] Bindshadler D.L., and E.M. Parmentier, *Lunar Planet. Sci. Conf. XX*, Lunar and Planetary Institute, Houston, 78-79, 1989; [25] Vorder Bruegge, R.W., and J.W. Head, *Lunar Planet. Sci. Conf. XX*, Lunar and Planetary Institute, Houston, 1162-1163, 1989; [26] Sukhanov, A.L., *Lunar Planet. Sci. Conf. XX*, Lunar and Planetary Institute, Houston, 1085-1086, 1989.

**RADAR SCATTERING FROM DESERT TERRAINS, PISGAH/LAVIC REGION, CALIFORNIA: IMPLICATIONS FOR MAGELLAN;** J. J. Plaut, R. E. Arvidson, McDonnell Center for the Space Sciences, Department of Earth and Planetary Sciences, Washington University, St. Louis, Missouri 63130, S. Wall, Jet Propulsion Laboratory, 4800 Oak Grove Drive, Pasadena, California 91109.

A major component of the 1988 Mojave Field Experiment (Wall et al., 1988) involved the simultaneous acquisition of quad-polarization multi-frequency airborne SAR imaging radar data and ground measurements thought to be relevant to the radar scattering behavior of a variety of desert surfaces. In preparation for the Magellan mission to Venus, the experiment was designed to explore the ability of SAR to distinguish types of geological surfaces, and the effects of varying incidence angles on the appearance of such surfaces. The airborne SAR system acquired images at approximately 10 m resolution, at 3 incidence angles (30°, 40°, 50°) and at 3 wavelengths (P: 68 cm, L: 24 cm, C: 5.6 cm). The polarimetric capabilities of the instrument allow the simulation of any combination of transmit and receive polarizations during data reduction (Zebker et al., 1987; vanZyl et al., 1987). Calibrated trihedral corner reflectors were deployed within each scene to permit absolute radiometric calibration of the image data. We will report on initial analyses of this comprehensive radar data set, with emphasis on implications for interpretation of Magellan data.

Detailed site characterization and sample collection were conducted at 5 compositionally and/or texturally distinct sites within the Pisgah Volcanic Field/Lavic Lake area. These included: a smooth undisturbed playa surface; a playa surface covered with basaltic cobbles; a moderately vegetated alluvial surface; and 2 basaltic lava flow surfaces of contrasting roughness.

Total (unpolarized) backscattered power values are well-correlated with ground determinations of wavelength-scale roughness for the various sites. For example, differences in measured backscattered power between the smooth and cobble-strewn playa surfaces are minor in P-band (<1 dB) and L-band (<4 dB), but are large (>5 dB) in C-band. This is clearly due to the presence of scattering elements (cobbles) which occur primarily at the scale of the C-band wavelength (5-20 cm). A similar effect is seen at the two lava flow sites. Backscattered power differences between the rough (aa) and less rough (pahoehoe) surfaces are >4 dB in P- and L-band but <2 dB in C-band. In this case the longer wavelength bands are sensitive to the dominant roughness differences of the two sites, while the relatively uniform C-band response results from a common small-scale roughness.

Preliminary analysis of incidence angle effects indicates that all of the surface types exhibit the expected decrease in backscatter strength with increasing incidence angle. Future work will examine this effect in more detail, in the context of model scattering laws. In HH-polarized data, the two playa surfaces are better separated at large incidence angles, as are the aa and pahoehoe lava flows. Near-range (low incidence angle) observations suffer from increased speckle noise and saturation from radar-facing slopes.

Work to be reported in the workshop poster session will address the effects of incidence angle, look azimuth and resolution on distinguishing among units. Future work will utilize the unique polarimetric data, along with absolute calibrations at

multiple wavelengths, to develop and test models for inversion of image data for extracting geologically important properties of surfaces.

#### REFERENCES

- VanZyl, J.J., H.A. Zebker, and Charles Elachi (1987) Imaging radar polarization signatures: Theory and observation; Radio Sci., 22, 529-543.
- Wall, S., vanZyl, J.J., Arvidson, R.E., Theilig, E., and R.S. Saunders (1988) The Mojave field experiment: Precursor to the planetary test site (abstract), Bull. Am. Astr. Soc., 20, 809.
- Zebker, H.A., J.J. vanZyl, and D.N. Held (1987) Imaging radar polarimetry from wave synthesis; J. Geophys. Res., 92, 683-701.

**LAKSHMI PLANUM: A DISTINCTIVE HIGHLAND VOLCANIC PROVINCE;** Kari M. Roberts and James W. Head, Dept. of Geological Sciences, Brown University, Providence, R. I. 02912

**Introduction-** Lakshmi Planum, a broad smooth plain located in western Ishtar Terra and containing two large oval depressions (Colette and Sacajawea), has been interpreted as a highland plain of volcanic origin.<sup>1-5</sup> Lakshmi is situated 3-5 km above the mean planetary radius and is surrounded on all sides by bands of mountains interpreted to be of compressional tectonic origin (Fig. 1).<sup>5-7</sup> Four primary characteristics distinguish Lakshmi from other volcanic regions known on the planet, such as Beta Regio: 1) high altitude, 2) plateau-like nature, 3) the presence of very large, low volcanic constructs with distinctive central calderas (Colette and Sacajawea), and 4) its compressional tectonic surroundings. Building on the previous work of Pronin,<sup>5</sup> the purpose of this study is to establish the detailed nature of the volcanic deposits on Lakshmi, interpret eruption styles and conditions, sketch out an eruption history, and determine the relationship between volcanism and the tectonic environment of the region. The following is revised and reprinted from a previous abstract,<sup>13</sup> intended as a review for the Flagstaff Venus Geoscience Workshop. A more detailed, thorough discussion and interpretation of features and units on Lakshmi Planum may be found in a paper to be submitted to the *Journal of Geophysical Research*, entitled "Characterization and Interpretation of Lakshmi Planum, Venus: A Distinctive Highland Volcanic Province."

**Observations and Interpretations-** On the basis of our detailed mapping we have compiled a province map (Fig 1.) that illustrates some of the basic characteristics and relationships in Lakshmi Planum. **Major shields/calderas:** Two major caldera structures (Colette, C; Sacajawea, S) and their circumferential low-shield-forming flow deposits dominate the region. Colette is 130 x 180 km, elongated in a N-S direction, is approximately 1-2 km deep<sup>4,5</sup> and is surrounded by an extensive radiating system of flows having an average width of 15 km, and lengths of 100-300 km. The shield structure surrounding Colette is about 500 x 700 km in dimension and descends about 1 km from the rim to the surrounding plains. Sacajawea is a 200 x 120 km oval-shaped depression elongated in a SW-NE direction, approximately 1.5-2 km deep, and lacks the distinct radial lobate flow patterns of Colette, although mottled deposits surrounding Sacajawea, and distinct from the undivided plains, have been mapped extending about 300 km from the center of Sacajawea. The Sacajawea shield structure (defined by the caldera and the surrounding deposits) is very low (less than 1 km from the rim to the surrounding plains). On the basis of the relative crispness and distinctiveness of the flows and structures comprising the Colette shield, it is interpreted to be younger than Sacajawea.<sup>4,5</sup> Elsewhere, we have described the characteristics and relationships of Colette and Sacajawea calderas.<sup>8</sup>

A wide range of additional structures interpreted to be **volcanic source vents** have been mapped including: 1) **domes and cones**, which range from 1-50 km in diameter and include **small cones** (<10 km diameter) scattered throughout the region; **small domes** (10-15 km in diameter) sometimes containing summit depressions and apparently preferentially located in association with structural features (e.g., inside Colette, along a rift associated with Sacajawea, and within the Ridged Terrain); and **low shields**, up to 75 km across, almost indiscernible topographically, and containing a summit pit; 2) **Diffuse halo** (Fig. 1, [1]); SE from Colette is a large, dark semicircular feature about 50 km in diameter surrounded by an elongated halo of diffuse radar-bright deposits that are apparently superimposed on the more distinct flow deposits of Colette. The diffuse character, the lack of distinctive lobate patterns, the elongation and the superposition of the deposits suggest that they may be of pyroclastic origin; 3) **Vent Complex** (Fig. 1, [2]); flanking Sacajawea to the S-SW is a very broad (~200 km diameter) radar-bright feature that lacks distinctive topographic expression in the currently available altimetry. It appears to be a localized center of volcanism, characterized by very mottled lobate flow deposits which become more continuous towards a central region containing numerous volcanic craters and domes.

**Plains units** dominate the surface of Lakshmi and are interpreted to be volcanic on the basis of their embayment relationships, their flatness and uniform albedo, and their association with volcanic source vents. **Undivided Plains units (PU)** are characterized as smooth low-albedo plains in which individual flow features are not seen in either Venera 15/16 or Arecibo data. They cover a large part of Lakshmi, and may be derived from the major shields, from the numerous domes and cones, or from presently buried sources. **Grooved Plains (PG)** occur in a single patch about 150 km to the north of Sacajawea and are typified by very finely spaced furrows or grooves arranged in sweeping curvilinear sets trending generally N-S but frequently curving to the NE or NW. This system of faults<sup>5</sup> appears to be extensional in origin, and is embayed by Sacajawea deposits and undivided plains. **Ridged Plains (PR)** are defined by faint bright lineaments on plains material arranged in subparallel sets that follow the borders of the planum or trend S-SE across it. On the basis of the ridge-like nature of some of these bands, and their association with the compressional deformation in the surrounding orogenic belts, we have interpreted them to be of compressional origin. The parallelism of many of these ridged units with the adjacent orogenic belts, and the general tilting of the ridged plains away from the mountains, strongly suggest that the plains have been involved in at least the latter phases of deformation producing the orogenic belts.

**Structural features and units** occur within the plains, as well as dominating the surrounding mountains. **Ridged Terrain (RT)** is characterized by a very rough-textured system of ridges and grooves and is concentrated in east central Lakshmi where, in at least one occurrence, the ridges and grooves are arranged in rhomboidal sets with the small angle subtending about 35° and the bisectrix oriented about N35°W. Virtually all other units are superposed on or embay RT, and we thus concur with Pronin<sup>5</sup> that this unit is representative of an episode of deformation early in the history of Lakshmi. Adjoining Sacajawea to the SE is a system of linear features interpreted by Pronin<sup>5</sup> to be fault scarps with characteristics similar to graben, at least one of which contains a volcanic dome. This may be a flanking rift zone similar to those occurring on

Hawaii. In addition, a series of domes and cones appear to be arrayed in a preferred orientation, trending E-SE along a line connecting Colette and Sacajawea.

#### Conclusions-

1) Volcanic style: The range of deposits and structures mapped in Lakshmi Planum indicates that the region is dominated by at least three styles of volcanism: a) centralized effusive, very large low shield structures (>500 km) with numerous long flows and extremely large calderas<sup>8</sup> (100-200 km); b) distributed effusive, with a wide range of source vents most typically forming cones and domes in the 1-50 km diameter size range; although dispersed throughout Lakshmi, many are localized along structural trends; on the basis of their radar characteristics, most mapped effusive deposits appear to be relatively smooth at scales of decimeters to meters; c) possible pyroclastic, represented by the Diffuse Halo; if further mapping confirms a pyroclastic origin, this would imply the presence of volatile-rich magmas on Venus.<sup>9</sup>

2) Sequence and Geologic History: Formation of the Ridged Terrain was followed by emplacement of plains which were subsequently deformed to produce the Grooved Plains N of Sacajawea. Sacajawea was formed and its related deposits embayed the Grooved Plains and Ridged Plains. Although brighter than those of Sacajawea, the deposits of the Vent Complex appear truncated by the large caldera; we thus interpret it to be older than Sacajawea. Colette and its associated flows were formed subsequent to Sacajawea, but it is not known if activity in the two structures overlaps in time. The Diffuse Halo appears to postdate Colette. Ridged Plains appear to have formed throughout the history of Lakshmi, apparently deforming in response to compressional deformation and regional tilting in the adjacent mountain ranges. Ivanov et al<sup>10</sup> have argued that the radar brightness (decimeter to meter scale roughness) associated with fresh impact crater haloes is lost by a smoothing process after about 120-250 my. If this is true, and bright units on Lakshmi have a similar roughness, then this may imply that at least some of the volcanism occurred relatively recently.

3) Relation to Tectonic Deformation: There is abundant evidence for the synchronicity of volcanism and tectonism (elongation of calderas, rift zones adjacent to calderas, association of domes and cones with preexisting structure, Grooved Plains, Ridged Plains of various ages and orientations, etc.). Further analysis is required to determine the sequence of deformation in the adjacent orogenic belts and its link to Lakshmi volcanic history, but it tentatively appears that the center of volcanism has migrated from east to west during the history of Lakshmi. 4) Distinctiveness of Lakshmi Planum: Our studies further emphasize the unique nature of Lakshmi Planum in terms of its compressional tectonic environment, altitude, and presence of large low shields with extremely large calderas. No other such volcanic province has yet been identified on Venus.

5) Origin of Lakshmi Planum: On the basis of the presence of distributed regional compressional deformation surrounding Lakshmi Planum,<sup>6-7,11-12</sup> the sense of tectonic transport in toward Lakshmi from the north<sup>11</sup> and the east,<sup>12</sup> the evidence for crustal thickening in Freyja and Maxwell Montes in excess of several tens of kilometers,<sup>11-12</sup> and the topographic elevation of the plateau itself, we interpret Lakshmi Planum to be the locus of convergence and crustal thickening, and the volcanic activity there to be linked to melting associated with processes of convergence and crustal thickening. This model is in contrast to that of Pronin,<sup>5</sup> who attributes the volcanism to a large hot spot upwelling below Lakshmi, and spreading laterally to cause the surrounding deformation.

References: (1) H. Masursky, *et al.* (1980) *JGR*, **85**, 8232; (2) V. Barsukov, *et al.* (1986) *JGR*, **91**, D378; (3) A. Basilevsky, *et al.* (1986) *JGR*, **91**, D399; (4) E. Stofan *et al.* (1987) *Earth, Moon*, **38**, 183; (5) A. Pronin (1986) *Geotectonica*, **4**, 26 (in Russian); (6) Campbell *et al.* (1983) *Science*, **221**, 644; (7) Crumpler *et al.* (1986) *Geology*, **14**, 1031; (8) Magee and Head (1988) *Lunar Planet. Sci.*, **XIX**, 711; (9) Head and Wilson (1986) *JGR*, **91**, 9407; (10) B. Ivanov, *et al.*, (1986) *JGR*, **91**, D413; (11) Head (1988) *Lunar Planet. Sci.*, **XIX**, 467; (12) Vorder Bruegge and Head (1988) *Lunar Planet. Sci.*, **XIX**, 1220, (13) Magee and Head (1988) *Lunar Planet. Sci.*, **XIX**, 713.

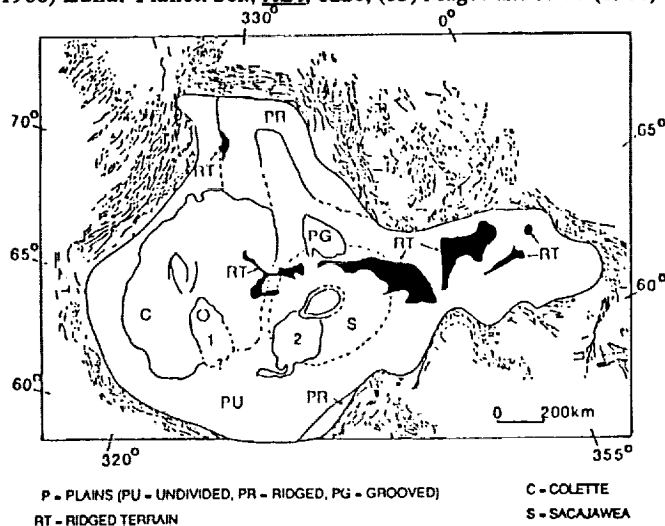


Figure 1. Province map of Lakshmi Planum. See text for explanation. Lines outside of Lakshmi Planum indicate structural trends in adjacent deformed terrain.

**VOLCANISM ON VENUS: LARGE SHIELDS AND MAJOR ACCUMULATIONS OF SMALL "DOMES"; G.G. Schaber and R.C. Kozak; U.S. Geological Survey, Flagstaff, Arizona 86001**

The outer layers of the Venusian lithosphere appear to dissipate heat from the interior through mantle-driven thermal anomalies ("hot spots", "swells"). As a result, Venus exhibits diverse forms of "thin-skin" tectonism and magmatic transfer to and extrusion from countless numbers of volcanic centers (e.g., shields, paterae, domes) and volcano-tectonic complexes (e.g., coronae, arachnoids) [1]. We will summarize what is known about the distribution and morphologies of major Venusian shields, and describe the evidence for possible structural control of major accumulations as long as 5000 km of small volcanic "domes".

**LARGE VENUSIAN SHIELDS-** Approximately 40 major shields whose basal diameters exceed 200 km have been tentatively identified on Venus between lat 90° N. and 65° S. from analyses of PV, Venera 15/16, and Earthbased radar data. The gross morphologies and estimated volumes of ten major shields between lat 30° and 90° N. have been determined from Venera 15/16 data [2]. Nine of these shields have extremely low heights (0.7 to 2.3 km) despite large basal diameters (300 to 782 km); in this respect, the shields are similar to highland paterae on Mars (e.g., Hadriacia and Tyrrhena Paterae) and some paterae (e.g., Ra Patera) on Io. The tenth shield, Tepev Mons (western Bell Regio), is the notable exception. This shield is probably young [3]. It has a substantial height of 5.2 km and a basal diameter of 253 km, and it possesses a well-defined ring moat resulting from flexure of the lithosphere below the load [3].

Most large shields within the northern quarter of Venus are associated with the large concentration of coronae between lat 30° and 80° N. and long 238° and 272° and with Lakshmi Planum. The heights of 30 other shieldlike constructs (basal diameters >200 km) between lat 30° N. and 65° S. were found from PV altimetry to range between 0.8 and 3.9 km (average = 2.9 km). The larger Venusian shields, unlike the Tharsis shields on Mars, cannot achieve great heights, probably because of thermal conditions in the crust and lithosphere.

**MAJOR ACCUMULATIONS OF VOLCANIC "DOMES"-** Small (2- to 20-km-diameter) conical and domical landforms ("domes") are abundant on the surface of Venus; they are probably volcanoes [1]. Slyuta et al. [4] reported that domes in small "groups" (50-80 km across) and larger "clusters" (few hundred kilometers across) in some regions form "accumulations," which can extend for over 5000 km. Examples of accumulations have been identified in Tethus Regio and Atalanta and Niobe Planitiae; they are especially well developed between Akkruva Colles (northeastern Niobe Planitia) and Allat Dorsa ("Akkruva-Allat") and between Ananke Tesserae and Akkruva Colles ("Ananke-Akkruva"). Smaller concentrations of domes are found in Ganiki, Guinevere, Bereghinya, and Snegurochka Planitiae [4].

The largest lineal accumulation of small domes in the

northern quarter of Venus, Akkruva-Allat, is best developed at Akkruva Colles (lat 45°; long 118°). It is 600-1000 km wide and extends northwest-southeast for over 5000 km from northeastern Niobe Planitia (lat 40°, long 135°) to Allat Dorsa (lat 65°, long 70°) [4]. Most of the Akkruva-Allat heavily domed terrain is about 1 km higher than the adjacent smooth plains; a lineal positive gravity anomaly as great as 25 mgal is associated with this dome accumulation [4,5]. The concentration of domes in the middle and southern parts of Akkruva-Allat reaches 2344 domes per 10<sup>6</sup> km<sup>2</sup>, while the average number of domes within the entire area surveyed by Venera 15/16 (excluding areas of tesserae) is 200 per 10<sup>6</sup> km<sup>2</sup> [4].

The size, shape, and frequency distribution of domes within the Akkruva-Allat accumulation are similar to those of seamounts on the Earth's ocean floor, e.g., in the East Pacific Rise [4, 6-9]. Syluta et al. [4] concluded that some of the largest Venusian dome accumulations may be independent tectonic structures; however, they recognized no large-scale tectonic dislocations in the Akkruva-Allat and Ananke-Akkruva accumulations to support the idea that they are analogous to a linear heat anomaly of the ocean-ridge type. We have, however, recognized evidence for northeast- and northwest-trending structural control of these dome accumulations.

Most terrestrial oceanic seamounts are formed on very young, thin lithosphere that permits the passage of small volumes of magma; in older, thicker lithosphere, small magma bodies would cool before reaching the surface, although larger bodies might not. Thus, smaller seamounts are generally more abundant on the youngest, thinnest crust near a ridge crest, while the number of larger seamounts tends to increase on older, thicker crust away from the ridgecrest [6]. This suggests that small sources of melt exist near the ridge crests on the ocean floor to supply the small seamounts; sources of melt may also exist along the structures controlling the Ananke-Akkruva and Akkruva-Allat accumulations. Such magma sources are likely trapped remnants of extended heat anomalies originating at considerable depth. The Magellan image and altimetric data can be used to better understand the origin of these and other dome accumulations and to confirm or reject their analogy to an oceanic spreading ridge.

**REFERENCES CITED** [1] Barsukov, V.L. and 29 others, 1986, Proc. Lunar and Planet. Sci. Conf. XVI, J. Geophys. Res., 91, B4, D378-D398; [2] Schaber, G.G. and Kozak, R.C., 1989, Lunar and Planet. Sci. XX, Part 3, 954-955; [3] Janle, R.C., Janssen, D., and Basilevsky, A.T., 1988, Earth, Moon, and Planets, 41, 127-139; [4] Syluta, E.N., Nikolaeva, O.V., and Kreslavskii, M.A., 1988, Astron. Vestnik (in Russian), XXII, no. 4, 287-297; English transl. in Solar System Res., in press; [5] Bowin, C., 1983, Icarus, 56, 2, 345-372; [6] Abers, G.A., Parsons, B., and Weissel, J.K., 1988, Earth Planet. Sci. Lettrs., 87, 137-151; [7] Aubele, J.C., Head, J.W., and Syluta, E.N., 1988, Lunar and Planet. Sci. XIX, 21-22; [8] Smith D.K. and Jordan, T.H., 1988, J. Geophys. Res., 93, B4, 2899-2918; [9] Smith, D.K., 1988, Earth Planet. Sci. Lettrs., 90, 457-466.

IMPACT CRATERING AND THE SURFACE AGE OF VENUS: THE PRE-MAGELLAN CONTROVERSY; G.G. Schaber, Shoemaker, E.M., Shoemaker, C.S., and Kozak, R.C.; U.S. Geological Survey; Flagstaff, Arizona 86001

The average surface age of a planet is a major indicator of the level of its geologic activity and thus of the dynamics of its interior. Radar images obtained by Venera 15/16 from the northern quarter of the Venus (lat 30° to 90°) reveal about 150 features that resemble impact craters, and they were so interpreted by Soviet investigators B.A. Ivanov, A.T. Basilevsky, and their colleagues [1, 2]. These features range in diameter from about 10 to 145 km. Their areal density is remarkably similar to the density of impact structures found on the American and European continental shields [3].

The Soviet investigators interpreted the record of apparent impact craters as indicating a mean age for the observed surface of Venus of about 1 b.y. ( $\pm 0.5$  b.y.) [1,2,4]. Schaber et al. [5], however, pointed out that the observed Venusian craters may imply an average crater-retention age for the region surveyed no greater than the 450-million-year mean age of the Earth's crust, a result consistent with the expected thermal and tectonic history of Venus (whose size and mass, and probable composition are similar to Earth's).

The basic difference between the Soviet and American estimates of the average surface age of Venus's northern quarter is due to which crater-production rate is used for the Venusian environment. Cratering rates based on the lunar and terrestrial cratering records, as well as statistical calculations based on observed and predicted Venus-crossing asteroids and comets, have been used in both the Soviet and American calculations. The single largest uncertainty in estimating the actual cratering rates near Venus involves the shielding effect of the atmosphere. Melosh [6] has determined that breakup of stony asteroids during penetration of Venus' atmosphere would inhibit formation of craters much smaller than 20 km in diameter. In fact, the Venera 15/16 data indicate that relatively few of the apparent impact craters on Venus are smaller than 20 km.

Shoemaker and Shoemaker [3] suggested that the size distribution of Venusian impact craters with diameters >20 km is similar to the size distribution of young craters on the Moon. Because most young craters larger than 60 km in diameter on the Earth and Moon are probably due to cometary impact, most of the largest impact craters on Venus were also probably produced by cometary impact [3]. Applying their best estimate of the proportion of craters produced by asteroid impact, and using the cratering rate down to 20-km diameter found for the last 120 million years on Earth [7], Shoemaker and Shoemaker [3] found the mean age indicated for the surface surveyed by Venera 15/16 to be  $210 \pm 105$  million years, consistent with Venus' surface age reported earlier by Schaber et al. [5]. For the largest craters (50-100 km in diameter), assuming the expected crater production by cometary impact, Shoemaker and Shoemaker [3] found an average surface age of about 400 million

The Pre-Magellan Controversy  
Schaber G. G. et al.

years, which they recently concluded [3] is the most probable average age. Should some fraction of the impact craters identified by the Soviet scientists ultimately prove to be of volcanic origin [8], the average surface age could of course be younger. Statistical evidence for a non-random distribution of the suspected impact craters on Venus [9-11] strongly suggests the presence of terrains of different ages that may include regions of active volcanism and tectonism.

REFERENCES CITED: [1] Ivanov, B.A., Basilevsky, A.T., Kryuchkov, V.P., and Chernaya, I.M., 1986, Proc. 16th Lunar and Planet. Sci. Conf., J. Geophysical Res., 91, D413-430; [2] Basilevsky, A.T. and seven other authors, 1987, J. Geophys. Res., 92, B12, 12,869-12,901; [3] Shoemaker, E.M. and Shoemaker, C.S., in The New Solar System (revised edition by J. Kelly Beatty; Sky Publishing Corp., Cambridge, Mass. and Cambridge Univ. Press, Cambridge, England; [4] Ivanov, B.A. and Basilevsky, 1987, Solar System Res., 21, 2, 84-89 (translation from *Astronomicheskii Vestnik*, 21, 2); [5] Schaber, G.G., Shoemaker, E.M., and Kozak, R.C., 1987, Solar System Res., 21, 2, 89-94; [6] Melosh, H. J., 1981, in Multi-ringed Basins; Proc. 12th Lunar Planet. Sci. Conf., part A, 29-36; [7] Grieve, R.A.F., 1984, Proc. 14th Lunar Planet. Sci. Conf., J. Geophys. Res., 89, B403-B408; [8] Kozak, R.C. and Schaber, G.G., Repts. of the Planet. Geol. and Geophys. Program-1986, NASA TM 89810, 443-445; [9] Burba, G.A., 1989, Lunar Planet. Sci. XX, Abs. submitted to XX Lunar Planet. Sci. Conf., 123-124; [10] Plaut, J.J. and Arvidson, R.E., 1988, J. Geophys. Res., 93, B12, 15,339-15,340; [11] Plaut, J.J. and Arvidson, 1988, Repts. of the Planet. Geol. and Geophys. Program-1987, NASA TM4041, 410-412; [12] Wood, C.A. and Coombes, C.R., 1989, this volume.

## GEOLOGY OF THE VENUS EQUATORIAL REGION FROM PIONEER VENUS RADAR IMAGING. D. A. Senske and J. W. Head, Brown University, Providence, RI 02912.

**Introduction.** The surface characteristics and morphology of the equatorial region of Venus were first described by Masursky *et al.* (1) who showed this part of the planet to be characterized by two topographic provinces, rolling plains and highlands, and more recently by Schaber (2) who described and interpreted tectonic zones in the highlands. Using Pioneer Venus (PV) radar image data (15° S to 45° N), Senske and Head (3,4) examined the distribution, characteristics, and deposits of individual volcanic features in the equatorial region, and in addition classified major equatorial physiographic and tectonic units on the basis of morphology, topographic signature, and radar properties derived from the PV data (5). Included in this classification are: plains (undivided), inter-highland tectonic zones, tectonically segmented linear highlands, upland rises, tectonic junctions, dark halo plains, and upland plateaus. In addition to the physiographic units, features interpreted as coronae and volcanic mountains have also been mapped. In this paper, we briefly describe the latter four of the physiographic units along with features interpreted to be coronae.

**Upland rises** are defined as broad, radar-dark, topographic highs containing individual peaks which are commonly radar-bright and express typically 1.0- to 3.0-km of relief (4). Two regions designated as upland rises are Bell Regio and Eisila Regio. Bell Regio is a radar-dark topographic rise on which are located four peaks, Api Mons, Nefertiti, Tepev Mons, and an unnamed peak. On the basis of the presence of both radar-bright and radar-dark flows these mountains are interpreted to be volcanoes (4,6). Gravity modeling by Janle *et al.* (7) suggests a deep apparent depth of compensation (~200 km) for this region which they interpret along with geologic mapping to indicate support of topography by dynamic processes in the mantle. The second upland rise, Eisila Regio, length of 8000 km, forms the westward extension of Aphrodite Terra. The western part of Eisila Regio is a broad radar-dark topographic rise which exhibits properties similar to the surrounding plains. Located on the crest of the high topography are two volcanic mountains, Sif Mons and Gula Mons. Flows associated with these volcanoes appear to be of limited extent, forming a thin veneer, suggesting that this region was not built up entirely by volcanic construction. On the basis of the interpretation of volcanic deposits representing a thin veneer, the presence of material on broad topographic rises similar to that on the adjacent plains, and deep apparent compensation, formation of upland rises related to doming due to thermal uplift is proposed.

**Tectonic junctions** are radar-bright highlands located at the convergence of three or more inter-highland tectonic zones, and are centers of volcanism possessing individual mountains typically located at the crest of a domal topographic rise. Features mapped as tectonic junctions include Beta Regio, Atla Regio, Asteria Regio, northern Phoebe Regio, the region of convergence of Ulfrun Regio and Hecate Chasma, and an elevated region southeast of Atla Regio. The largest tectonic junctions, Atla Regio and Beta Regio are broad domal topographic rises on which are located large volcanic edifices, Ozza Mons and Maat Mons in Atla Regio, and Theia Mons and Rhea Mons in Beta Regio. On the basis of geologic mapping (8,9) and modeling of gravity data (10), these regions have been interpreted to be associated with deep mantle thermal anomalies. The tectonic junctions located at Asteria Regio and northern Phoebe Regio possess characteristics similar to Beta and Atla, and may have formed in similar manners, but are smaller. The combination of inter-highland tectonic zones and tectonic junctions forms an interconnecting network extending over half the circumference of the planet.

**Dark halo plains** are defined as broad quasi-circular regions of very low radar backscatter located in low lying areas and extending for hundreds of kilometers (4). A radar-bright circular feature or ring, which itself has a radar-dark interior is often found in the dark material. In high resolution image data these circular features correspond to craters, several of which are located on local topographic rises and are surrounded by lobate flow deposits suggesting a volcanic origin (5). The most extensive regions of dark halo plains are located to the west of Eisila Regio and west of Atla Regio. In the region west of Eisila Regio the radar-dark material appears to embay areas of higher topography suggesting emplacement by lava flooding. On the basis of the embayment relations expressed by the radar-dark material and the presence of deposits associated with the interior craters which are interpreted to be volcanic, it is suggested that the dark halo plains are regions of smooth lava flows with the interior crater being a source region of some of these deposits.

**Upland plateaus** are broad, bright to mottled-bright, plateaus covering areas of hundreds of square kilometers typically bounded by steep scarps standing 1 to 2 kilometers above the surrounding plains (5). Few individual peaks are present or they are entirely absent. Central troughs similar to those associated with Beta and Aphrodite are not observed. Specific upland plateaus are located north of Asteria Regio, on the eastern flanks of Beta Regio, at Phoebe Regio, adjacent to Ovda Regio and Thetis Regio, in the southern hemisphere at Alpha Regio, and at Tellus Regio. Venera imaging of Tellus Regio shows it to possess a complex tectonic structure of intersecting valleys and ridges and is mapped as tessera (11). A comparison of radar properties indicate that both upland plateaus and tessera are characterized by high roughness, low values of uncorrected reflectivity, and that they contain a large percentage of wavelength-scale (5-50 cm) diffuse scatterers (12). On the basis of topographic signature, radar properties, and correlations with units mapped as tessera from Venera imaging, it is suggested that areas mapped as upland plateaus are tectonic units similar to tessera (5).

Within the PV data **coronae** are characterized by locally elevated topography, narrow radar-bright discontinuous rims, and radar-dark interiors (13). Similar characteristics are observed for coronae mapped in Mnemosyne Regio from both Arecibo and Venera radar images (14). On the basis of this characterization, two large circular features interpreted as coronae are identified in the area imaged exclusively by PV. The first, Pavlova, is located in eastern Eisila Regio (15° N, 40° E), is elliptical with dimensions of 525 km x 370 km, and is characterized by a 50-km wide discontinuous

rim which exhibits 200 to 600 m of relief. The discontinuous part of the rim corresponds with flanking topographic depressions mapped as very dark that are similar to units mapped elsewhere as volcanic plains and suggests that lava flows have breached the rim. The second (840 km diameter) corona is located to the south of western Eisila Regio (2.0° N, 355.0°). Like Pavlova, this structure is characterized by a discontinuous rim which is radar-bright and elevated to the south while the northern rim possesses no topographic relief and is mottled dark (5). Stratigraphic relations between the rim and radar-dark interior deposits suggests lava flooding, forming plains, has occurred in the interior of this structure. From this analysis, we find that the number of large coronae in the equatorial region to be much less than in the northern high latitudes (14,15).

**Discussion and Conclusions.** On the basis of variations in structure and morphology, the physiographic units are divided into three distinct longitudinal zones: upland rises (330° to 55°), tectonically segmented linear highlands-upland plateaus (55° to 145°), and inter-highland tectonic zones-tectonic junctions (145° to 315°). The zone of upland rises contains the two highland structures of Bell Regio and Eisila Regio whose volcanic nature has been previously established (4,6,7). Eisila Regio is characterized by three distinct regions, western Eisila with its volcanic peaks Sif Mons and Gula Mons, central Eisila with the volcanic peak Sappho (16,17), and eastern Eisila Regio with its corona structure, Pavlova. Detailed analysis of western Eisila Regio suggests that the volcanoes and their deposits represent a thin veneer of material superimposed on a broad topographic high. In addition, ridges in the lowlands along the eastern flanks of western Eisila Regio are interpreted to be normal faults (18) whose relation to high topography is consistent with a model of uplift under extension (19). This arrangement of structures and association with volcanism in western Eisila suggests formation by doming associated with thermal uplift. A similar model has been previously proposed for Bell Regio (6,7). The region of tectonically segmented linear highlands and upland plateaus is made up of the highlands of western Aphrodite and Tellus Regio. Previous studies of the tectonically segmented linear highland of western Aphrodite show it to be characterized by bilaterally symmetric topography and an en echelon central trough offset in a right lateral sense along cross-strike structural and topographic discontinuities (CSD's) (20,21). The structure of western Aphrodite is similar to that of terrestrial mid-ocean ridges, and has on this basis been interpreted to be a site of possible spreading (20,21). The upland plateaus of Tellus Regio and the units flanking northern Aphrodite form a second distinctive set of highland features in the equatorial region (13). The location of an upland plateau adjacent to Thetis Regio, a region interpreted to be the site of crustal spreading (20,21), suggests two possible models for formation of this upland plateau: 1) the plateau is a preexisting old crustal block; doming and rifting analogous to that of old terrestrial continental crust, followed by spreading as suggested by Head and Crumpler (20), have split the block and formed the intervening high topography associated with Thetis; 2) the upland plateau originated by crustal spreading. In this second model, developed by Sotin *et al.* (22), an increase in mantle temperature and associated production of thicker crust created the high topography in central Thetis Regio. The region of inter-highland tectonic zones and tectonic junctions has previously been described as zones of extension (2). Unlike the upland rises and tectonically segmented linear highlands, which are predominantly linear features striking east-west, the inter-highland tectonic zones have a variety of orientations forming an interconnecting radial pattern between tectonic junctions (13). The presence of a bilaterally symmetric topographic rise with a central trough offset along CSD's suggests that the inter-highland tectonic zone of eastern Aphrodite is a site of rifting and possible crustal spreading (23). This and other inter-highland tectonic zones converge at tectonic junctions. Two of these junctions, Beta Regio and Atla Regio, have been interpreted to be associated with deep mantle thermal anomalies (5,9,10).

The highlands in the equatorial region of Venus form a near-global network of volcanic centers and interconnecting tectonic zones, composed of several distinctive terrain types. The relationship between tectonic junctions and inter-highland tectonic zones suggests that the junctions are nodal points of the network. The inter-highland tectonic zones which extend to the north and do not connect with tectonic junctions die out in this direction. In some places in the equatorial network crustal spreading may be occurring (inter-highland tectonic zones) (23) whereas at other places (tectonic junctions) hot spots and thermal uplift activity is apparently occurring. These characteristics and correlations suggest that both vertical thermal uplift and lateral movement are occurring in the Venus equatorial highlands. In contrast to the equatorial region, the northern high latitudes are characterized by several broad zones of compression forming highlands and orogenic belts (24,25).

**References:** (1) Masursky, H., *et al.*, *JGR*, 85, 8230, 1980. (2) Schaber, G., *GRL*, 9, 499, 1982. (3) Senske, D.A. and J. W. Head, *LPSC XVIII*, 908, 1987. (4) Senske, D. A. and J. W. Head, *LPSC XIX*, 1061, 1988. (5) Senske, D. A., M. S. Thesis, in preparation, 1989. (6) Basilevsky, A. T. and P. Janle, *Astron Vestnik*, 21,109, 1987. (7) Janle, P. *et al.*, *Earth Moon, and Planets*, 39, 251, 1987. (8) Stofan, E. R., *et al.*, *GSA Bulletin*, 143, 1989. (9) Senske, D. A. and J. W. Head, *LPSC XIX*, 1063, 1988. (10) Esposito, P. B., *et al.*, *Icarus*, 51, 448, 1982. (11) Barsukov, V. L. *et al.*, *JGR*, D378, 1986. (12) Bindschadler, D. L. and J. W. Head, *Earth, Moon, and Planets*, 133, 1988. (13) Senske, D. A. and J. W. Head, *LPSC XX*, 986, 1989. (14) Stofan, E. R. and J. W. Head, submitted to *Icarus*, 1989. (15) Nikoleava, O. V. *et al.*, *Geokhimiya*, 5, 579, 1986. (16) Burns, B. and D. B. Campbell, *JGR*, 90, 3037, 1985. (17) Stofan, E. R., M. S. Thesis, 1-64, 1985. (18) Senske, D. A. and J. W. Head, *IGC*, in press, 1989. (19) Withjack, M. D. and C. Scheiner, *AAPG Bull.*, 66,302, 1982. (20) Head, J. W. and L. S. Crumpler, *Science*, 238, 1380, 1987. (21) Crumpler, L. S., and J. W. Head, *JGR*, 93, 301, 1988. (22) Sotin, C. *et al.*, submitted to *EPSL*, 1988. (23) Crumpler, L. S. and J. W. Head, *LPSC XIX*, 223, 1988. (24) Crumpler, L. S. *et al.*, *Geology*, 14, 1031, 1986. (25) Vorder Bruegge, R. M. S. Thesis, 1987.

VENUS GRAVITY: MEASUREMENTS, REDUCTIONS AND RESULTS; W.L. Sjogren,  
Jet Propulsion Laboratory

This presentation will include a description of what gravity data are and how gravity data measurements are obtained. There will be a brief discussion of the error sources that corrupt the raw data and how Magellan data will be superior to the previous Pioneer Venus data set.

A summary of present data coverage and what will be obtained by Magellan will be shown. The various reduction techniques using spherical harmonics, line-of-sight profiling and direct mass estimates for local feature modeling will be described. The published results from these various approaches will be summarized and inferences suggested. There'll be a list of things we hope to resolve in the MGN extended mission with new high resolution data. For the conscientious participant at this conference, he would be in good shape to ask intelligent questions if he reads the Venus V-gram #14, May 1988.

VENUS AND THE ARCHEAN EARTH: THERMAL CONSIDERATIONS, N. H. Sleep,  
Department of Geophysics, Stanford University, Stanford CA 94305

The Archean Era of the Earth is not a direct analog of the present tectonics of Venus. In this regard, it is useful to review the state of the Archean Earth. Most significantly, the temperature of the adiabatic interior of the Earth was 200°C to 300°C hotter than the current temperature. Mid-oceanic ridges thus resembled Iceland to a considerable extent. The oceanic crust was thicker about 20 km. Melting of ascending material began at greater depths than now. Young oceanic crust was more difficult to subduct and more easily remelted to form continental crust. The global rate of seafloor spreading, or equivalently the average age of oceanic crust, was similar to now. This is inferred because the thickness of continental crust accreted in a compressional orogeny scales to the driving forces available from the decrease in buoyancy of oceanic plates as they cool with age. This observation further indicates that the increased temperature and decreased viscosity of the adiabatic interior did not greatly enhance the rate of convection within the Archean Earth.

Preservation biases limit what can be learned from the Archean record. Archean oceanic crust, most of the planetary surface at any one time, has been nearly all subducted. Preserved orogenic sequences are possibly related to back-arc rifting and subsequent closure. The classic rules for designating supercrustal rocks ensialic or ensimatic do not apply in such a situation. Similar to a modern break-up margin, continuous strata overlay both stretched continental crust and nearby oceanic crust.

More speculatively, the core of the Earth has probably cooled more slowly than the mantle. Thus the temperature contrast above the core-mantle boundary and the vigor of mantle plumes has increased with time on the Earth. That is, hot material which was ubiquitous in the Archean is now restricted to distinct hotspots.

The most obvious difference between Venus and the present Earth is the high surface temperature and hence a low effective viscosity of the lithosphere. In addition, the temperature contrast between the adiabatic interior and the surface, which drives convection, is less on Venus than on the Earth. Both the Earth and Venus are complicated enough that it is not obvious whether the hot lithosphere enhances convection within Venus more than the lower temperature contrast will decrease it. However, it cannot be expected that the hotter lithosphere of Venus enhances convection and affects tectonics in the same way that the hot interior affected the early Earth.

It appears that the hot lithosphere enhanced tectonics on the early Venus significantly enough that its interior cooled faster than the Earth's. The best evidence for a cool interior of Venus comes from long-wavelength gravity anomalies. Unlike the Earth, gravity anomalies on Venus are large and show strong correlation with topography. Upwelling plumes beneath elevation and gravity highs are thus more massive than plumes on the earth. For such plumes or blobs to be steady-state features, the viscosity of the interior of Venus must be significantly higher than the viscosity of the Earth's interior. Otherwise the plumes would have already quickly ascended to the surface and no longer be present. The most obvious explanation for higher viscosity is lower temperatures in the interior.

The low interior temperatures retard seafloor spreading on Venus. The normal interior temperature is low enough that ascending material does not melt significantly and a cool lid of crust and mantle resists spreading. More melting occurs where plumes impinge on the surface. This situation will not exist on the earth for at least several hundred million years.

The high surface temperatures on Venus enhance crustal deformation. That is, the lower crust may become ductile enough to permit significant flow between the upper crust and the mantle. There is thus some analogy to modern and ancient areas of high heat flow on the Earth. Archean crustal blocks typically remained stable for long intervals and thus overall are not good analogies to the deformation style on Venus.

CORONAE ON VENUS: OBSERVATIONS AND MODELS OF ORIGIN; E.R. Stofan, Dept. Geological Sciences, Brown University, Providence RI 02912

The Venera 15/16 spacecraft revealed a number of features of unknown origin including *coronae*, elongate to circular structures with a complex interior surrounded by an annulus of concentric ridges (1) (Figure 1). Eighteen coronae have been identified in Venera 15/16 data of Venus (2); an additional thirteen possible coronae are found in Pioneer Venus and Arecibo data (3). Coronae, with maximum widths of 160 to over 650 km, are found primarily in two clusters in the northern hemisphere located to the east and west of Ishtar Terra. Another possible cluster is located in Themis Regio in the southern hemisphere. The majority of coronae are at least partially raised less than 1.5 km above the surrounding region, and over half are partially surrounded by a peripheral trough (2, 4).

Coronae are characterized by an annulus of concentric ridges, composing 15-60% of the radius of a corona (2). Ridges within the annulus are spaced 5-10 km apart, and vary in length from 10-100's of kilometers. The majority of ridges within the annulus are interpreted to be compressional in origin (2, 5). The interiors of coronae are cut by lineaments of compressional, extensional and unknown origin. Volcanic flows, domes and edifices are found in the interior; flows also frequently overlap the annulus and pond in the peripheral trough. The distribution and variety of volcanic landforms indicates that volcanism associated with coronae is not concentrated at a few large edifices or shields as it is major domal uplifts such as Beta Regio (6).

A sequence of events for coronae has been determined through mapping (2, 5). Prior to corona formation, regional compression or extension creates bands of lineaments along which coronae tend to later form (2). During the early stages of corona formation, relatively raised topography is produced by uplift and volcanic construction. The interiors of coronae are characterized by central extensional deformational features and volcanic features that formed in the middle- to late- stages of evolution. In the final stages of corona evolution, volcanism continues accompanied by lowering of topographic relief. Some coronae are cut by later regional tectonic activity. Many of the coronae with the most subdued relief, interpreted to be older, are located at lower (below 40°N) latitudes.

The evolution of coronae and their general characteristics have been compared to two models of corona origin: hotspots and sinking mantle diapirs (7) (Figure 2). In the hotspot or rising mantle diapir model, heating and melting at depth create uplift at the surface. Uplift is accompanied by central extension, facilitating volcanism. Gravitational relaxation of the uplifted region follows producing the compressional features within the annulus and the peripheral trough. Sinking mantle diapirs may form as a result of a phase transformation at depth (such as the basalt/eclogite transition) or cooling of the lithosphere, resulting in denser material detaching from the base of the lithosphere and sinking. Early-time compression is predicted, followed by uplift, central extension and peripheral compression, and formation of a peripheral trough. Both models can predict the major characteristics and evolutionary sequence of coronae. The sinking diapir model does predict an early-time low and central compression as well as broadening and shallowing of the peripheral trough with time, all of which are not observed at current data resolution. In addition, the sinking mantle diapir model predicts more simultaneous formation of the high topography,

annulus and trough unlike the hotspot or rising mantle diapir model. High resolution Magellan data will be used to distinguish between the two models of corona origin.

**References** 1) V.L. Barsukov *et al.*, *JGR*, **91**, 378, 1986. 2) A.A. Pronin and E.R. Stofan, in prep., 1989. 3) E.R. Stofan and J.W. Head, in prep., 1989. 4) E.R. Stofan and J. W. Head, *LPSC XVIII, Suppl.*, 1033. 5) E.R. Stofan and J.W. Head, in review, *Icarus*, 1989. 6) E.R. Stofan *et al.*, *GSA Bull.*, **101**, 143, 1989. 7) E.R. Stofan *et al.*, in prep., 1989.

Figure 1. Venera 15/16 image of Anahit Corona. Anahit is centered at 77N, 278, and is about 430 km across. Figure 2. Diagrams of hotspot or rising mantle diapir and sinking mantle diapir models of corona origin.



Figure 1.

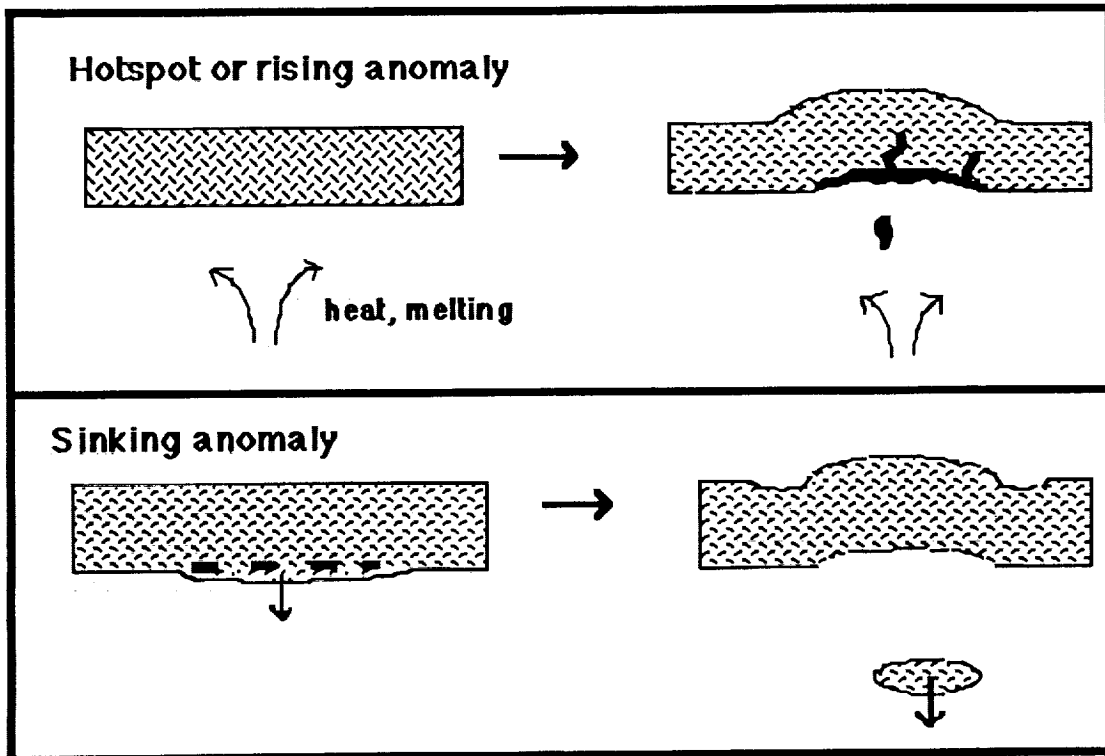


Figure 2

CRUSTAL DEFORMATION: EARTH VS. VENUS; D.L. Turcotte, Department of Geological Sciences, Cornell University, Ithaca, NY 14853

It is timely to consider the possible tectonic regimes on Venus both in terms of what we know about Venus and in terms of deformation mechanisms operative on the earth. Hopefully the Magellan mission will answer many questions. Plate tectonic phenomena dominate tectonics on the earth. Horizontal displacements are associated with the creation of new crust at ridges and destruction of crust at trenches. The presence of plate tectonics on Venus is debated<sup>1,2</sup>, but there is certainly no evidence for the trenches associated with subduction on the earth.

An essential question is what kind of tectonics can be expected if there is no plate tectonics on Venus. Mars and the moon are reference examples. Volcanic constructs appear to play a dominant role on Mars but their role on Venus is not clear. Volcanism, either intrusive or extrusive, will lead to elevated terrains. Elevated terrains will have tensional deviatoric stresses even if fully compensated<sup>3</sup>. For example, 5 km of topography will generate a 700 bar tensional stress in a lithosphere 100 km thick. This mechanism could be associated with the tensional tectonics associated with Beta Regio and Aphrodite.

On single plate planets and satellites tectonic structures are often associated with thermal stresses. Cooling of a planet leads to thermal contraction and surface compressive features. It should be noted that thermal stresses are nonrenewable; once relieved by, for example, transient creep they are gone whereas bending and other stresses are renewable. Thermal stresses can be very high but the role of relaxation processes is unclear.

Delamination has been proposed for Venus by several authors<sup>4,5</sup>. Delamination is associated with the "subduction" of the mantle lithosphere and possibly the lower crust but not the upper crust. The surface manifestations of delamination are unclear. There is some evidence that delamination is occurring beneath the Transverse Ranges in California<sup>6</sup>. Delamination will certainly lead to lithospheric thinning and is likely to lead to uplift and crustal thinning.

A word of caution should be given, however. With all the knowledge of the earth's surface the plate tectonic hypothesis only evolved in the 1960's. And even with this hypothesis many aspects of tectonics are still controversial. For example, does the Eurasian plate override the Indian plate in Tibet. Thus, even with improved imaging it is likely that many aspects of the tectonics of Venus will remain a mystery.

#### References

1. Kaula, W.M. and Phillips, R.J. (1981), *Geophys. Res. Let.* 8, 1187.
2. Head, J.W. and Crumpler, L.S. (1987), *Science* 238, 1380.
3. Turcotte, D.L. (1983), *J. Geol. Soc. London* 140, 701.
4. Head, J.W. (1986), *Lunar Planet. Sci.* 17, 323.
5. Turcotte, D.L. (1989), *J. Geophys. Res.* 94, 2779.
6. Humphreys, E., Clayton, R.W. and Hager, B.H. (1984) *Geophys. Res. Let.* 11, 625.

**EASTERN ISHTAR TERRA: TECTONIC EVOLUTION DERIVED FROM RECOGNIZED FEATURES.** R.W. Vorder Bruegge and J.W. Head, Dept. of Geo. Sci., Brown Univ., Providence, RI 02912 (SPAN BRNPSG::VBRUEGGE).

**Introduction:** Previous analyses have recognized several styles and orientations of compressional deformation, crustal convergence, and crustal thickening in Eastern Ishtar Terra [1-11]. An east to west sense of crustal convergence through small-scale folding, thrusting, and buckling is reflected in the high topography and ridge-and valley morphology of Maxwell Montes and the adjacent portion of Fortuna Tessera [5-11]. This east to west convergence was accompanied by up to 1000 km of lateral motion and large-scale strike-slip faulting within two converging shear zones which has resulted in the present morphology of Maxwell Montes [5-7]. A more northeast to southwest sense of convergence through large-scale buckling and imbrication is reflected in large, northwest-trending scarps along the entire northern boundary of Ishtar Terra, with up to 2 km of relief present at many of the scarps [11,12]. We have previously suggested that both styles of compression have occurred at the expense of pre-existing tessera regions which have then been overprinted by the latest convergence event [11]. The difference in style is attributed mostly to differences in the properties of the crust converging with the tessera blocks. If one, presumably thick, tessera block converges with another tessera region, then the widespread, distributed style of deformation occurs, as observed in western Fortuna Tessera. However, if relatively thin crust (such as suggested for the North Polar Plains [13]) converges with thicker tessera regions, then localized deformation occurs, as reflected in the scarps along Northern Ishtar Terra.

Our purpose in this abstract is to identify the types of features observed in Eastern Ishtar Terra. In this abstract and the accompanying poster presentation, we will describe their potential temporal and spatial relationships, suggest possible origins for them, and show how the interpretation of some of these features has led to the multiple-style tectonic evolution model described above.

**Craters** - These are elliptical or circular depressions described and interpreted as impact craters by Basilevsky and others [14]. They include: Cleopatra (66N/7E), Fernandez (76N/17E), Rossetti (57N/7E), Unnamed #1 (75.5N/30E), Ulrique (76N/55.5E), Frida (68N/55.5E), Unnamed #2 (66.5N/58E).

**Montes** - Recognized as a very high relief rise or chain of rises [15], these mountain ranges are characterized by sub-parallel linear ridges and valleys that strike parallel to the trend of the rise and by linear features that cut across the trend of the ridges and valleys. The ridges and valleys have been interpreted as compressional features [1, 3-5, 16] and the linear features as strike-slip faults [5, 16]. The only major mountain chain in Eastern Ishtar Terra is Maxwell Montes, centered at 65N/4E.

**Dorsae (Ridge Belts)** - Ridge belts are similar to montes in that they are characterized by sub-parallel linear ridges and valleys often cut by linear features. However, they differ from montes in that they are more irregular in plan [15] and have less topographic relief (always less than 3 km). The nature of these features is uncertain, with compressional [17], extensional [18], and transpressional origins all possible. Those in and around Eastern Ishtar Terra include: Semuni (70N/3E-78N/12E), Dyan-Mu (78N/28E-75N/43E), Sel-Anyu (84N/75E-75N/80E), Allat (60N/65E-65N/80E), Kamari (62N/45E-50N/60E), Ausra (45N/20E-55N/28E), Auska (59N/356E-62N/2E), and Unnamed #1 (76.5N/56E-71N/84E).

**Rupes (Scarps)** - These steep scarps are often up to thousands of km long and can have over 2 km of relief. They commonly occur along the edges of highland and tessera areas, often separating regions of highly deformed terrain (such as tessera) from relatively less deformed areas (such as smooth plains). The nature of these scarps is variable, with some scarps interpreted to be related to compressional deformation involving large-scale crustal buckling, imbrication, and underthrusting [12,13], while others may represent fault surfaces associated with rifting [19]. Several dozen unnamed scarps over 100 km long have been mapped in Eastern Ishtar Terra [11], with particular concentrations occurring along the northern and eastern flanks and in the central portion of this region (see chasmata).

**Chasmata** - Chasmata are deep, steep-sided linear depressions [15] with flat floors that are often covered by relatively smooth plains units. Parallel, inward-facing scarps, with up to 2 km of relief define the boundaries of chasmata, which can be up to 100 km wide and over 1000 km long. The nature of these features is also uncertain, since some have been interpreted as extensional graben [19], while others may represent incipient suture zones between converging crustal blocks or slices [12]. Those recognized in and around Eastern Ishtar Terra include: Morana (67N/25E-71N/25E), Varz (71N/27E-70N/30E), Lasdona (66N/30E-72N/35E), Daura (74N/50E-73N/55E), Aranyani (73N/73E-68N/74E), Unnamed #1 (73N/28E-69N/38E), Unnamed #2 (68N/27E-72N/34E), Unnamed #3 (71N/40E-73N/47E).

**Fossae** - Fossae are long, linear, narrow, shallow, depressions [15]. They differ from chasmata in that they are very narrow (less than 20 km wide) and lack flat floors. A simple extensional origin is favored for most of these features, but some may be graben related to large-scale shearing [4], while others (not previously identified as fossae, but as 'troughs') may represent strike-slip or shear faults [11]. Three major sets of fossae are recognized around Eastern Ishtar: Sigrun (48N/17E-53N/19E), Rangrid (63N/355E-62N/0E), and Manto (-63N/54E-64N/69E).

**Syntaxes (No official nomenclature)** - Syntaxes on Venus are broad, arcuate, loop-like features converging at the apical end and opening at the antapical end, with lengths of 250-600 km and widths of 100-400 km [20]. Individual

## EASTERN ISHTAR TERRA, R.W. Vorder Bruegge & J.W. Head

ridges and valleys between 5 and 20 km wide and 20 and 300 km long define the interiors of these features. On Earth, they represent a bend in an orogenic belt, such that two or more compressional (ridge) trends form an acute angle at their intersection. Two such features are recognized in Eastern Ishtar, including: Unnamed #1 (south-opening, apex at 65N/22E) and Unnamed #2 (south-opening, apex at 73N/75E).

**Septae** - These features are broad linear rises, often bounded by steep rupes. They exhibit a mottled appearance dominated by very narrow (< 5 km) intersecting ridges and/or fossae. Their origin is uncertain. Three are recognized in Eastern Ishtar: Unnamed #1 (64.5N/32E-64.5N/37E), Unnamed #2 (64N/31E-63N/33E), and Unnamed #3 (67N/50E-68N/65E).

**Basins** - These are broad topographic depressions often bounded by steep scarps, but far less linear than chasmata. They are usually floored by smooth plains areas, although disrupted areas are often observed within them. Those basins in and around Eastern Ishtar include: Snegoruchka Planitia (North Polar Plains), Audra Planitia (southeast of Ishtar), Unnamed #1 (centered at 58N/5E, just south of Maxwell Montes), Unnamed #2 (centered at 69N/355E, just north of Maxwell), Unnamed #3 (74N/9E), Unnamed #4 (72N/11E), Unnamed #5 (65N/26E), and Unnamed #6 (61N/32E).

**Chevrons (No official nomenclature)** - Chevrons are curved features that consist of either individual or paired scarps, that are distinct from rupes or chasmata because they exhibit a sharp change in trend that produces an acute angle [8]. Numerous chevrons are observed concentrated in central Fortuna Tessera [8], where they may represent either syntaxes-like structures or the sharp edges of individual tectonic blocks. One such chevron opens to the south at 72N/26E.

**Tesserae** - Tesserae are regions of orthogonal to obliquely oriented sets of ridges and valleys [1]. Three sub-types of tessera have been identified on Venus [21], including: *Sub-parallel ridged terrain* (Tsr), *Trough and ridge terrain* (Ttr), and *Disrupted Terrain* (Tds). Tsr consists of sub-parallel ridges and valleys, often disrupted along linear zones, possibly indicating strike-slip offset. Ttr consists of parallel troughs separated by regions of parallel ridges and valleys oriented orthogonal to the troughs. Tds lacks continuous ridges or valleys and is often characterized by a blocky appearance. Tesserae occur as either individual blocks of one sub-type or as large regions made up of a collage or mosaic of tessera blocks and sub-types. Eastern Ishtar Terra represents one such collage region, with all three sub-types recognized there: Tsr is recognized just east of Maxwell Montes (65N/15E); Ttr in Eastern Fortuna (70N/59E); and Tds in Central Fortuna (68N/45E). The origin of tessera is uncertain, though a variety of models have been suggested [22]. We have previously interpreted the Tsr as resulting from the overprinting of the Ttr through compressional deformation oriented normal to the strike of the ridges and valleys in the Tsr [11]. This is reflected in the gentle transition from the Ttr pattern to that of the Tsr in Eastern Fortuna. Similarly, the Tds may result from the gravitational relaxation of Ttr or Tsr in Central Fortuna. In these ways, one tessera sub-type may be transformed to another.

**Discussion.** In our previous analyses we have interpreted the deformation in most of Eastern Ishtar Terra to be the result of several styles and orientations of compressional deformation and crustal thickening [5-11]. The various features in Eastern Ishtar Terra and their relationships to one another reflect these different styles and orientations. The sub-parallel ridges and valleys of Maxwell Montes and the Sub-parallel ridged terrain (tessera) of western Fortuna Tessera reflect an east-west sense of convergence in this region, with deformation characterized by small-scale folding and buckling [5-11]. This sense of convergence may also be reflected in the north-south orientation of the syntaxis structure at 66N/22E, as well as the numerous north-south chevrons in Central Fortuna Tessera [8], and in the north-south trend of Semuni Dorsa [9,10]. The more northeast-southwest sense of convergence suggested for Northern Ishtar Terra is predominantly characterized by large-scale buckling and crustal imbrication, which is reflected in the sub-parallel rupes, chasmata, and dorsae striking west-northwest along this boundary [11-13]. Present analysis is focused on the detailed mapping and synthesis of the units, features, and their relationships.

**References:** 1) A.T. Basilevsky *et al.*, (1986) *J.G.R.*, **91**, 399-411. 2) V.L. Barsukov *et al.*, (1986) *J.G.R.*, **91**, 378-398. 3) A.T. Basilevsky, (1986) *Geotektonika*, **4**, 42-53. 4) L.B. Ronca & A.T. Basilevsky, (1986) *E.M.P.*, **36**, 23-39. 5) R.W. Vorder Bruegge *et al.*, Orogeny and large-scale strike-slip faulting: Tectonic evolution of Maxwell Montes, Venus, submitted to *J.G.R.*, 1989. 6) R.W. Vorder Bruegge *et al.*, (1986) *LPSC XVII*, 917-918 (abs.). 7) R.W. Vorder Bruegge *et al.*, (1987) *LPSC XVIII*, 1047-1048 (abs.). 8) R.W. Vorder Bruegge & J.W. Head, Fortuna Tessera, Venus: Evidence of horizontal convergence and crustal thickening, submitted to *G.R.L.*, 1989. 9) R.W. Vorder Bruegge & J.W. Head, (1988) *LPSC XIX*, 1218-1219 (abs.). 10) R.W. Vorder Bruegge & J.W. Head, (1988) *LPSC XIX*, 1220-1221 (abs.). 11) R.W. Vorder Bruegge & J.W. Head, (1989) *LPSC XX*, 1162-1163 (abs.). 12) J.W. Head, (1988) *LPSC XIX*, 467-468 (abs.). 13) S.C. Solomon & J.W. Head, (1989) *LPSC XX*, 1032-1033 (abs.). 14) A.T. Basilevsky *et al.*, (1987), *J.G.R.*, **92**, 12,869-12,901. 15) G.A. Burba, (1988) *Nomenclatura detalei reliefa Veneri* (Nomenclature of the detailed relief of Venus, in Russian), Nauka Press, Moscow. 16) L.S. Crumpler *et al.*, (1986) *Geology*, **14**, 1031-1034. 17) S.L. Frank & J.W. Head, (1988) *LPSC XIX*, 348-349 (abs.). 18) A.L. Sukhanov & A.A. Pronin, Indications of spreading on Venus (in Russian), in press *Doklady an CCCP*, 1988. 19) R.C. Kozak & G.G. Schaber, (1987) *LPSC XVIII*, 513-514 (abs.). 20) J.W. Head, (1988) *LPSC XIX*, 469-470 (abs.). 21) D.L. Bindschadler & J.W. Head, (1988) *LPSC XIX*, 76-77 (abs.). 22) D.L. Bindschadler & J.W. Head, (1988) *LPSC XIX*, 78-79 (abs.).

**STRESS DISTRIBUTION AND TOPOGRAPHY OF TELLUS REGIO, VENUS; Williams, David R., and Ronald Greeley, Department of Geology, Arizona State University, Tempe, AZ 85287**

The Tellus Regio area of Venus represents a subset of a narrow latitude band where Pioneer Venus Orbiter (PVO) altimetry data (1), line-of-sight (LOS) gravity data (2), and Venera 15/16 radar images (3,4) have all been obtained with good resolution. Tellus Regio also has a wide variety of surface morphologic features, elevations ranging up to 2.5 km, and a relatively low LOS gravity anomaly. This area has therefore been chosen in order to examine the theoretical stress distributions resulting from various models of compensation of the observed topography. These surface stress distributions are then compared with the surface morphology revealed in the Venera 15/16 radar images. Conclusions drawn from these comparisons will enable constraints to be put on various tectonic parameters relevant to Tellus Regio.

The stress distribution is calculated as a function of the topography, the equipotential anomaly, and the assumed model parameters. The topography data is obtained from the PVO altimetry. The equipotential anomaly is estimated from the PVO LOS gravity data. The PVO LOS gravity represents the spacecraft accelerations due to mass anomalies within the planet. These accelerations are measured at various altitudes and angles to the local vertical and therefore do not lend themselves to a straightforward conversion. A minimum variance estimator of the LOS gravity data is calculated, taking into account the various spacecraft altitudes and LOS angles and using the measured PVO topography as an a priori constraint. This results in an estimated equivalent surface mass distribution, from which the equipotential anomaly is determined.

Banerdt (6) has solved equations for a global thin elastic shell, representing the elastic portion of the lithosphere. The assumptions inherent in these solutions are that the shell thickness is less than about 1/10 the planetary radius, that the shell is isotropic, single-layered, and continuous, and that the toroidal terms, representing rotational forcing, can be neglected compared to the poloidal terms, which account for pure loading. Solving these equations requires one further assumption, which will vary depending on the particular model chosen. These models currently include: 1) topographic support due entirely to a combination of density anomalies in the mantle, lithospheric flexure, and the resulting deflection of the crust-mantle boundary, 2) support due to crustal thickness variations combined with lithospheric flexure and deflection of the crust-mantle boundary, and 3) a support model where both mantle density anomalies and crustal thickness variations are considered, and the shell flexure is proportional to the topography. The equations are solved for subsurface mass distribution and lithospheric flexure using the topography and surface equipotential anomaly as data. We also assume a lithospheric, crustal, and upper mantle thickness for a given model. The flexure and mass results are used to solve for a surface stress distribution, which is represented as magnitudes and directions of principal tensile and compressive stresses.

Banerdt's original formulation (6) solves for the surface spherical harmonic coefficients on a spherical shell. We have recast the solutions to be applicable to Fourier coefficients in order to solve for regional scale in addition to global scale stresses. The dependence of the solutions on spherical shell geometry has been retained. The solutions themselves give the short and intermediate wavelength stresses generated by topography and flexure in the immediate vicinity of the Tellus Regio area. These regionally induced stresses are combined with the long-wavelength global stress field, calculated using the spherical harmonic formulation. The stress distribution is then compared to the surface features shown in the high resolution Venera radar images of the Tellus Regio area.

The Tellus Regio area exhibits a wide range of geological features (figure 1). These include complex systems of long sub-parallel ridges and grooves (trending in various directions) and associated wide valleys and flat depressions. A large proportion of the central part of this region is characterized by a chaotic parquet terrain. The northern and southern margins of the elevated region are covered with plains-forming material. A preliminary sketch map is being

STRESS DISTRIBUTION AND TOPOGRAPHY OF TELLUS REGIO  
Williams, D.R. and Greeley, R.

prepared for comparison with the stress distribution results. Preliminary calculations of regional stress distribution show close correlation between principal stress directions and various surface features. For the case of density anomalies in the mantle loading the lithosphere from below, or supporting a lithosphere loaded at the surface, unreasonably high stresses on the order of 1 to 3 kbars result. If crustal thickness variations are included in the solution, and the lithospheric flexure is assumed to be proportional to the topography, more reasonable values for the regional surface stresses result, on the order of 0.1 to 0.5 kbar. Assuming a thinner lithosphere decreases the magnitude of these stresses only slightly. Calculations for an end-member lithosphere with a thickness of only 1 km show stresses ranging up to ~ 0.3 kbar. Variations in assumed crustal thickness have almost negligible effect on the magnitude of the stresses. The principal tensional and compressive directions are perpendicular to the dominant linear surface features for values of flexure consistent with a lithosphere loaded from above. Solutions for regional stresses for a lithosphere loaded from below do not show a good qualitative match between stress direction and surface morphology.

References

- (1) Pettingill *et al.*, *J. Geophys. Res.*, 85, 8261-8271, 1980, (2) Sjogren *et al.*, *J. Geophys. Res.*, 85, 8295-8302, 1980, (3) Barsukov *et al.*, *J. Geophys. Res.*, 91, D378-D398, 1986, (4) Basilevsky *et al.*, *J. Geophys. Res.*, 91, D399-D411, 1986, (5) Kaula, *Theory of Satellite Geodesy*, 1966, (6) Banerdt, *J. Geophys. Res.*, 91, 403-419, 1986, (7) Phillips *et al.*, *J. Geophys. Res.*, 83, 5455-5464, 1978.

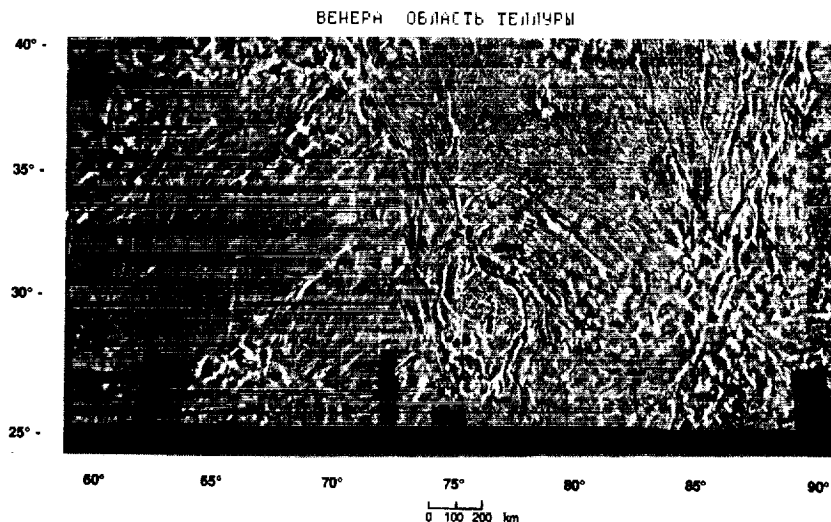


FIGURE 1  
Venera 15/16 radar image of Tellus Regio

ORIGINAL PAGE  
BLACK AND WHITE PHOTOGRAPH

## THREE AGES OF VENUS

Charles A. Wood and Cassandra R. Coombs, NASA Johnson Space Center, Houston, TX 77058

A central question for any planet is the age of its surface. Based on comparative planetological arguments, Venus should be as young and active as the Earth (Wood and Francis, 1988). The detection of probable impact craters in the Venera radar images provides a tool for estimating the age of the surface of Venus. Assuming somewhat different crater production rates, Bazilevskiy et al. (1987) derived an age of  $1 \pm 0.5$  billion years, and Schaber et al. (1987) and Wood and Francis (1988) estimated an age of 200-400 million years. The known impact craters are not randomly distributed, however (Wood and Francis, 1988; Plaut and Arvidson, 1988), thus some areas must be older and others younger than this average age.

We have derived ages for major geologic units on Venus using the Soviet catalog of impact craters (Bazilevskiy et al., 1987) and the most accessible geologic unit map (Bazilevskiy, 1989). Table 1 presents the crater counts (diameters >20 km), areas, and crater densities for the 7 terrain units and coronae. Our procedure for examining the distribution of craters is superior to the purely statistical approaches of Bazilevskiy et al. (1987) and Plaut and Arvidson (1988) because our bins are larger (average size  $16 \times 10^6 \text{ km}^2$ ) and geologically significant.

Crater densities define three distinct groups: relatively heavily cratered (Lakshmi, mountain belts), moderately cratered (smooth and rolling plains, ridge belts, and tesserae), and essentially uncratered (coronae and domed uplands). Following Schaber et al. (1987), we use Grieve's (1984) terrestrial cratering rate of  $5.4 \pm 2.7$  craters >20 km/ $10^9$  years/ $10^6 \text{ km}^2$  to calculate ages for the geologic units on Venus. To improve statistics we aggregate the data into the three crater density groups, deriving the ages in Table 2. For convenience, the three similar age groups are given informal time stratigraphic unit names, from youngest to oldest: Ulfrunian, Sednaian, Lakshnian.

These results suggest that (1) there are significant differences in the age of units on the surface of Venus, (2) the age differences are geology dependent (not random), (3) some activity is extraordinarily young, and (4) geologic activity on Venus may be episodic rather than continuous, i.e. periods of activity were centered at 330, 150 and 10 m.y. ago. This is different, for example, from the generally continuous seafloor spreading that has occurred on Earth for the last 150 m.y. Changes in the pace of activity are also pronounced (Table 2), with approximate resurfacing rates (in  $10^6 \text{ km}^2/10^9 \text{ yr}$ ) of 10 during the Lakshnian, 700 during the Sednaian, and 400 during the Ulfrunian.

The derived ages and photogeologic observations provide evidence concerning the stratigraphic relations of various units. **(a)** Recent volcanism (Bazilevskiy et al., 1989) cuts all units except tesserae, and coronae (also thought to be volcanic; Stofan et al., 1988) cut all but tesserae and Lakshmi and surrounding mountains. The lack of these recent volcanic landforms on tesserae suggest that either magma generation does not occur under them or that magma can not rise to the surface (thick or low density crust?). **(b)** Mountain belts surrounding Lakshmi are old; the deformation forming them is thus ancient and not contemporary (or crater outlines would be distorted). **(c)** Ridge belts are the same age as (not younger than) the plains which surround them, thus they are not like active terrestrial spreading ridges which are commonly of zero age while nearby ocean floor may be tens of millions of years older. **(d)** Impact craters are not uniformly distributed within all terrains; some large areas of ridge belts and tesserae have no detected impact craters, and Lakshmi has most of its impacts concentrated in the western half. **(e)** The two youngest units - domed uplands and coronae - appear to be superposed on smooth and rolling plains and ridge belts. One corona cuts domed uplands, and small patches of domed uplands occur in the middle of tesserae.

The broadscale distribution of time stratigraphic units (Fig. 1) is not random. All but one patch of the young domed upland is south of roughly  $40^\circ\text{N}$  latitude, suggesting a younging toward the equator. Coronae, which are also very young, are widely dispersed in latitude and longitude. The oldest units (Lakshmi and mountain belts) are tightly clumped in one patch,

**Three Ages of Venus:** Wood, C.A. and Coombs, C.R.

almost like terrestrial Precambrian shields with surrounding greenstone belts.

All of these observations and inferences depend on the distribution of 96 craters >20 km in diameter on ~25% of Venus. Fortunately these speculations can be confirmed, extended or rejected when the higher resolution, full-planet radar images from Magellan become available.

**REFERENCES:** Bazilevskiy A.T. (1989) *Sky and Telescope*, April, 1989, 360-368. Bazilevskiy A.T., B.A. Ivanov, G.A. Burba, I.M. Chernaya, V.P. Kryuchkov, O.V. Nikolaeva, D.B. Campbell, and L.B. Ronca (1987) *J. Geophys. Res.*, 92, 12,869-12,901. Bazilevskiy A.T., V.P. Kryuchkov, N.N. Bobina (1989) *Lunar and Planet. Sci. Conf. XX*, 48-49. Griev R.A.F. (1984) *Proc. Lunar and Planet. Sci. Conf. 14th*, in *J. Geophys. Res.*, 89, B403-B408. Plaut J.J. and R.E. Arvidson (1988) *NASA Tech. Mem.* 4041, 410-412. Schaber G.G., E.A. Shoemaker, and R.C. Kozak (1987) *Lunar and Planet. Sci. Conf. XVIII*, 874-875. Stofan, E.R., J.W. Head, and E.M. Parmentier (1988) *Lunar and Planet. Sci. Conf. XIX*, 1129-1130. Wood C.A. and P.W. Francis (1988) *Proc. Lunar and Planet. Sci. Conf. 18th*, 659-664.

**TABLE 1: CRATER STATISTICS**

<u>Terrain Unit</u>	<u>Number of Craters</u>	<u>Area (10<sup>6</sup>km<sup>2</sup>)</u>	<u>Craters /Area</u>
Domed Uplands	0	5.1	0.0
Coronae	0.5	2.3	0.2
Rolling Plains	74	55.8	1.3
Smooth Plains	22	24.8	0.9
Ridge Belts	17.5	13.4	1.3
Tesserae	13	12.6	1.1
Lakshmi	6	2.0	3.0
Mountain Belts	5	1.3	3.8

**TABLE 2: TIME -STRATIGRAPHIC UNITS**

<u>Unit</u>	<u>Time-stratigraphic Name</u>	<u>Age<sup>1</sup></u>	<u>Resurfacing Rate<sup>2</sup></u>
Domed Uplands } Coronae }	Ulfrunian	13	392
Rolling Plains } Smooth Plains } Ridge Belts } Tesserae }	Sednaian	150	710
Lakshmi } Mountain Belts }	Lakshmian	330	10

Units: 1: 10<sup>6</sup>yr; 2: 10<sup>6</sup>km<sup>2</sup>/10<sup>9</sup>yr

**Fig.1:** Time-stratigraphic map of northern portion of Venus. U = Ulfrunian (age 10 m.y.); S = Sednaian (150 m.y.), L = Lakshmian (330 m.y.). Unlabeled outlines are Coronae of Ulfrunian age.

